

HERON contains contributions based mainly on research work performed in I.B.B.C. and STEVIN and related to strength of materials and structures and materials science.

Contents

Biaxial testing of normal concrete

Adapted from the thesis:

twee-assig onderzoek van grindbeton.

L. J. M. Nelissen (Stevin)

Jointly edited by:

STEVIN-LABORATORY
of the Department of
Civil Engineering of the
Technological University, Delft,
The Netherlands
and
I.B.B.C. INSTITUTE TNO
for Building Materials
and Building Structures,
Rijswijk (ZH), The Netherlands.

EDITORIAL STAFF:

F. K. Ligtenberg, *editor in chief*
M. Dragosavić
H. W. Loof
J. Strating
J. G. Wiebenga

Secretariat:

L. van Zetten
P.O. Box 49
Delft, The Netherlands

Samenvatting	3
Summary	5
0 Introduction	7
1 Review of previous investigations	8
1.1 Solid cylindrical specimen	8
1.2 Hollow cylindrical specimen	8
1.2.a Axial compression (tension) combined with an internal or external fluid pressure	8
1.2.b Axial compression (tension) combined with a moment of torsion	10
1.3 Cubes and plates	10
1.4 Conclusions from previous investiga- tions	16
2 Elaboration of the conditions	17
2.1 Sizes of the specimen and the trans- mission of the forces	17
2.2 Estimation of the ultimate load and deformations	20
2.2.a Loading and measurement apparatus	23
2.2.b Influence of the way of loading on the bearing capacity of struc- tures	25
2.3 Variables in the biaxial testing pro- gram	29

3 Testing frame	31
3.1 The transmission of the external load by rod platens	31
3.2 Loading frame	35
3.3 Scheme of measurements	38
4 Concrete mixes and manufacture of the specimen	40
5 Test results	41
5.1 Properties of the concrete	41
5.2 Failure modes	44
5.3 Ultimate load	46
5.4 Stress-strain curves	50
5.4.a Maximum deformation	57
5.5 Energy	57
6 Failure criterion	61
6.1 Long-term strength under biaxial loading	63
7 Conclusions	65
7.1 The ultimate load	68
7.2 Stress-strain relationship	68
7.3 Some remarks about the practical use of the test results	71
Appendix I	
Survey of previous investigations	80
Appendix II	
Calculations of the rod-platens	88

Twee-assig onderzoek van grindbeton

Samenvatting

In vele betonconstructies treden twee-assige spanningstoestanden op. Er is echter nog weinig bekend omtrent het maximale weerstandsvermogen en de vervormingen van beton onder een dergelijke belasting. Zeer vele proefnemingen zijn in de afgelopen 7 decennia reeds op dit onderwerp verricht. Een kritische beschouwing leert dat bij vele van deze onderzoeken (voornamelijk verricht op holle en massieve cilinders en op kuben en schijven) de werkelijk optredende spanningstoestand in het proefstuk sterk afwijkt van de berekende spanningstoestand. De kube of schijf lijkt het meest geschikte proefstuk om twee-assige proefnemingen op te verrichten. Met behulp van een dergelijk proefstuk kan iedere willekeurige combinatie van druk- en trekspanningen op gelijke wijze op het proefstuk aangebracht worden. Uit een vergelijking van de bezwijkvormen die optreden bij de kubus- en prismadrukproef volgt reeds dat de spanningstoestand in een dergelijk proefstuk ondubbelzinnig is te bepalen wanneer de schuifspanningen die optreden in het grensvlak tussen de belastingsplaat en het proefstuk ten gevolge van het verschillende vervormingsgedrag van beton en staal in belangrijke mate worden beperkt.

Hiertoe is een belastingsplaat toegepast die is opgebouwd als een pakket van staafjes, welke staafjes afzonderlijk ten opzichte van elkaar kunnen bewegen. De belasting in de beide richtingen werd bij praktisch alle proefnemingen in een constante verhouding opgevoerd ($\sigma_1/\sigma_2 = K$), terwijl tegelijkertijd de vervorming in een van de beide belastingsrichtingen met een constante snelheid toenam ($d\varepsilon/dt = c$). Hierdoor kon op een eenvoudige wijze het vervormingsgedrag van beton worden gevolgd, terwijl bovendien de duur van de beproeving en de maximale belasting waartegen het proefstuk nog weerstand kon bieden alsmede de bij deze belasting behorende vervormingen ("maximale" vervorming) ondubbelzinnig en onafhankelijk van uitwendige invloeden, zoals bijvoorbeeld de stijfheid van de beproevingsbank, worden vastgelegd.

Bij een vooronderzoek werden een-assige drukproeven verricht waarbij de belasting zowel via een constante snelheid van belasten ($d\sigma/dt = K$) als via een constante snelheid van vervormen ($d\varepsilon/dt = c$) werd opgevoerd. De invloed van de wijze van belasten en de beproevingsduur op het maximale weerstandsvermogen is weergegeven in de figuren 16 en 17.

Het onderzoek is uitgevoerd op beton met een maximale korrelafmeting van 32 mm. De afmetingen van het proefstuk bedroegen $18 \times 18 \times 13$ cm. Twee betonkwaliteiten werden onderzocht, te weten K250 en K350. Om een mogelijke invloed van de snelheid van belasten bij twee-assige proefnemingen te onderzoeken werd de belasting opgevoerd via respectievelijk $d\varepsilon/dt = 1^0/_{00}/100'$ en $d\varepsilon/dt = 1^0/_{00}/5'$. Deze constante vervormingssnelheid werd in het druk-trek en trek-trek gebied gehandhaafd in de richting van de (grootste) trekkrachten in het druk-druk gebied in de richting van de grootste drukkracht. Bij één serie proefnemingen werd in de drie belastingsgebieden de constante vervormingssnelheid juist in de andere belastingsrichting gehandhaafd.

Bij enkele proefnemingen werd de belasting in de beide richtingen niet in een constante verhouding opgevoerd, maar via een “willekeurig” belastingspad. De beproevingsresultaten tonen aan dat het maximale weerstandsvermogen ten opzichte van de prismadruksterkte bij de verschillende spanningsverhoudingen praktisch niet beïnvloed wordt door de wijze waarop de belasting wordt opgevoerd alsmede door de betonkwaliteit. In het druk-druk gebied bleek het maximale weerstandsvermogen groter te worden wanneer een tweede drukkracht aanwezig was. Bij de spanningsverhouding $\sigma_2 : \sigma_1 = 1 : 2$ was de toeneming het grootst en wel ca. 30% ten opzichte van het maximale weerstandsvermogen bij de een-assige drukproef. Bij de spanningsverhouding $\sigma_2 : \sigma_1 = 1 : 1$ bedroeg deze toeneming nog slechts ca. 20%. In het druk-trek gebied bleek het maximale weerstandsvermogen bij de verschillende spanningsverhoudingen het beste gekarakteriseerd te kunnen worden door een rechte die het maximale weerstandsvermogen dat gevonden werd bij de een-assige trek-, respectievelijk een-assige drukproef verbindt.

Het maximale weerstandsvermogen in het trek-trek gebied bleek, in tegenstelling met de twee hiervoor beschreven belastingsgebieden, niet beïnvloed te worden door een belasting in de tweede richting (zie fig. 33).

Deze beproevingsresultaten ten aanzien van het maximale weerstandsvermogen bij twee-assige belasting zijn niet te verklaren met behulp van de klassieke breukhypothese.

De maximale vervorming bleek wel afhankelijk te zijn van de wijze waarop de belasting werd opgevoerd en het gevolgde belastingspad. Vooral in het druk-druk gebied was de maximale vervorming in de richting van de grootste drukkracht (ε_1) sterk afhankelijk van de duur van de beproeving (een langere proefneming gaf een grotere ε_1), zodat ook de richting waarin de constante vervormingssnelheid werd gehandhaafd nog van invloed was op de maximale vervorming (zie fig. 37). Het uiteindelijke breukbeeld was in het trek-trek en in het druk-trek gebied tot aan de spanningsverhouding $\sigma_2 : \sigma_1 = -1 : 30$ hetzelfde en wel één breukvlak loodrecht op de richting van de (grootste) trekkracht en loodrecht op het vlak van belastingen. De proefnemingen met een spanningsverhouding tussen $\sigma_2 : \sigma_1 = -1 : 25$ en $\sigma_2 : \sigma_1 = 3 : 10$ gaven verschillende breukvlakken te zien in dezelfde richting als hiervoor beschreven. De proefnemingen waarbij de spanningsverhouding groter was dan $\sigma_2 : \sigma_1 = -1 : 100$ leidden tot verschillende breukvlakken evenwijdig aan het vlak van belastingen (in dit gebied tot aan de spanningsverhouding $\sigma_2 : \sigma_1 = 3 : 10$ ontstonden dus kolommetjes in de richting van de grootste drukkracht). Bij alle proefnemingen werd geconstateerd dat het breukvlak door slechts ca. 10% van de aanwezige korrels liep, terwijl bij de overige korrels het breukvlak door het grensvlak mortel – toeslagkorrels liep. In 7.1 is een rekenvoorbeeld gegeven hoe het maximale weerstandsvermogen en de rekenwaarde hiervoor bij twee-assige belasting kunnen worden berekend, terwijl in 7.2 een methode wordt beschreven om het vervormingsgedrag van beton onder twee-assige belasting te bepalen.

In 7.3 wordt ingegaan op het nut van de twee-assige beproevingsresultaten voor de praktijk.

Biaxial testing of normal concrete

Summary

In many structures there exists a biaxial stress condition. However, little is known about the strength and the deformation of concrete when loaded in that way. Many tests on this subject have already been carried out in the past seventy years. A critical examination of these tests (mainly done on hollow and massive cylinders and on cubes and plates) shows, that the real stresses in the specimen strongly differ from the calculated ones.

Apparently the cube or plate will be the most suited specimen to use for biaxial tests. On such a specimen, any combination of compression and tension can be introduced into the specimen in an identical way. Comparing the crack pattern that occurs when a cube and a prism are loaded by uniaxial compression, it is shown that the stresses in such a specimen can be determined unambiguously providing the shear stresses, which occur between the loading platen and the specimen, can be eliminated to a large extent. The shear stresses are a result of the difference in deformation behaviour of the loading platen in comparison to the specimen. In this case a loading platen has been used which is composed of small rods. These rods can deform independently of each other. In the tests described the load in both directions has been increased in a constant ratio ($\sigma_1/\sigma_2 = K$), keeping the rate of deformation constant ($d\varepsilon/dt = c$) in one of the loading directions.

As a result it was possible to follow the deformation behaviour of concrete. In addition the duration of the tests and the maximum load which can be borne ("strength") as well as the deformations which occur at that stage ("maximum" deformation) can be ascertained unambiguously and independent of external influences, such as the stiffness of the testing machine. At a preliminary investigation, uniaxial loading tests were carried out at a constant rate of stressing ($d\sigma/dt = K$) as well as at a constant rate of deformation ($d\varepsilon/dt = c$). The influence of the way of loading and the duration of the test on the strength is shown in fig. 16 and 17.

Biaxial investigation has been carried out on a concrete with a maximum grain size (gravel) of 32 mm. The measurements of the specimen were about $18 \times 18 \times 13$ cm. Two qualities of concrete were investigated, namely K250 and K350 (cube strength in kgf/cm^2 after 28 days of age). To study a possible influence of the rate of loading of biaxial tests, the load was increased by $d\varepsilon/dt = 1^0/00/100'$ resp. $d\varepsilon/dt = 1^0/00/5'$. This constant rate of deformation was maintained in the regions of compression-tension and tension-tension in the direction of the (greatest) tension force and in the region of compression-compression in the direction of the greatest compression force.

For one series of tests the constant rate of deformation in the three regions of loading was maintained in the opposite direction. During some tests the load in both directions was not increased in a constant ratio, but in an "arbitrary" loading path.

The test results prove, that the strength in comparison with the prism strength at

the various ratios of stress were not significantly influenced by the method of increasing the load or by the quality of concrete. In the region of compression-compression the strength appeared to be increased due to the stress in the second direction. At the stress ratio $\sigma_2 : \sigma_1 = 1 : 2$ the increase was greatest, about 30% in respect of the uniaxial compression strength. At the stress ratio $\sigma_2 : \sigma_1 = 1 : 1$ this increase was only about 20%. In the region of compression-tension the strength at the several stress ratios could be characterized best by a straight line that connects the uniaxial compression and the uniaxial tension strength. However, the strength in the region of tension-tension appeared not to be influenced by a force in the second direction (see fig. 33). These test results with regard to the strength under biaxial loading cannot be explained by the classical fracture theories.

The maximum deformation appeared to be influenced by the method in which the load was increased and by the loading path. Especially in the region of compression-compression the maximum deformation in the direction of the greatest compression force (ε_1) was strongly dependent upon the duration of the test (a longer test duration led to a greater ε_1), so that the maximum deformation was also influenced by the direction in which the constant rate of deformation was maintained (see fig. 37).

The crack patterns observed were similar in the region of tension-tension and in the region of compression-tension until the stress ratio $\sigma_2 : \sigma_1 = -1 : 30$. The fracture was perpendicular to the direction of the (greatest) tension force and also perpendicular to the plane of loading. The tests with a stress ratio between $\sigma_2 : \sigma_1 = -1 : 25$ and $\sigma_2 : \sigma_1 = 3 : 10$ resulted in different fractures in the same direction as described above. The tests in which the stress ratio was greater than $\sigma_2 : \sigma_1 = -1 : 100$ gave different fractures parallel to the plane of loading (in this region until the stress ratio $\sigma_2 : \sigma_1 = 3 : 10$ the fracture consisted of columns in the direction of the greatest compression force). In all tests it was noted that the fracture passed through only about 10% of the grains, while for the remaining grains the fracture passed through the boundary between the paste and the grain.

In 7.1 and 7.2 a numerical example is given. In 7.1 it is shown how the strength and the design quantity of this strength at biaxial loading can be estimated. In 7.2 it is shown how the deformation behaviour of concrete under biaxial loading can be determined.

In 7.3 the use of the biaxial testresults for the practice is shown.

Biaxial testing of normal concrete

0 Introduction

Many structures have a multi-axial state of stress, e.g. the plates and the shells. Such a stress condition can also occur in structures which are normally considered as linear: in a beam loaded by shearing forces, in the region behind the anchorage zone of a prestressed beam and in a concrete hinge. Nowadays the design of these structures is mainly based on the knowledge of uniaxial tests.

When multi-axial compressive forces act, this will probably lead to an underestimation of the ultimate bearing capacity. When a combined compressive and tensile force acts, an overestimation of the ultimate load is possible. Furthermore little is known about the deformations of structures and the capacity to withdraw large rotations under multi-axial stresses. In order to calculate the several limit states, it will be necessary to know more about the properties of concrete under biaxial loading.

Unless otherwise stated, in the rest of this article when we speak of the state of stress, we mean the mean state of stress calculated from the external load. Every arbitrary state of stress can be characterized by the principal stresses. Several principal stress conditions are possible, viz. the tri-, bi- and uniaxial one (fig. 1). A further subdivision of the biaxial state of stress is given in fig. 2.

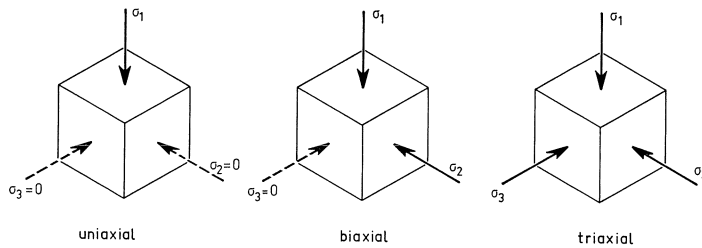


Fig. 1. Definition of the several states of stress.

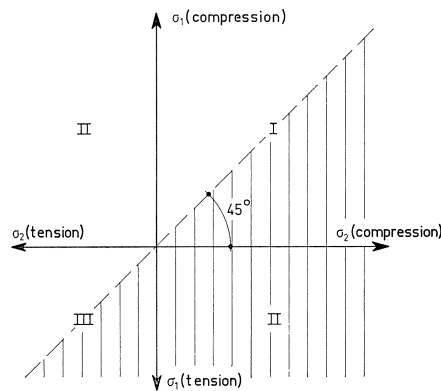


Fig. 2. A subdivision of the biaxial state of stress.
 Region I: compression-compression
 Region II: compression-tension
 Region III: tension-tension

This paper describes an experimental investigation performed on the properties of normal concrete under biaxial loading in each of the three regions as given in fig. 2.

1 Review of previous investigations (see appendix I)

1.1 *Solid cylindrical specimen* [1–7]

When a concrete cube is subjected to an uniaxial compressive load in a normal way, the load is applied to the specimen through steel machine platens. In addition to the longitudinal compressive stress, differences between the lateral deformation of the platens and the concrete specimen induce stresses in the direction normal to the applied load at the platen-specimen interface. This results in an unknown irregular state of stress in the specimen and an apparent increase in the uniaxial strength of concrete. The loading effects are confined mainly to the ends of the specimen and gradually fade out, and a uniform strain distribution is obtained at a distance from the end equal to the width or the diameter of the specimen.

Long specimens have a central zone which is subjected to the desired state of uniaxial compression. Consequently, a prism or a cylinder is used in many countries to estimate the real uniaxial compressive strength.

Many investigators have used this knowledge to investigate the properties of concrete under multi-axial loading. For this purpose, solid cylindrical specimens were subjected to a hydrostatic pressure (biaxial compression, $\sigma_2:\sigma_1 = 1:1$) or a hydrostatic pressure combined with an axial tensile or compressive force (triaxial, $\sigma_1 \neq \sigma_2 = \sigma_3$). The drawback in testing the concrete in this way is the possibility of penetration of the pressure fluid into the pores of the concrete. When this occurs a more sudden rupture at a smaller ultimate load (30 till 60%) and at a smaller axial strain occurs. Most of the investigators surrounded the specimen by a membrane in order to prevent this penetration.

It is also necessary to avoid a restraint of the axial deformation of the specimen in order to get a real biaxial state of stress.

Most of the investigators have not completely fulfilled both of the afore mentioned requirements.

Some investigators ([4, 8–11]), used stirrups or a spiral reinforcement instead of fluid pressure in order to get a multi-axial state of stress. The lateral deformations of concrete loaded by an axial compressive force are prevented by this reinforcement. The results of such a uniaxial compression test is a triaxial compression state of stress in the specimen.

The results of both types of the tests showed that an increase in lateral pressure gives a considerable increase in maximum load. At the same time the axial deformation grows considerably.

1.2 *Hollow cylindrical specimen*

1.2.a Axial compression (tension) combined with an internal or an external fluid pressure

When testing in such a way it is difficult to speak of a biaxial state of stress in the specimen because the fluid pressure gives a triaxial state of stress at one side of the wall. Besides, the stresses in the specimen cannot be calculated directly from the external load because these depend on the deformations of the material. As an example the state of stress in the wall of a cylinder for a linear-elastic material is given in fig. 3.

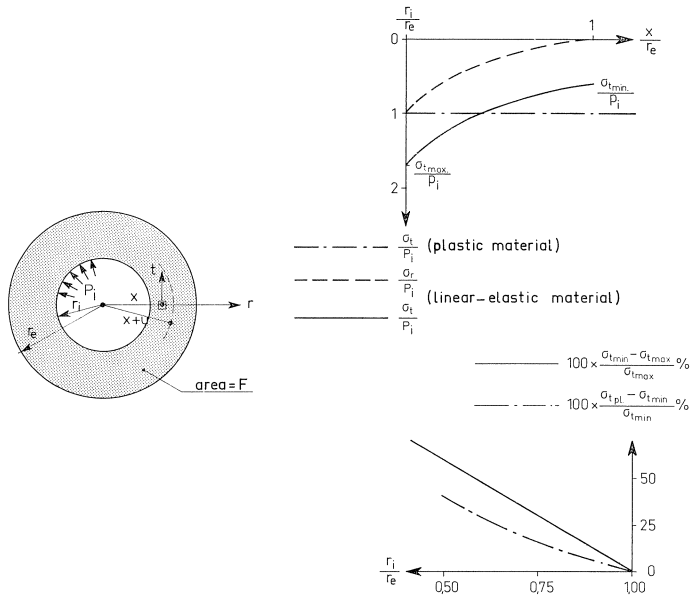


Fig. 3. Calculation of the stresses in the wall of a cylinder loaded by an internal pressure.

The stresses will be more uniform when the behaviour of the material is more plastic (this is to be expected in the phase of rupture of concrete). The difference in σ_t over the wall will also be smaller when the thickness of the wall is small in comparison with the diameter of the cylinder. When aiming at equal properties in all directions, it is necessary, however, for testing concrete that the sizes of the specimen be at least 3 to 4 times the maximum size of the course aggregate.

Most of the investigators [12–14], who have used this kind of testing, calculated the stresses in the specimen by assuming a plastic behaviour of the material (see appendix I), because they were looking for the strength of concrete under biaxial loading.

Mal'cov-Pak [14] have also estimated the load at which the internal micro-cracking increases noticeably by measuring the transverse speed of sound. This load is often assumed to be the discontinuity load or the long-term strength. Such a load was not found at the combined tension tests. With the combined compression tests this load was higher than normally found in uniaxial tests (at $\sigma_1 = \sigma_2$ about 10%) and at compression-tension tests lower.

1.2.b Axial compression (tension) combined with a moment of torsion

This method of loading renders possible every combination of stresses in the region of compression-tension. Assuming a material that behaves in a linear-elastic way, the shear stresses in the wall of a cylinder due to a moment of torsion can be calculated by:

$$\tau_x = \frac{M_T}{\pi(r_u^4 - r_i^4)} \cdot 2x \quad (\text{see fig. 3})$$

It can be seen from this formula that for such a material the difference in stresses at the outside and inside of the wall will be greater when the thickness of the wall increases. For a plastic material the shear stresses can be calculated by:

$$\tau_p = \frac{3M_T}{2\pi(r_u^3 - r_i^3)}$$

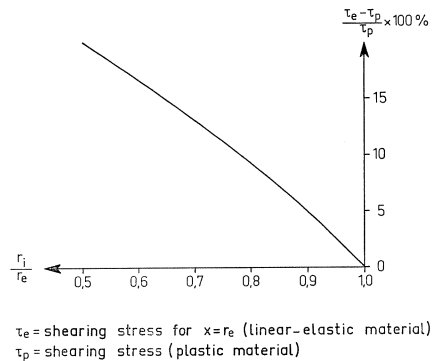


Fig. 4. Shearing stresses in a hollow cylinder, loaded by a moment of torsion.

In fig. 4 these stresses are compared with the stresses at the outside of the wall when testing a linear-elastic material. These figures show that the thickness of the wall must be small in comparison to the diameter of the cylinder. Furthermore, the length of the specimen has to be large so that in the middle part of the cylinder disturbances of the loading platens and the mechanism for the moment of torsion do not occur. Besides, this mechanism has to follow the change of length of the specimen without friction, so that no extra axial loading can be introduced. Finally, it is necessary to know which part of the external moment of torsion is lost by friction in the mechanism itself and by slip.

1.3 Cubes and plates

It has already been mentioned in 1.1 that by testing a cube, the state of stress in the specimen is influenced by the medium between the loading system and the specimen. This influence depends, for instance, on the deformations of concrete under loading,

the thickness of the loading platen and the coefficient of friction between the medium and the concrete.

At the moment it is impossible to calculate the influence exactly. For this purpose it is necessary to know the deformations of concrete under a multi-axial state of stress. However, it is possible, by assuming certain uncertainties, to show the necessity of investigating this friction when cubes or plates are used for biaxial tests on concrete.

With the help of the finite element method [20] we calculated how the state of stress in a plate is affected by the loading platen when this platen is connected stiffly to the plate. For this calculation it was assumed that concrete behaves in a linear-elastic way.

When the real deformations of concrete under multi-axial loading are known and also the coefficient of friction between the concrete and the loading platen is known (which probably depends on the normal stresses) then the finite element method can lead to a more realistic calculation.

The calculated stresses are given in fig. 5. This figure shows that the quality of the concrete has a great influence on the state of stress in the specimen. At a larger deformation of the concrete under equal loading this difference between the real

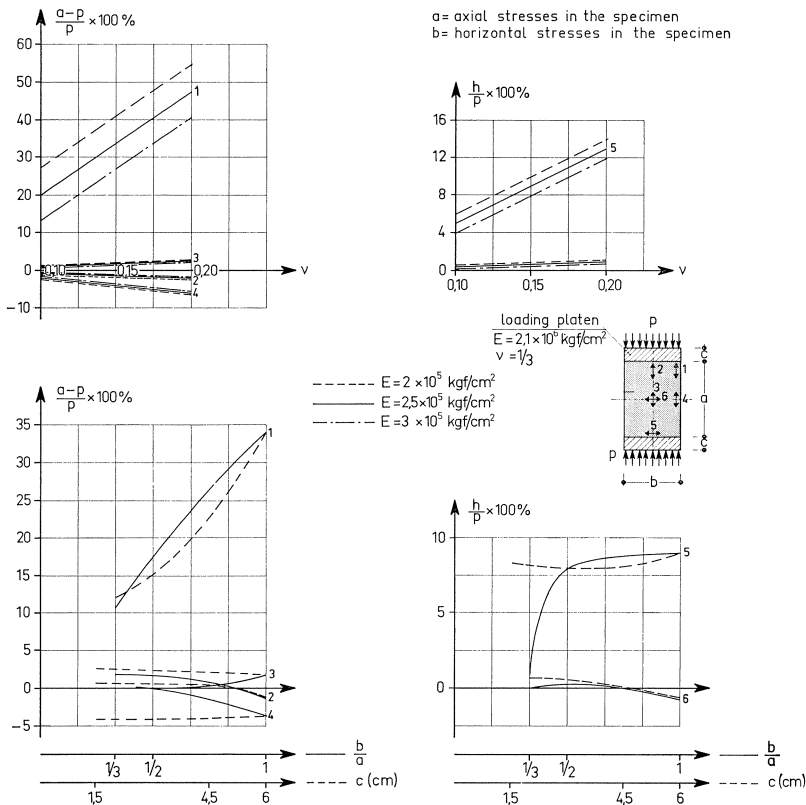


Fig. 5. Influence of the quality of the concrete, the slenderness of the specimen and the thickness of the loading platen on the state of stress in the specimen under uniaxial compressive loading.

state of stress in the specimen and the calculated one will be greater. We have to remember, however, that the given deviations in fig. 5 are valid only when the suppositions are fulfilled. The deviations will be smaller because in such a test the loading platen is not completely connected to the specimen. On the other hand the deviations will be greater in the case of non linear-elastic behaviour of concrete and the relative increase of the lateral deformation. It is not known which of these influences is the most important. Also the thickness of the loading platen is very important (standardizing this thickness seems very significant).

Finally, fig. 5 gives the well-known fact that by increasing the slenderness of the specimen, the deviations will be smaller. A real uniaxial state of stress is realized when the slenderness of the specimen is about 3.

When testing a cube or a plate in a biaxial way, in addition to the above-mentioned influences a deviation of the external state of stress will also occur by the adjacent platens. A part of the applied external load will be borne by these platens. As a result the stresses in the specimen will be much lower than the external stresses. This will give an apparent increase of strength.

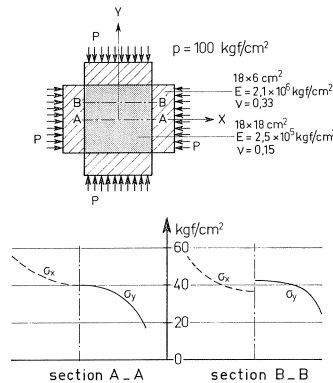


Fig. 6. The state of stress in a cube or a plate under biaxial loading.

This was also investigated with the help of the finite element method (see fig. 6). The difference between the external stresses and the stresses in the specimen will be smaller when the friction between the loading platens and the specimen is smaller, but will be greater as a result of the non-linear stress-strain relationship of concrete.

Föppl [21] was the first investigator who carried out biaxial tests on concrete. He was aware of the influence of the friction between the loading platen and the specimen and tried to avoid this influence by a lubricant. This lubricant may not be too tough, because otherwise the deformations of the concrete cannot be followed and a kind of prestressing of the concrete will result (fig. 7a). The lubricant also cannot be too weak because then it will flow away to the sides of the specimen which results in an irregular stress condition and an apparent decrease in strength (see fig. 7b).

Furthermore there is a chance that the lubricant will penetrate the pores of the concrete. This will give tensile stresses in the concrete and also because of this splitting action an apparent decrease in strength (see also 1.1).

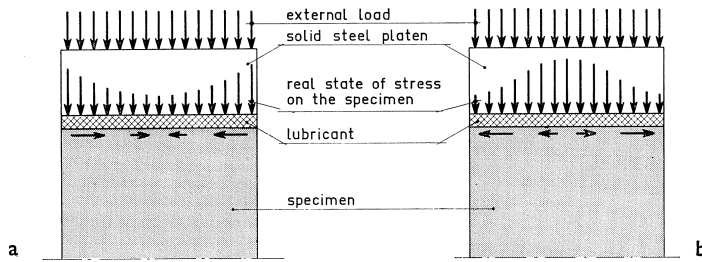


Fig. 7. State of stress on a specimen by using lubricants with different stiffness.

Föppl found the following values for the strength in comparison to the cube strength:

- cube strength – without lubricant: 1
- cube strength – with lubricant: 0,58
- biaxial compression strength – without lubricant: 1,87
- biaxial compression strength – with lubricant: 0,56

From these results it can be concluded that the lubricant has a very important influence on the test results.

Further some tests were carried out with a very thin layer of brass between the lubricant and the specimen to avoid the lubricant penetrating the pores of the concrete:

- a. uniaxial compression strength – without lubricant
without brass 1
- b. uniaxial compression strength – with lubricant
without brass 0,52
- c. uniaxial compression strength – with lubricant
with brass 0,56
- d. uniaxial compression strength – without lubricant
with brass 0,83

These results show that a possible penetration of the lubricant into the pores of the concrete had little influence on the test results (compare b–c).

Weigler/Becker [24] investigated $10 \times 10 \times 2,5$ cm plates. The thickness of the plate, compared to the other two sizes, was chosen after an investigation into the influence of the thickness of the plate on the strength of concrete under uniaxial and biaxial loading (see fig. 8).

This figure shows that the sizes of the specimen have a greater influence on the biaxial strength than on the uniaxial strength and that after a certain thickness, compared to the other two sizes, there is not any influence at all. Tests carried out by Fumagalli [6], with different stress ratios, also showed this influence of the thickness. This influence appeared to be the greatest at a stress ratio of $\sigma_1:\sigma_2 = 1:1$.

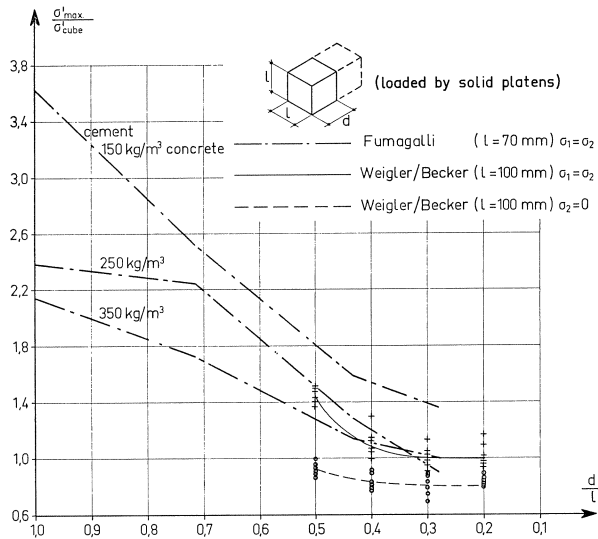


Fig. 8. Influence of the thickness of the plate on the strength of concrete.

Weigler/Becker thought to reduce all shear stresses between the loading platens and the specimen by using thin plates in their biaxial investigation. In the direction perpendicular to the free planes they did indeed reduce the restraint of deformations, but in the plane of loading this influence is maintained as is proved by strain measurements at a uniaxial compression test (the strain in the direction of the thickness was greater than in the other lateral direction).

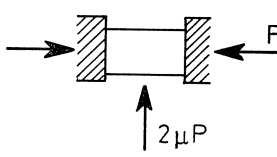
Sundara Raja Iyengar et al [25] used a testing frame with one frame in a vertical position fitted to the floor, and the frame in the other direction in a horizontal position suspended by contraweights. This allowed the two frames to move independent of each other without introducing secondary stresses in the specimen. In this way it was possible to follow the change in length of the frames and the specimen and at the same time maintain a real biaxial loading.

Vile [26] loaded the plates (25 × 25 × 10 cm) directly by steel platens. He investigated the possible introduction of shear stresses by strain measurements. These measurements showed in the middle part of the specimen (15 × 15 cm) a uniform state of deformation. He concluded that there also had to be a uniform stress condition and calculated these stresses by dividing the external load by the total area. Just like Weigler/Becker he disregarded the bearing of load by the adjacent platens (as given in fig. 6). During the tests, strains were measured in the three principal directions with strain gauges with a measuring length of 3 cm. This is very small compared to the maximum size of the aggregate. He also measured the discontinuity point (see Mal'cov-Pak). The loading frame of Kupfer et al [31] consisted of one frame fitted to the floor and another one suspended from the first one by means of steel rods and springs (both frames were very rigid, made of prestressed concrete). They used brush-

bearing platens to avoid the restraining action of these platens on the specimen. An effort was made to maintain a constant strain rate during the test. It was chosen such that the maximum load was reached after about 20 min. In contradiction to the combined compression tests, there was a sudden rupture as a result of an increasing strain rate during the tests in the region of compression-tension and tension-tension. Therefore a comparison of the test results in these two regions with the results in the region of compression-compression is difficult. Besides, with almost all tension tests the fracture was directly next to the connection of the brush loading platens and the specimen probably due to a weak layer of glue.

Strain measurements also gave an excentricity of loading as a result of a difference in properties of the mould side and the open side of the specimen. This investigation proved that the module of elasticity was independent of the state of stress, but the Poissons ratio was about 10% higher at tension tests compared to compression tests. In the tests under biaxial compression one major crack developed at failure, which had an angle of about 18–27 deg. to the free surfaces of the specimen.

Several of the above-mentioned tests and also some of those in appendix I can easily be transferred to triaxial tests. This was done by Niwa et al [32], by means of a complete symmetrical loading frame (six vessels!). To diminish the friction between the loading platens and the specimen, the most suitable lubricant was chosen:

lubricant	μ	$0,2P_{\max} \leq P \leq 0,9P_{\max}$
non	0,46 –0,65	
graphith powder	0,28 –0,31	
cup grease	0,15 –0,24	
teflon sheet 0,05 mm + silicon grease	0,018–0,023	
rubber sheet + silicon grease	0,008–0,012	

The lubricant consisting of a rubber sheet with silicon grease was used in their investigation. They did not look for the other difficulties mentioned in fig. 7. After 28 days of hardening, the cube strength was about 300 kgf/cm² and the maximum size of the aggregate was 15 mm (which kind of lightweight aggregate was used is not mentioned). The load was raised with a constant rate of loading (3 to 4 kgf/cm²/sec) in the direction of the greatest stress.

In the biaxial tests constant stress ratios were maintained as well as an increase in load following several stress paths in order to examine the effect of loading history on the strength. In the triaxial investigation most tests were carried out in such a way that the sum of the principal stresses was kept constant. The results are given in fig. 9.

There appeared to be a good relationship between the sum and the difference of the maximum and minimum stresses. This does not mean that the failure occurs by maximum shear stress. The angle of cracking did not correspond to the slip

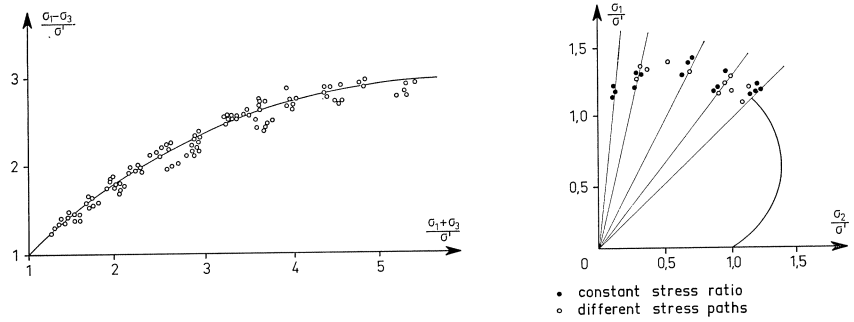


Fig. 9. Test results of Niwa, et al. [32].

angles of Mohr's criterion and a lot of aggregates were split in the cracked planes.

Almost all the multi-axial tests carried out on concrete up to now were for the purpose of comparing the strength under such a loading with the uniaxial strength and of creating a failure criterion for concrete.

Only a few investigators have also carried out some strain measurements to look for the influence of the second and sometimes also third principal stress on the deformations of concrete. The influence of the factor time was almost always disregarded, although a few investigators have mentioned their rate of loading. In only a few investigations is the influence of the factor time determined by doing creep tests under biaxial loading ([33, 35] and appendix I).

1.4 Conclusions from previous investigations

One of the major problems dealing with multi-axial tests on concrete is the development of a well-defined and uniform state of stress in the concrete. Most investigators have mentioned this difficulty and almost everyone has tried to solve this problem.

A comparison of all the results of the different investigations would for this reason be very difficult. Furthermore, less is reported about the set-up of the investigation (the way of loading, the mixes of concrete, the treatment of the specimen, etc.), although this can have a great influence on the test results. Uniaxial compression tests have shown that the size of the specimen has an influence on the results. Most investigators have used different specimen in the different regions of the biaxial state of stress.

In spite of the previously mentioned difficulties, some information can be concluded from previous investigations. In the region of combined compression, the strength of concrete is greater than the uniaxial compression strength. The increase in strength depends on the stress ratio and has a maximum of about 20% to 70% compared with the uniaxial compression strength (the different investigations show 30% to 400%, and even in some tests a decrease of strength was found.) In the region of compression-tension the strength decreases compared with the uniaxial compression strength. In almost every investigation a large variation in the results occurred in this

region. Only a few investigations have been carried out in the region of combined tension. A conclusion regarding the strength of concrete in this region cannot be made.

The previous investigations do not provide very much information about the influence of the quality of the concrete in the three regions. Only a few investigators mentioned that by using another kind of concrete (cementstone and lightweight concrete) is the increase in strength in the region of biaxial compression less compared to normal concrete and the influence of the stress ratio on this increase is different by using different kinds of concrete. To what extent this increase in strength is maintained by a long-term loading has not been investigated directly. In some investigations the discontinuity point is estimated by doing strain or sound measurement. From these investigations it appeared that the ratio between the long-term strength and the short-term strength was constant at the different stress ratios. How much this ratio is cannot be concluded from the previous tests.

Less is known about the influence of a biaxial state of stress on the deformations of concrete because almost all strain measurements were stopped before reaching the ultimate load for protecting the instruments against damage.

Following different loading paths had in general no influence on the strength of concrete but to what extent the deformations were influenced by this is not investigated.

In general it can be concluded that for doing biaxial tests on concrete very severe requirements with regard to the loading equipment and the set-up of the test has to be fulfilled.

The following conditions are drawn up for the tests described in this report:

- the state of stress in the specimen has to be uniform and biaxial. It must be easy to calculate these stresses from the external load and they have to be independent of the deformations of the specimen.
- it must be possible to get every state of stress required in the same way and with identical specimens, in order to compare the results in the three regions of biaxial loading.
- it is important to investigate the influence of the factor time on the strength and deformations of concrete under a biaxial state of stress. For this reason it is important to standardize the duration of the test beforehand and to vary this duration.
- the stress ratio has to be constant during the test in order to follow in an easy way the deformations of concrete under biaxial loading. Some additional tests are necessary to check the influence of following different loading paths.
- the strain measurements must be conducted in an easy way.

2 Elaboration of the conditions

2.1 Sizes of the specimen and the transmission of the forces

Compared to other shapes of specimen, cubes and plates have the advantage that any

bi- or triaxial state of stress on the same specimen and in the same way can be transmitted, so that a direct comparison of the different biaxial regions is possible. Strain measurements can easily be carried out on such a specimen and the sizes of the specimen are such with testing normal concrete that the specimen is still easy to handle. The state of stress in a cube or plate is undefined, when cubes or plates are loaded in the normal way by the usual platens of the testing machine (see 1.3). The cube or plate is the most suitable specimen for conducting multi-axial tests, when the shear stresses, due to the friction between the loading platens and the concrete can be reduced or eliminated. This can be achieved by:

- a. a slender specimen
- b. applying a lubricant to the loaded surfaces of the specimen
- c. using such a loading platen that the deformations of the specimen can easily be followed.

a. Uniaxial compression tests, carried out by Newman [36] (see fig. 10) and also the calculation with the finite element method (see fig. 6) have showed that a real uniaxial state of stress is achieved when the slenderness of the specimen is about $2\frac{1}{2}$ to 3. The strain measurements, given in fig. 10, can also serve to explain a phenomenon found by testing rocks. In this tests cylindrical specimen were loaded uniaxial and unloaded just before rupture.

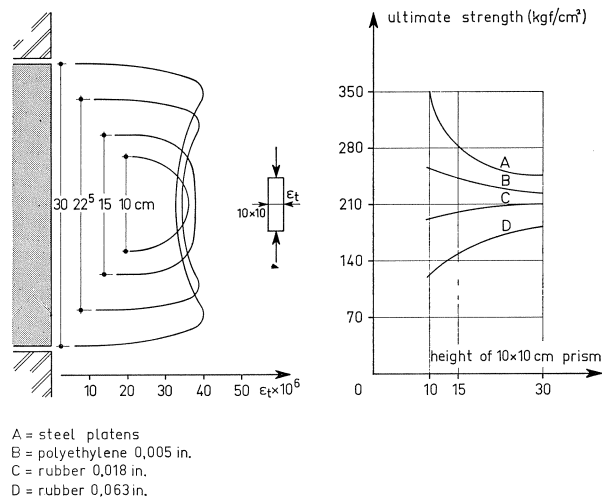


Fig. 10. Variation of ultimate strength of concrete with height of specimen and type of packing.

It appeared that a little distance from the loading platens microcracks occurred [37]. The influence of the loading platens can be neglected in the middle part of a slender specimen. For this reason in some countries (for instance England, U.S.A.) a cylindrical specimen is used for control tests. This method no longer helps with biaxial

tests. The influence of the loading platens in the direction normal to the plane of loading can be reduced (see fig. 8), but in the plane of loading this influence still remains and depends on the deformations of the concrete and the friction between the loading platens and the concrete.

b. A lubricant (paraffine, rubber etc). is mostly used to reduce the friction. Choosing a good lubricant is very difficult while the deformations of concrete under loading are not linear. Some other affects can also occur such as an irregular loading or penetration of the lubricant into the pores of the concrete (see fig. 7 and the tests of Föppl).

For tension tests it is also necessary to have a good glue with a low coefficient of friction.

c. This way of loading seems to be the most suitable one for doing multi-axial tests on concrete. For testing constructions or parts of it sometimes movable stamps are used to follow the deformations of the specimen and as a result to avoid secondary stresses. This principal can also be used for testing cubes, as has already been done by Kjellman [38] for testing soil samples and by Hilsdorf [30]. The conventional solid bearing platens of the testing frame are replaced by bearing platens built up from small rods (mentioned rod-platens), which can move independently of each other. These rods have to fulfill the following conditions:

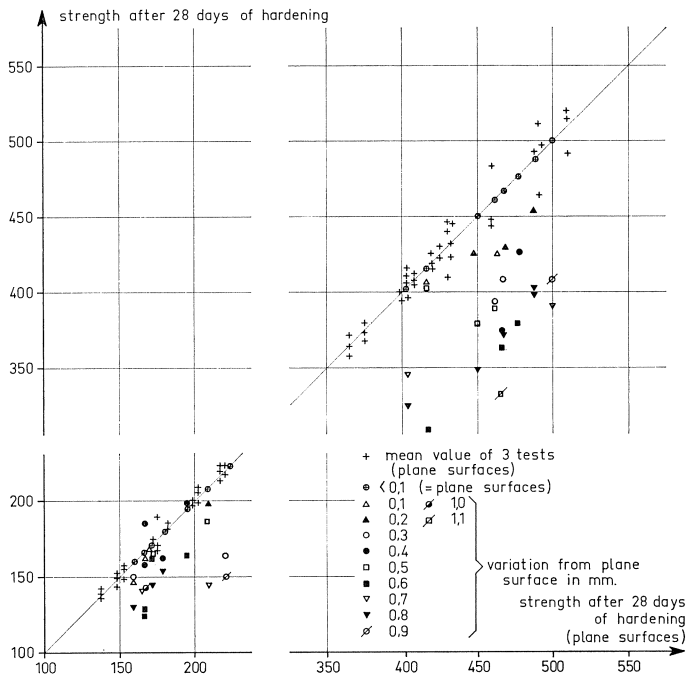


Fig. 11. Influence of the variation from plane surface on the ultimate strength [39].

- they have to be strong enough
- their buckling stability has to be sufficient
- they have to be flexible enough to follow the deformations of the concrete without introducing extra stresses in the specimen.

A compression force can be transmitted directly into the specimen. The platens have to be flat, just like the surfaces of the specimen, while otherwise the apparent strength of the concrete will be decreased by introducing splitting stresses into the specimen [39, 40] (see fig. 11). For this reason it is necessary to standardize the flatness of the bearing platens and the surfaces of the specimen in our codes.

The specimen and the rod-platens have to be glued to transmit tensile forces. In order to insure a good effect of the rod platens this layer of glue has to be very thin and the separate rods may not be glued to each other.

2.2 *Estimation of the ultimate load and the deformations*

When a compression test on a prism is carried out in the conventional way to estimate the stress-strain relationship and the prism strength the load is raised with a constant or a quasi-constant speed. Such a method of loading produces a sudden and explosive rupture by the release of energy out of the testing frame. The shape of the stress strain diagram and the maximum load that can be borne by the specimen are dependent on the rate of loading. From strain measurements of the compression zone of loaded beams, Talbot (1904) learned that the strain of concrete under compression can be greater than the maximum strain measured in the conventional way. Furthermore, Talbot found from calculations of the equilibrium of the internal and external bending moment that the stress-strain relationship of concrete under uniaxial compression also has a descending portion. To get a good insight into the rupture of concrete it is necessary to estimate the maximum load and the deformation in that stage of loading. For this purpose a complete stress-strain curve is necessary. The descending part of the diagram cannot be estimated by the conventional prism test. Because of the influence of the stiffness of the testing frame in comparison with the stiffness of the specimen, the descending part of the stress-strain curve cannot be reached. There exists a stable equilibrium between the specimen and the testing frame when the test is in the rising part of the stress-strain curve (see fig. 12). In this part of the diagram a raising of the load is necessary to get a shortening of the specimen. Because of this compression force the columns of the testing frame will lengthen and the bearing platens will bend. As a consequence of this lengthening of the testing frame the load will decrease and a stable equilibrium is attained.

When the test is in the descending part of the curve such an equilibrium is not possible, it will be a labile one. There still exists an equilibrium between the specimen and the testing frame when the stiffness of the specimen is smaller than the stiffness of the testing frame (see fig. 12, till point A). In a certain stage the stiffness of the testing frame will be greater than that of the specimen. As a result the shortening of the testing frame will be greater than the shortening of the specimen and a sudden

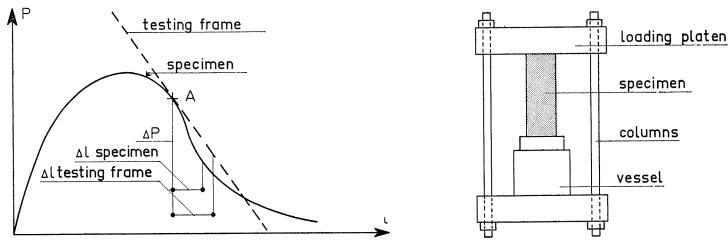


Fig. 12. Estimation of the equilibrium between the specimen and the testing frame.

rupture of the specimen will occur. For this reason the maximum apparent deformation of the concrete is dependent on the stiffness of the testing frame. This stiffness depends on the stiffness of the columns and the bearing platens, but also on the deformations of the hydraulic system. To get a complete stress-strain curve a very stiff testing frame is necessary. Turner and Barnard [41] even proposed to use mercury in stead of oil! In a tension test it appeared that in spite of the use of a very stiff testing frame an early rupture occurred as a result of the stiffness of the hydraulic system.

A very resilient (soft) testing frame can be considered as opposed to a very stiff (hard) testing frame. Glucklich [42] made a soft frame by using springs between the specimen and the bearing platen. It appeared that the strength in such a loading frame was about 30% of the strength in a normal frame. The essential difference between the two types of loading is that when testing with a soft frame a practically unlimited store of elastic energy is available whereas on the other hand with a hard frame the only energy available is that stored in the specimen. One idea is that it may be assumed that this reserve of energy is responsible for the low strength. In a non-homogeneous material when a crack growth was checked by a region of low energy, the presence of the spring contributed an additional supply of energy to overcome the obstacle. Actually this supply comes in the form of kinetic energy, the maximum being that of all the moving parts in the system. This reserve of energy therefore makes the first crack that starts growing the fatal one and that is why the strength in a soft frame is much lower than the strength in a hard frame where growing cracks soon reach stabilization. When the same experiment was carried out on a good homogeneous material there was not such a difference in strength. Tests in the Stevin-laboratory could not confirm this great decrease in strength. For this investigation prisms ($10 \times 10 \times 30$ cm) were made of normal concrete with a cube strength of 330 kgf/cm^2 after 28 days of hardening. The stiffness of the testing frame was between 2050 kgf/mm and the stiffness of a normal 500 tf loading frame. The load was raised by a constant rate of loading. The mean compression strength of the prisms was 276 kgf/cm^2 with a coefficient of variation of 3%. This variation in strength had no relation with the stiffness of the frame. It is possible that the stiffness of the loading frame was still too great but it is also possible that the coarse aggregate in normal concrete levels the process of internal cracking.

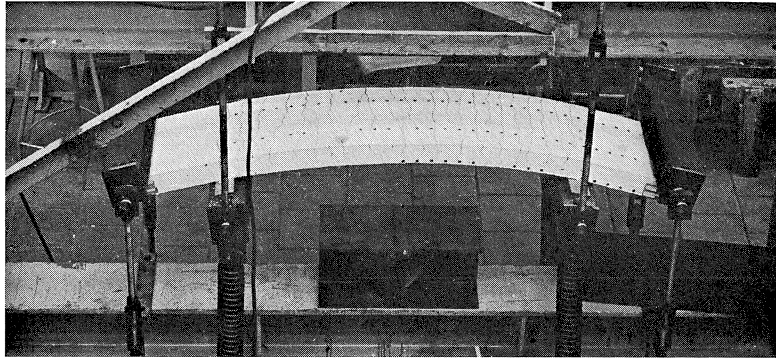


Fig. 13. Testing frame of a plate, in which the descending part of the moment-curvature diagram could be reached by fitting springs parallel to the specimen.

Another method used in the Stevin-laboratory (fig. 13) of getting into the descending part of the stress-strain curve is by fitting springs parallel to the specimen. These springs will sustain a part of the external loading and by raising the external loading the force on the specimen itself can descend and still a stable equilibrium is maintained between the loading frame and the combination of specimen-springs. Hughes and Chapman used for their purpose [43] a standard universal compression-tension loading frame. To obtain a stiffer machine a steel block was therefore placed in the compression testing space whilst the concrete specimen was being strained in the tension space. Which part of the external load is supported by the specimen, depends on the stiffness ratio between the specimen and the springs. The increase in load in the springs will be proportional to the deformation of the specimen, whereas the increase in load in the concrete specimen is not proportional to its deformation. As a result the loading of the specimen will not be proportional to the external load.

It is also possible to make an apparently stiff testing frame by raising the load with a constant strain rate. In this way the duration of the test can be determined beforehand and it is also possible to test certain properties of concrete independent of external influences. This constant strain rate can easily be attained by using a very stiff spring in the above-mentioned method!

When the load of these springs is great in comparison to the load on the specimen, then by raising the external load with a constant speed the distance between the loading platens will change with a constant speed. When there are no deformations between the specimen and the bearing platens the specimen itself will be loaded by a constant strain rate. The disadvantage of this method is that a very strong testing frame is needed.

After a lot of exercise a constant strain rate can be achieved manually. The regulation of the amount of oil to the vessel has to be regulated after visual strain measurements (see for instance Rasch [44]).

With uniaxial tension tests, however, it is impossible in this way to maintain a

constant strain rate [44–45]. The reaction of the operator is not fast enough and also the friction in the vessel and the long oilpipes are the cause of this.

To make a stiffer testing frame by the use of springs is not so suitable for doing biaxial tests because keeping a constant stress ratio in the specimen during the test is impossible even when the external forces in the both directions are equal to each other. With biaxial tests it is also difficult to maintain a constant strain rate manually. This method enabled Kupfer [31] to get over the top of the stress-strain curve in the region of combined compression, but the test results in the regions of compression-tension and tension-tension show an early rupture as a result of an increasing strain rate. This can be explained by the long oilpipes and the friction in the vessels necessary in order to maintain a constant stress ratio and to load the specimen.

As has already been mentioned, the ultimate load depends on the speed of loading. At the start of the tests the deformation is proportional to the stress so that by increasing the load via $d\varepsilon/dt = K$ and $d\sigma/dt = E_0K$ will give an equal rate of loading. When this proportionality no longer exists and the deformation increases faster, then by maintaining a constant strain rate the speed of loading will decrease and be zero when approaching the top of the stress strain curve. On the other hand by maintaining a constant rate of loading in the top of the stress strain curve the speed of deformation will be infinite and as a consequence the ultimate load will be greater by maintaining a constant rate of loading as compared to a constant strain rate.

When the rate of loading and the strain rate at a compression test on a concrete prism are chosen in such a way that at low stresses they both give the same speed of loading, then by the creep of the concrete the stress-strain curve at a constant strain rate, in comparison with that at a constant rate of loading will show a greater deformation under an equal stress and also the top of the stress-strain curve will be lower.

A constant rate of loading is often prescribed in the standardized cube test. In practice this way of loading is not maintained during the test to avoid a sudden and explosive rupture of the specimen and because the conventional loading apparatus cannot, in general, give sufficient oil per unit of time. As a consequence the constant rate of loading will gradually change in a constant strain rate.

In general it can be concluded that a sudden rupture is not a property of the concrete itself but is a result of the mechanical testing condition and that with the same quality of concrete there is no point in speaking of *the* strength and *the* stress-strain curve. These characteristics always have a connection with certain loading and testing conditions.

2.2.a Loading and measurement apparatus

Servo hydraulic loading apparatus is used to maintain a constant strain rate and at the same time a constant stress ratio. The scheme of the circuit of regulation is given in fig. 14.

A disadvantage of this method of regulation is that the specimen is a part of the circuit of regulation. The stiffness of the specimen also determines the possibility of

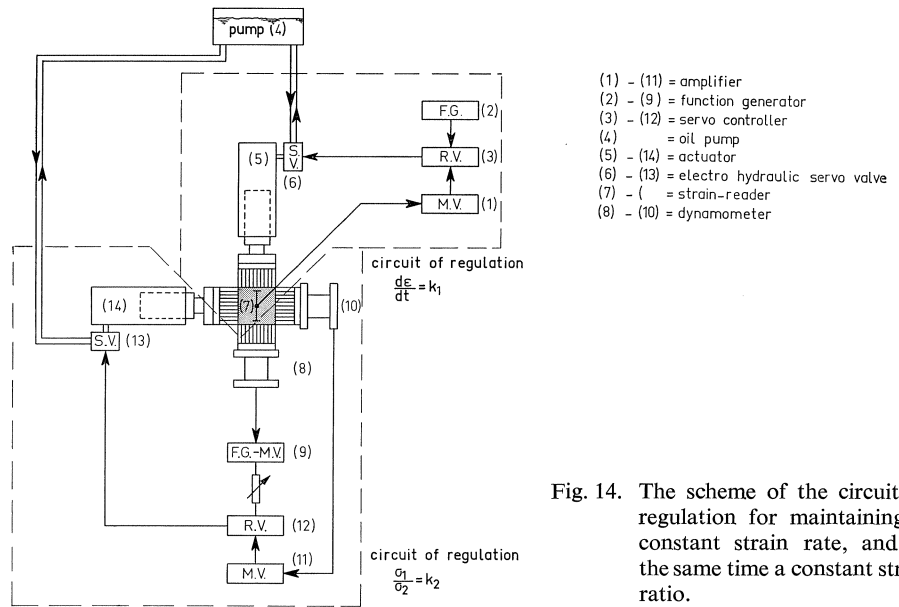


Fig. 14. The scheme of the circuit of regulation for maintaining a constant strain rate, and at the same time a constant stress ratio.

regulation. As a consequence the programmed way of loading is impossible when the stress ratio is about equal to the ratio of Poisson (see 5.4). For testing in such a way it is necessary to measure the load and the deformations in an electrical way. The load can be measured with a dynamometer and the deformations with the help of strain gauges of a sufficient length. The last method has the disadvantage that with biaxial tests it is very difficult to do measurements in the direction normal to the plane of loading and also a regulation and measurement of the deformations is impossible when cracks occur. For this purpose a removable, electrical instrument for measuring deformations (referred to hereafter as the strain reader) was developed (fig. 15), which can still functionate when a crack occurs.

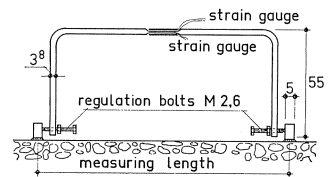


Fig. 15. Removable, electrical instrument for measuring deformations (strain-reader).

The working method of the strain reader is as follows: when the length of the concrete changes a curvature occurs in the thin part of the strain reader. Strain gauges are glued to both sides of this thin part. The difference of these strains is a yardstick for the curvature and also for the deformation of the concrete. There exists a linear relationship between this curvature and the deformation of the concrete. Only with great deformations (about 2 mm) does a deviation of this linearity occur because the lever (this is the distance between the thin part of the strain reader and the measuring

points on the concrete) will change. The accuracy of the strain reader depends on the thickness of the thin part in comparison with the other sizes and is about $0,5 \times 10^{-3}$ mm with a measuring length of 10 cm.

To obviate excentricities in loading and in concrete the four strain readers in the three principal directions are connected in such a way that the mean value is measured immediately and also the regulation of the constant strain rate is done on this mean value.

2.2.b Influence of the way of loading on the bearing capacity of structures

As has already been mentioned, the way of loading and the speed of loading has a great influence on the stress-strain curve of concrete and on the bearing capacity of concrete structures. At a preliminary investigation, which had the main purpose of testing the testing apparatus described above, the uniaxial stress-strain curve of concrete (the concrete mixes is given in 4.1) is estimated at different rates of straining and loading.

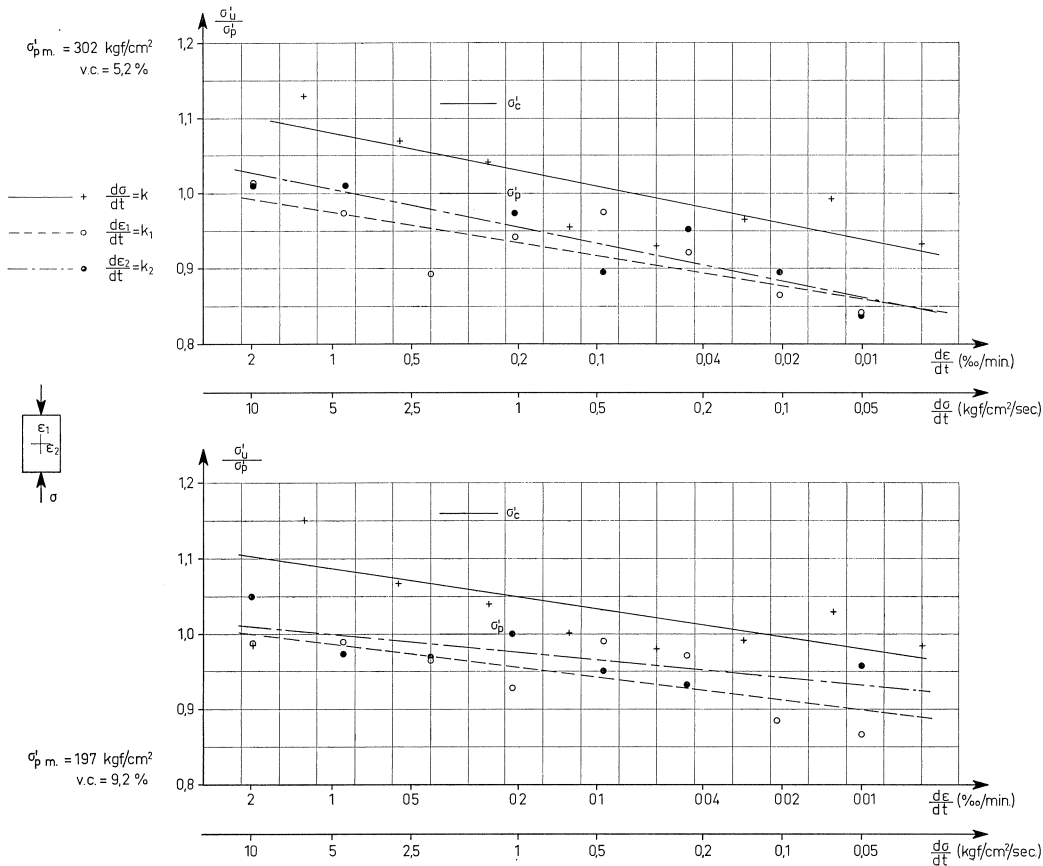


Fig. 16. The ultimate uniaxial compressive load as a function of the way of loading.

These rates were chosen in such a way that the ultimate load was reached within a maximum of 3 hours (in order to be able to speak about tests of short duration). The specimens were stored in a room with a humidity of 95% and $t = 21^{\circ}\text{C}$ for 26 days after mixing.

The specimens were tested after 27 or 28 days of hardening. From fig. 16 it can be seen that the ultimate load is a logarithmic function of the speed of loading (this is also found with tests on metals with a low melting point, such as copper, tin, lead, etc. [46]). This figure also shows that within a duration of the test of 3 hours already a difference in "strength" occurs of about 30%.

The prism strength estimated in the conventional way in a conventional testing frame proved to be lower than the uniaxial strength estimated with the same rate of loading. The prism strength proved on the contrary to be more equal to the uniaxial strength by maintaining a constant strain rate in the lateral direction. An explanation for this difference is that maintaining a constant rate of loading in a conventional testing frame is impossible, because the pumps cannot give enough oil per unit of time to maintain this constant speed. As a consequence the constant rate of loading will change during the test in a constant strain rate. The cube strength was higher than the uniaxial ultimate load, in spite of this difference in loading frame. The restraining action of the solid bearing platens is an explanation for this difference.

There was a sudden and explosive rupture in all tests in which the load was raised

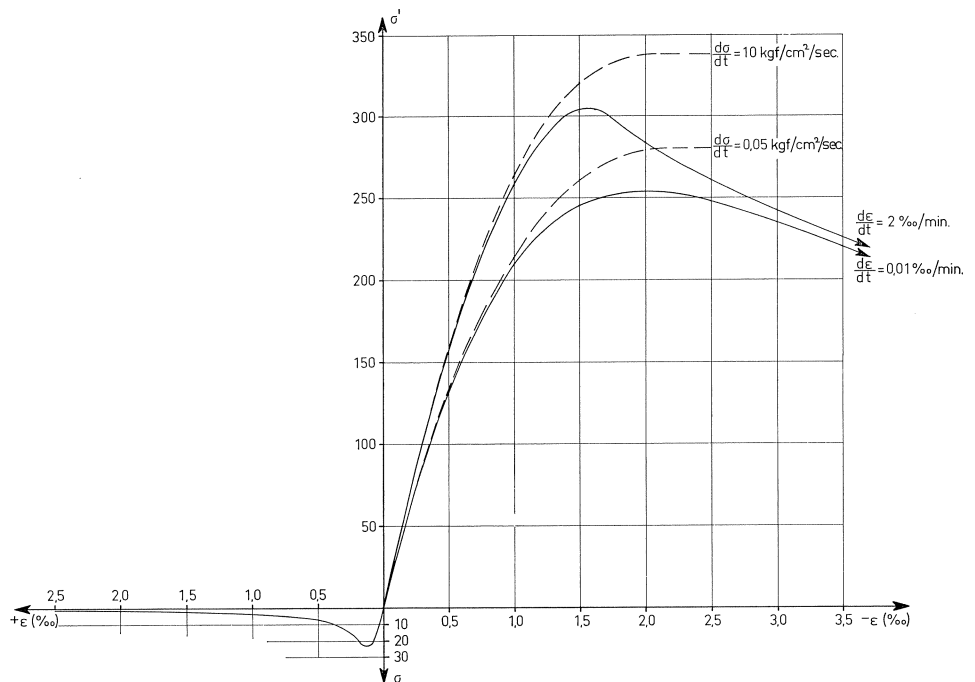


Fig. 17. The influence of the way of loading on the shape of the uniaxial stress-strain curve.

with a constant rate of loading. Such a rupture did not occur by maintaining a constant strain rate. Some of these tests were carried out up to an axial deformation of $6^{\circ}/_{00}$. At this deformation the stress appeared to be about 50% of the ultimate load. From fig. 17 it can be seen that, as has already been explained, the shape of the stress-strain curve is also influenced by the way of loading. As can be seen from the following it is necessary to have a lot of these diagrams to estimate the influence of these differences on the bearing capacity of structures.

With a 4-points bending test on a reinforced concrete beam, every fibre undergoes a different strain rate in the middle part of the beam. Suppose that the neutral axes does not change and also that flat sections remain flat after bending, then the most compressed fibre will undergo a certain strain rate but the strain rate of the neutral fibre will be zero. Every strain rate of every fibre can easily be calculated from the above-mentioned assumptions. As a result, one stress-strain curve belongs to every fibre, which curve depends not just on the way of loading but also on the type of cement, the amount of cement, the module of elasticity of the aggregate, the amount of aggregate, the temperature, the humidity, the age of loading, etc. [44, 47, 48]. To calculate a beam in this way there are not sufficient stress-strain curves available. For this reason in the next calculation of the influence of the way of loading on the bearing capacity of structures, two extreme curves ($d\sigma/dt = 10 \text{ kgf/cm}^2/\text{sec}$ and $d\varepsilon/dt = 0,01^{\circ}/_{00}/\text{min}$) will be compared directly.

A calculation is made of the bearing capacity of a column with constant starting excentricity over the length of the column. Columns with a square section and different slenderness and different amounts of reinforcement are investigated. The second order effect is taken into account. The calculation is made with the help of a method described in [49]. The method is based on the following assumptions:

- flat sections remain flat
- steel behaves in an elastic-plastic way with $\sigma_e = 4000 \text{ kgf/cm}^2$
- the influence of the shear stresses is neglected
- the column is straight before the load is applied
- the deformations of the column are small. As a result every section can be calculated with an equal normal force.

The ultimate bearing capacity of the column is attained when the maximum compression strain is reached in a section or when a column becomes unstable before reaching this maximum strain of concrete.

The calculated values are given in fig. 18a, b, c. From this figure it can be seen that within a duration of 3 hours the ultimate bearing capacity of the column is strongly influenced by the way of loading. With increasing slenderness the influence of the shape of the stress-strain curve under compression decreases because instability determines the collapse of the column. With increasing slenderness instability occurs under lower compression strains and the difference in the shape of the stress-strain curves diminish when the stresses decrease. The influence of the amount of reinforce-

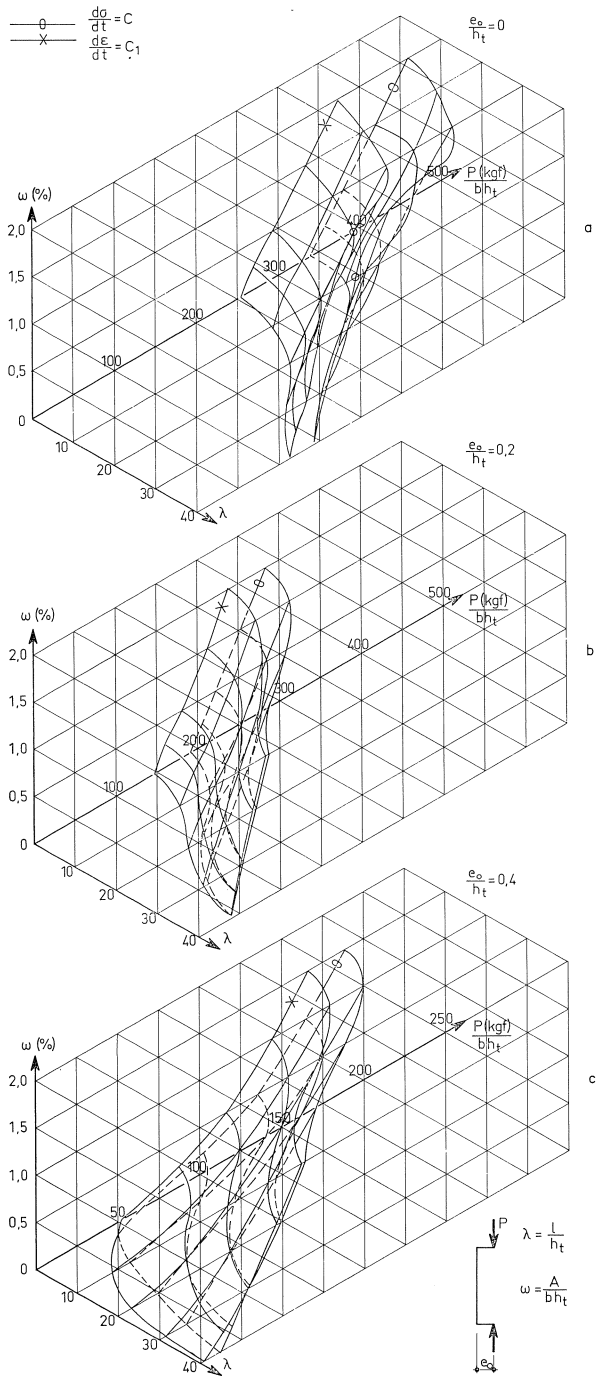


Fig. 18. The influence of the way of loading on the ultimate load of columns.

ment and the probability to withstand tensile stresses increase with increasing slenderness.

In general it can be concluded that a good calculation of the bearing capacity of a column is possible only when the chosen stress-strain curve is in agreement with reality. For this purpose research is necessary not only on separated columns but also in combination with column-beam-slab connections.

In general it is concluded from bending tests to the bearing capacity of reinforced concrete slabs that the shape of the stress-strain curve has not a great influence. A description is given in [50] of an investigation into the influence of a very fine spaced reinforcement on cracking, stiffness and strength of slabs loaded by a constant moment of bending. The testing frame was made in such a way that normal forces resulting from friction could not be introduced. The differences in properties found in the investigation could only be introduced by way of reinforcing. It was found that the stiffness in the cracked stage of the slabs (with an equal amount of reinforcement) increased when the distance between the separated bars of the reinforcement decreased and the amount of bars increased. A maximum increase of about 40% was found. Visual observation showed that in conventional reinforced slabs the cracks in the stage of rupture passed into the neutral axes but the cracks in the slabs with fine spaced bars did not pass the first layer of reinforcement in spite of a tension strain of about 1,5‰. This means that a great part of the concrete tension zone still bears the loading. In this kind of slabs it is possible for the concrete to reach the descending part of the stress-strain curve under tension. Via shearing stresses the concrete can transmit tension stresses to the steel. This is only possible when the bars are placed close to each other and the bond strength between the concrete and the steel is good, so that with thin bars this is more likely to happen as a results of the favourable ratio between circumference and surface.

Also in a tension test loaded by a constant strain rate the descending part of the stress-strain curve can be attained, and cracks can be seen only in the case of great strains. With the aid of the stress-strain curve given in fig. 17 the slabs described in [50] are calculated. The strength of lightly reinforced slabs appeared to be about 20% higher in comparison to conventional reinforced slabs when no cracks occur in the tension zone. This increase in strength is smaller when the amount of reinforcement increases. Furthermore, it was possible to demonstrate the increase in bending stiffness. The great differences in strength and stiffness from the tests could not be affirmed completely: an explanation for this could be the difference in the concrete mixes and the hardening circumstances of the slabs investigated and the specimen for estimating the complete stress-strain curve under tension. The slabs hardened under a higher humidity and the maximum size of the coarse aggregate was 11,2 mm.

2.3 *Variables in the biaxial testing program*

Here we investigate the three regions in a biaxial state of stress, namely compression-compression, compression-tension and tension-tension. The region of tension-tension

is less interesting for the construction of concrete. For this reason a few tests are carried out in this region as compared to the number of tests carried out in the other two regions, which are considered to be of equal importance. Till now it was usual to test three or four stress ratios in each region. From each ratio some tests were carried out and then a mean value for that stress ratio was calculated. However, it seems to be better to test each specimen with another stress ratio to get a better insight into the influence of the second stress on the deformations and failure of concrete under biaxial loading. By using servo-hydraulic loading apparatus it was possible to investigate almost every stress ratio. The stress ratios which were maintained during the whole test are given in fig. 19.

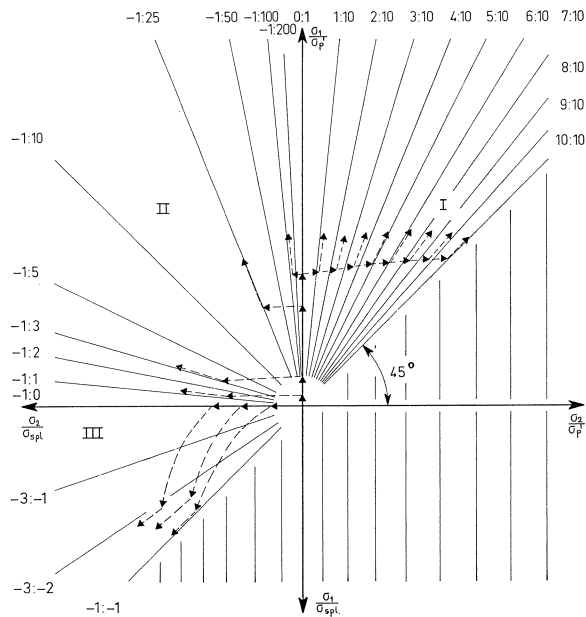


Fig. 19. The loading paths (---) and constant stress ratios (—) which were followed.

From the previous tests (described in appendix I) it cannot be seen whether a certain history of loading influences the deformations and the ultimate load under biaxial loading of concrete. To investigate this possible influence some tests are carried out in which the load was increased along different loading paths (see fig. 19).

The way of loading has a great influence on the properties of concrete under uniaxial loading, as mentioned already in 2.; it is not known whether the influence also exists in biaxial loading. Many methods of investigating this have been used in the past years but a direct comparison of these results is very difficult. The load is raised by a constant strain rate in order to fix the duration of the test beforehand and also to estimate the top of the stress-strain curve independently of external influences. The direction in which the constant strain rate was maintained and also the strain

rate itself were varied (such that the shortest test was as long enough for reliable measurements and the duration of the longest test had a maximum of about 8 hours).

All the above-mentioned tests were carried out with the rod-platens. Some tests were also done with the massive platens in order to provide a possible explanation for previous test results and also to investigate the influence of the solid loading platens.

Table I gives a survey of all the tests.

Table I: Survey of the variables in the biaxial testing program

Concrete quality	Strain rate	Direction of constant strain rate (fig. 2)	Testing period	Loading platen	Remarks
K250	1 ⁰ / ₀₀ /100'	Region III: σ_2 II: σ_2 I: σ_1	22-4 /25-4 5-9 /24-9 15-12/29-12	rod	all stress ratios
K250	1 ⁰ / ₀₀ /100'	III: σ_2 II: σ_2 I: σ_1	14-4 /18-4 26-9 / 7-10 30-12/ 7-1	massive	some stress ratios
K350	1 ⁰ / ₀₀ /100'	III: σ_2 II: σ_2 I: σ_2	7-5 /10-5 25-6 /21-7 4-11/13-11	rod	all stress ratios
K350	1 ⁰ / ₀₀ /100'	III: σ_1 II: σ_1 I: σ_1	21-5 /23-5 12-8 /27-8 20-10/ 3-11	rod	all stress ratios
K350	1 ⁰ / ₀₀ /5'	III: σ_2 II: σ_2 I: σ_1	16-5 /20-5 22-7 / 7-8 17-11/ 2-12	rod	all stress ratios
K350	1 ⁰ / ₀₀ /100'	III: σ_2 II: σ_2 I: σ_1	28-5 / 4-6 28-8 / 4-9 3-12/12-12	rod	loading path

3 Testing frame

3.1 The transmission of the external load by rod-platens

The difficulty in constructing rod-platens is the opposing condition which have to be fulfilled. On the one hand the separate rods have to be sufficiently strong and stable but on the other hand they have to be as flexible as possible to follow the deformations of the concrete without introducing important secondary stresses. The calculation of the rod-platens is based on a cube strength of 350 kgf/cm² after 28 days of hardening. The available vessels for the described tests had a maximum capacity of 100 tf. The sizes of the specimen used in the investigation are 17,7 × 17,7 × 12,6 cm in order to get reliable measurements of the strains (see fig. 20) and also to have a minimum size of the specimen of at least 3 to 4 times the maximum size of the coarse aggregate (32 mm). With these sizes of the specimen and with the available vessels it was possible to achieve an increase of 50% in strength as compared to the uniaxial

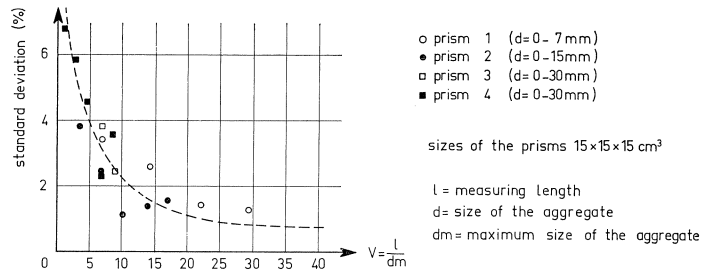


Fig. 20. Standard deviation in comparison to the mean value of the strain, dependent on the ratio l/dm [51].

strength. The rod-platens therefore had to transmit a normal force of 100 tf on a section of $17,7 \times 17,7$ cm. The calculation of the rod-platens is possible only when the possibility of distortion of the rods on the surface of the concrete is known. There are two extreme possibilities: effectively fixed or effectively pinned. Because the real properties are unknown, and because the rod-platens are very expensive the most unfavourable possibility is assumed in the calculation. At the other side of the rod-platens the separate rods are effectively fixed in a solid steel platen (see fig. 21). The calculation of the rod platens is given in appendix II.

From these calculations a rod-platen is chosen consisting of $4 \times 4 \times 100$ mm single rods. The space between the single rods is 0,2 mm. The rods are made of steel C35 with a tensile strength of about 55 kgf/mm². Every loading platen consists of 1260 of these rods (see fig. 21). Every single rod has to transmit a maximum normal force of 79,3 kgf.

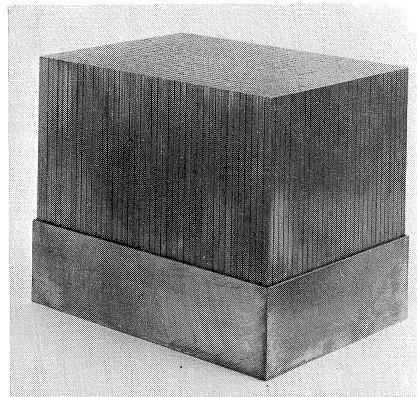


Fig. 21. Rod-platen.

From the previous tests in 1.3 and also from the calculation carried out with the help of the finite element method, it can be seen that a great part of the external load at biaxial tests is borne by the adjacent platens. This bearing of the load is strongly reduced when the load is transmitted to the specimen by rod-platens. The maximum bearing force of the adjacent platens can be calculated from $H_{tot} = 2 \cdot \frac{1}{4} m \cdot n / b^2 \cdot H \sim$

950 kgf (see appendix II). The minimum compressive force applied on the specimen in the region of biaxial compression will be about $0,85 \times 250 \times 12,6 \times 17,7 \sim 47.500$ kgf (cube strength 250 kgf/cm^2). Consequently, the stresses in the specimen will be about 2% lower than the stresses calculated directly from the external force. The separate rods will introduce a concentrated loading on the specimen. The maximum stress will be 9% greater than the mean stress and at a distance of about 1 cm of the loading surface the stress distribution will be uniform [53].

The bending which occurs in the single rods will be greater according as the distance from the middle of the specimen increases. As a result of this bending the length of the rods will be smaller in the direction of the load and a more concentrated loading will occur (compare 1.3 and fig. 7b). With an expected maximum compressive strain of the concrete of 3‰ this difference of length between the rod placed in the middle of the specimen and placed at the edge of the specimen will be about $3,5 \cdot 10^{-4}$ mm. To get a uniform loading the middle of the specimen has to deform about $7 \cdot 10^{-4}$ mm more than the deformation of the edge of the specimen. This will give a difference in stress of about

$$\Delta\sigma = 3 \cdot 10^5 \times \frac{7 \cdot 10^{-4}}{177} \sim 1 \text{ kgf/cm}^2,$$

which can be disregarded.

The tests described in 2.2.b were carried out with the rod-platens. From measurements in the middle part of the specimen and in the edges of the specimen (lateral

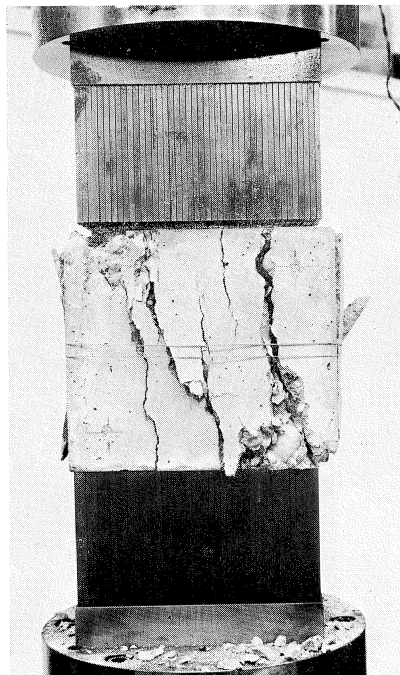


Fig. 22.
Mode of failure under
uniaxial compressive
loading.

and axial) it could be seen that the deformations were uniformly divided over the specimen so that the influence of the rod-platens on the deformations of the specimen could be disregarded. This could also be seen from the cracking of the specimen (see fig. 22).

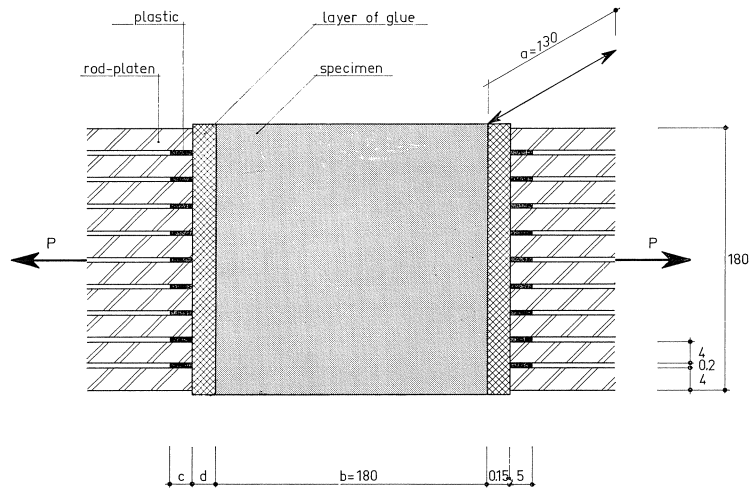


Fig. 23. Layer of glue for the transmission of tensile forces.

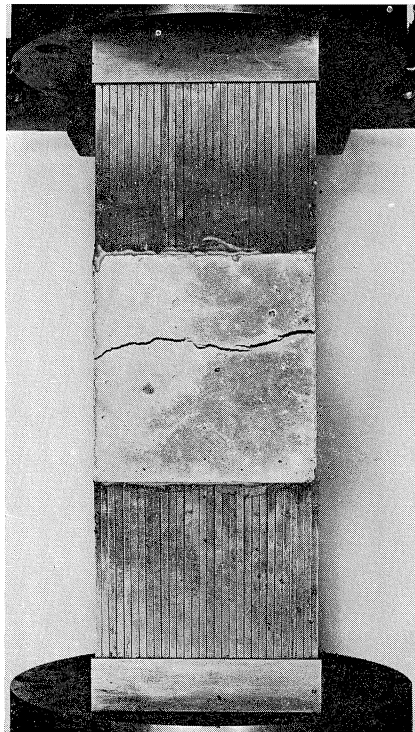


Fig. 24.
Mode of failure under uniaxial tensile loading.

The rod-platens must be glued to the specimen for the transmission of tensile forces. In order to maintain the “elastic working” of the rod-platens this layer of glue has to be as thin as possible and the separated rods may not be glued to each other. The layer of glue used had a thickness of about 0,15 mm and a tensile strength of 100 kgf/cm². The space between the separated rods was filled up with plastic ($E = 200$ kgf/cm²) over a length of about 5 mm (see fig. 23). It could be calculated that about 1% of the external force was borne by this connection between the rod-platens and the specimen. The results of some preliminary tension tests have also shown the good effects of this connection (see fig. 24).

3.2 Loading frame

One of the most important factors affecting the strength and the shape of the stress-strain curve is the method by which the load is applied to the specimen. Whether or not the ends of the specimen have to be effectively pinned or effectively fixed depends on the heterogeneousness and the slenderness of the specimen, the lateral stiffness of the loading frame, the possible misalignment of the specimen and the unparallel loading areas of the specimen [54]. If the specimen was homogeneous and the force co-linear with the axis of the loading frame there would be no difference in properties by using fixed or pinned ends of the specimen. The induced state of stress in the specimen when the material is not homogeneous is given in fig. 25.

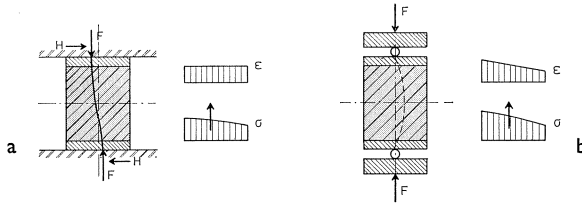
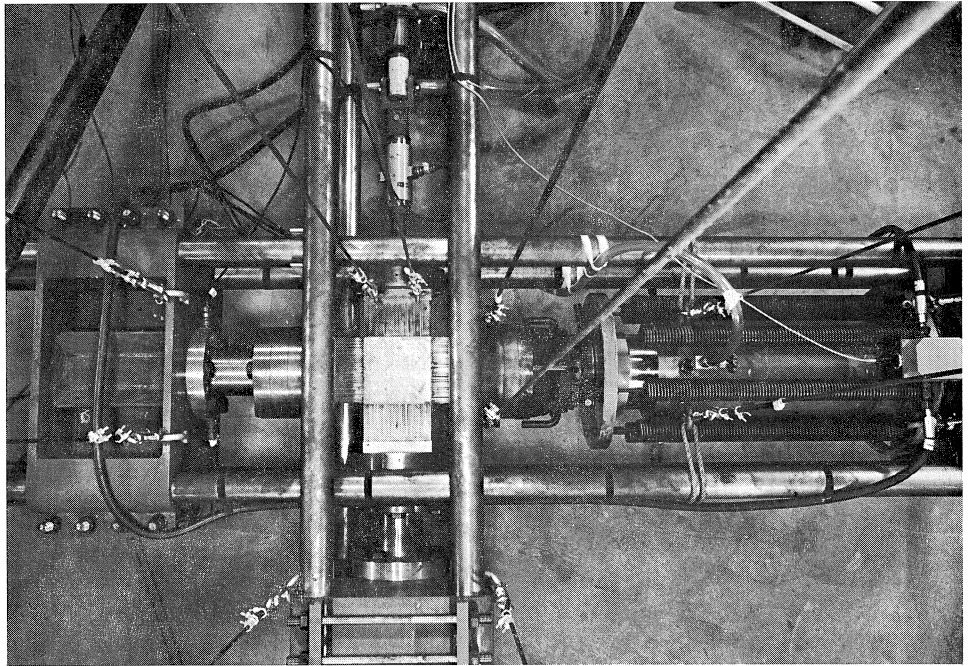
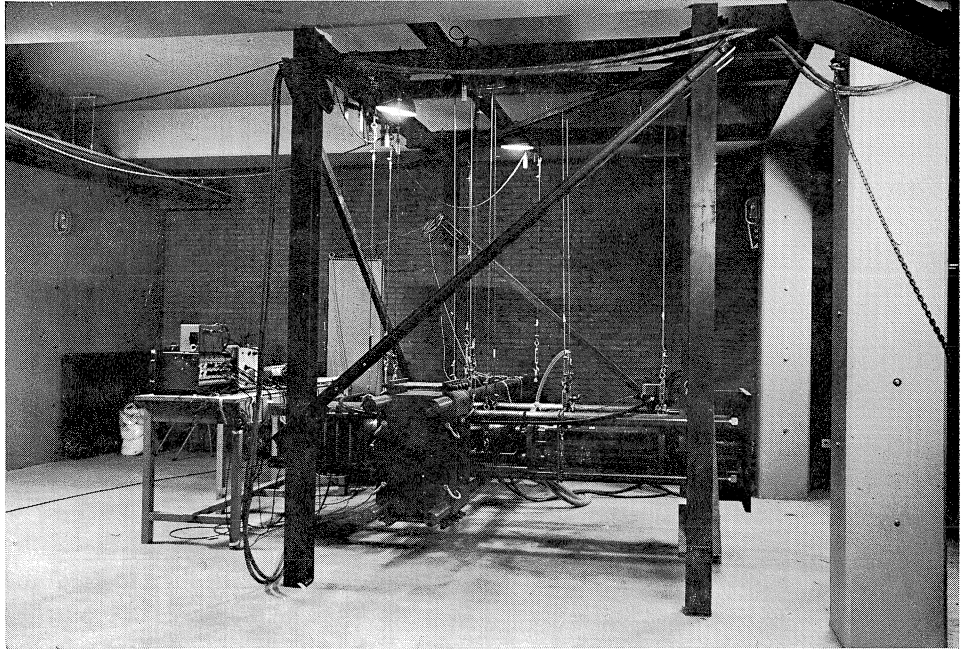


Fig. 25. Influence of effectively pinned or effectively fixed ends of a specimen on the state of stress in the specimen.

The method with fixed ends (fig. 25a) causes the condition that every axial section undergoes the same deformation. Consequently the stress in every section depends on the properties of the section and at the same time lateral forces will be introduced. With the method shown in fig. 25b the line of action of the stresses in every section is estimated by the pinned ends, and lateral forces cannot occur. When one side of the specimen is pinned and the other side fixed, then the stresses and deformations in every section will be between the above-mentioned extremes. In this case it is difficult to define the state of stresses and deformations at which the specimen collapsed. This last method seems to be unsuitable for testing materials.

From the point of view of the testing technique, it is less suitable to have both ends fixed because in that case there exists the possibility of lateral forces in the vessel which will raise the friction in the loading system and consequently maintaining a



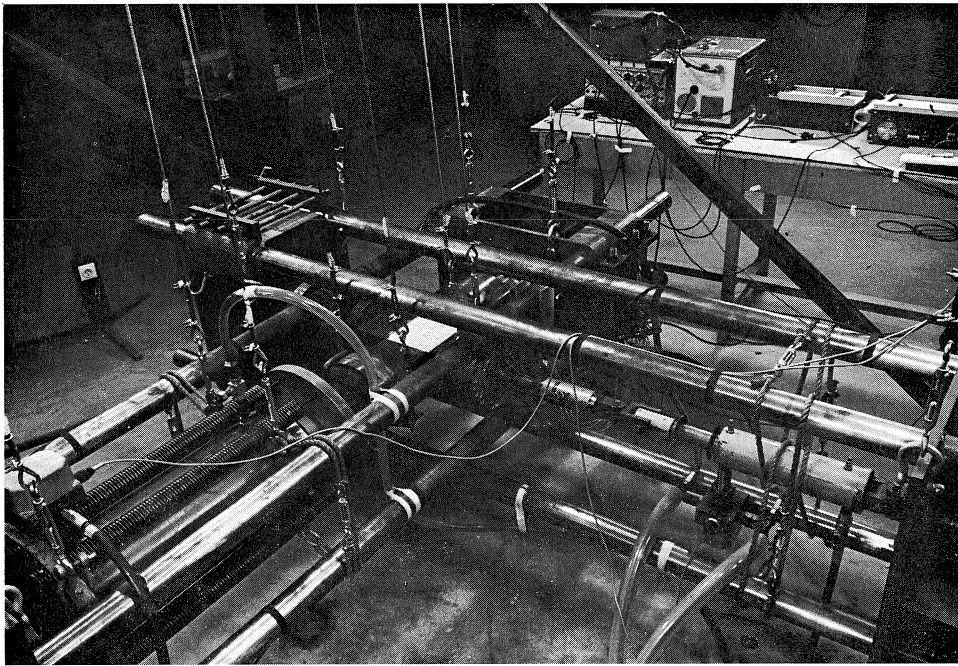
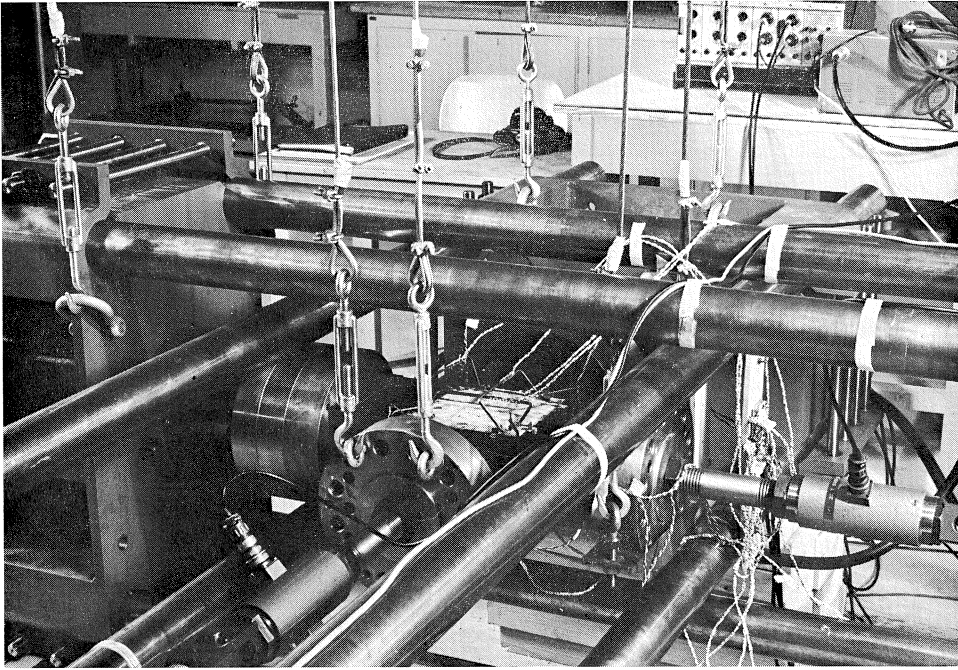


Fig. 26. Testing frame.

constant strain rate is very difficult. Also with biaxial tests it can be very important to have both ends pinned. When a shearing mode of failure occurs in such a test the fixed ends of the specimen could give an apparent raise in strength by a restraining action of the ends of the specimen.

With uniaxial tests and also with biaxial tests it is very important that the centroid of resistance of the specimen is co-linear with the line of action of the applied force. With uniaxial tests for this purpose the specimen has to be placed centrally in the loading frame and when this frame is symmetric in the lateral direction this centric placing is maintained during loading. With biaxial tests the specimen has also to maintain a centric loading in the second direction. For this purpose a completely symmetrical testing frame is most suitable (four identical vessels, two identical loading frames, etc.).

Because only two compression vessels and two tension vessels were available for the tests described, the testing frame could not be a symmetrical one and as a result there had to be taken into account a relative displacement of the specimen with respect to the loading frame in the second direction. The testing frame is constructed in such a way that the two loading frames can move independently of each other in order to maintain the best possible centric loading during the test. This is done by hanging the two loading frames on long, thin cables. As a result of this it is possible to follow the displacement of the specimen whereby secondary stress of the same order as the weight of the specimen occurs (see fig. 26). This testing frame also provides a symmetrical deformation of the specimen as mentioned in 3.1 and fig. II-1c.

3.3 *Scheme of measurements*

The forces in both directions are measured by dynamometers. The deformations in the three principal directions are measured by strain readers (see fig. 15). The measuring length in the direction normal to the plane of loading is fixed by the sizes of the specimen (12,6 cm). The deformations in this direction were measured directly as a mean value of the four strain readers placed in the 4 edges of the specimen. The measurement points on the concrete, necessary for the strain readers in this direction are also used for the strain readers in both directions of loading (measuring length 13,7 cm). By this the accuracy of the measurements in the three directions is almost equal to each other, so that a comparison of the strains in the principal directions is possible (see fig. 27). In the direction in which a constant strain rate was maintained the strain readers are connected in such a way that the mean value of the four separated deformations can be measured immediately.

Perpendicular to this direction in the plane of loading on both sides of the specimen, the mean values of the deformations of two separated strain readers were measured immediately, so that it was possible to check the centricity of loading.

In contradistinction to the above-mentioned measuring length there was, however, a different measuring length for compression-tension and tension-tension tests in the direction of the tensile force. It can be expected that perpendicular to the direction

of the tensile force only one crack occurs. The situation of this crack depends on the heterogeneousness of the material. This crack will occur inside the specimen before the top of the stress-strain curve is reached. It is impossible to come over the top of the stress-strain curve when this crack occurs outside the measurement length.

For this reasons the deformation of the entire specimen was measured by fixing the measurement points to the rod-platens. Hereafter, the deformations of the layers of

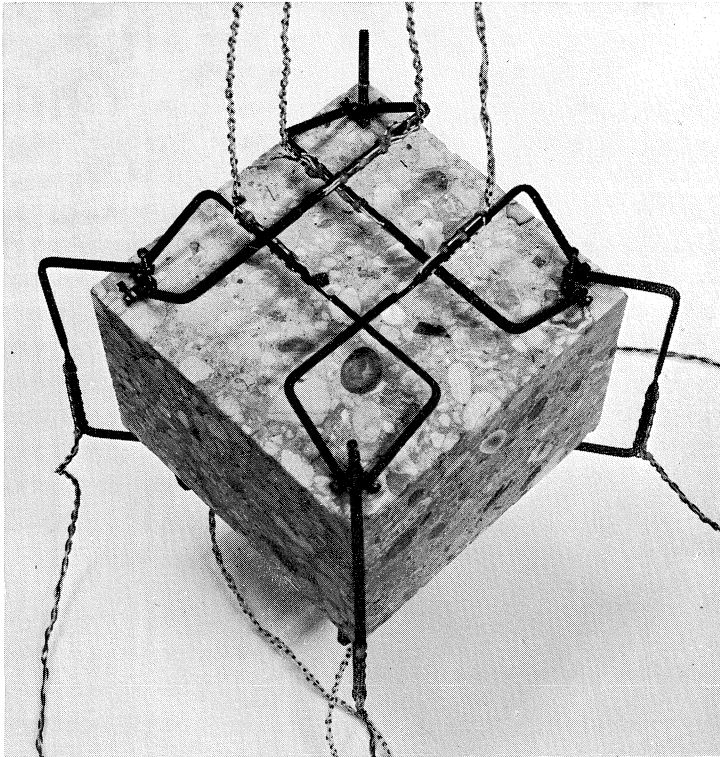


Fig. 27. Placing of the strain readers on the specimen.

glue were measured and the deformation under a certain state of stress was apparently higher. This mistake is, however, relatively small and will become smaller as the stress rises. At a low stress, when the concrete still behaves linear-elastically, this mistake can be calculated (see fig. 23):

the maximum expected mistake will be $\frac{\Delta l_g}{\Delta l_c} \times 100\% \sim 1\%$

deformation of the concrete $\Delta l_c = \frac{\sigma}{E_c} \times 177 \text{ mm}$

deformation of the layers of glue $\Delta l_g = 2 \times \frac{\sigma}{E_g} \times 0,15 \text{ mm}$

The apparatus used for regulation of the constant stress ratio and the constant strain rate and the measurement apparatus are shown in fig. 28.

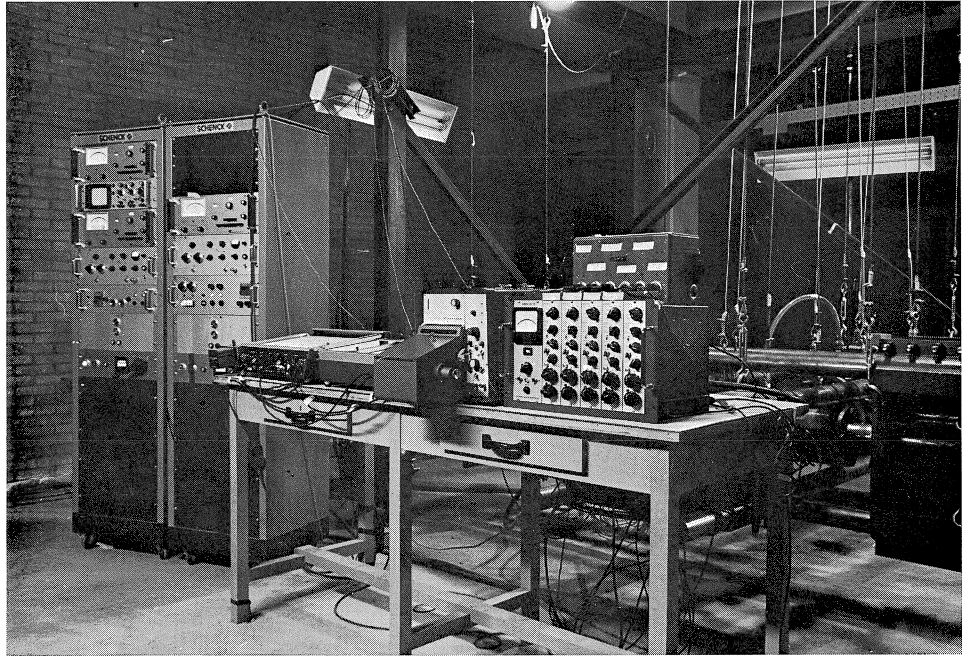


Fig. 28. Apparatus used for regulation and measurements.

4 Concrete mixes and manufacture of the specimen

As has already been mentioned, two qualities of concrete were investigated, namely K250 and K350 (cube strength after 28 days of hardening).

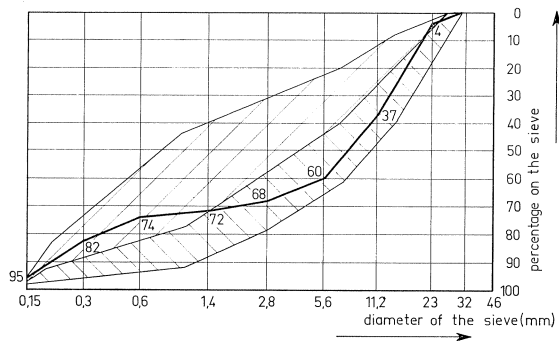


Fig. 29. Sieving curve for the qualities of concrete K250 and K350.

The concrete contained gravel aggregate with a maximum size of 32 mm. The sieving curve for both qualities of concrete is given in fig. 29. For 1 m³ of concrete, with an expected air content of 1½%, the used amounts of aggregate, cement and water are mentioned in table II:

Table II: Concrete mixes

	K250	K350
aggregate (sand-gravel)	1999 kg	1899 kg
cement (P.C.-A)	220 kg	300 kg
water	160,6 L (w/c-ratio = 0,73)	165 L (w/c-ratio = 0,55)

It appeared from previous tests that at the finished side of the specimen (with a skin of cement) the deformations can be twice as much as the deformations at the side of the mould, and also the cracks were seen in an earlier stage. This difficulty disappears by manufacturing a specimen of larger sizes and afterwards sawing from each side of the specimen a slice of about 2,5 cm. This sawing of the specimen was also the only possible way of getting a good layer of glue of sufficient strength between the specimen and the bearing platens. A more homogeneous specimen is also the result of this sawing. The loading surfaces of the specimen were polished after sawing to avoid a concentrated loading by irregularities on these surfaces.

The specimens for the biaxial tests and some specimens to control the quality of the concrete (cubes, 20 × 20 × 20 cm and prisms, 10 × 10 × 30 cm) were manufactured in an identical way. About 2 hours after pouring the concrete, the specimens were covered by plastic. As a result the humidity was about 95% and the temperature about 20° C. The further treatment of the specimen is given in table III.

Table III: Treatment of the specimens, cubes and prisms

week 1		week 2				week 3				week 4				week 5			
pouring	dismantling																
95%–21° C		97%–21° C												testing			
first half of the specimens 43%–21° C																	
second half of the specimens 43%–21° C																	

5 Test results

5.1 Properties of the concrete

In every batch 8 cubes and 6 prisms were manufactured to estimate the quality of the concrete of the specimens which were tested respectively, after 26, 27, 28 days of

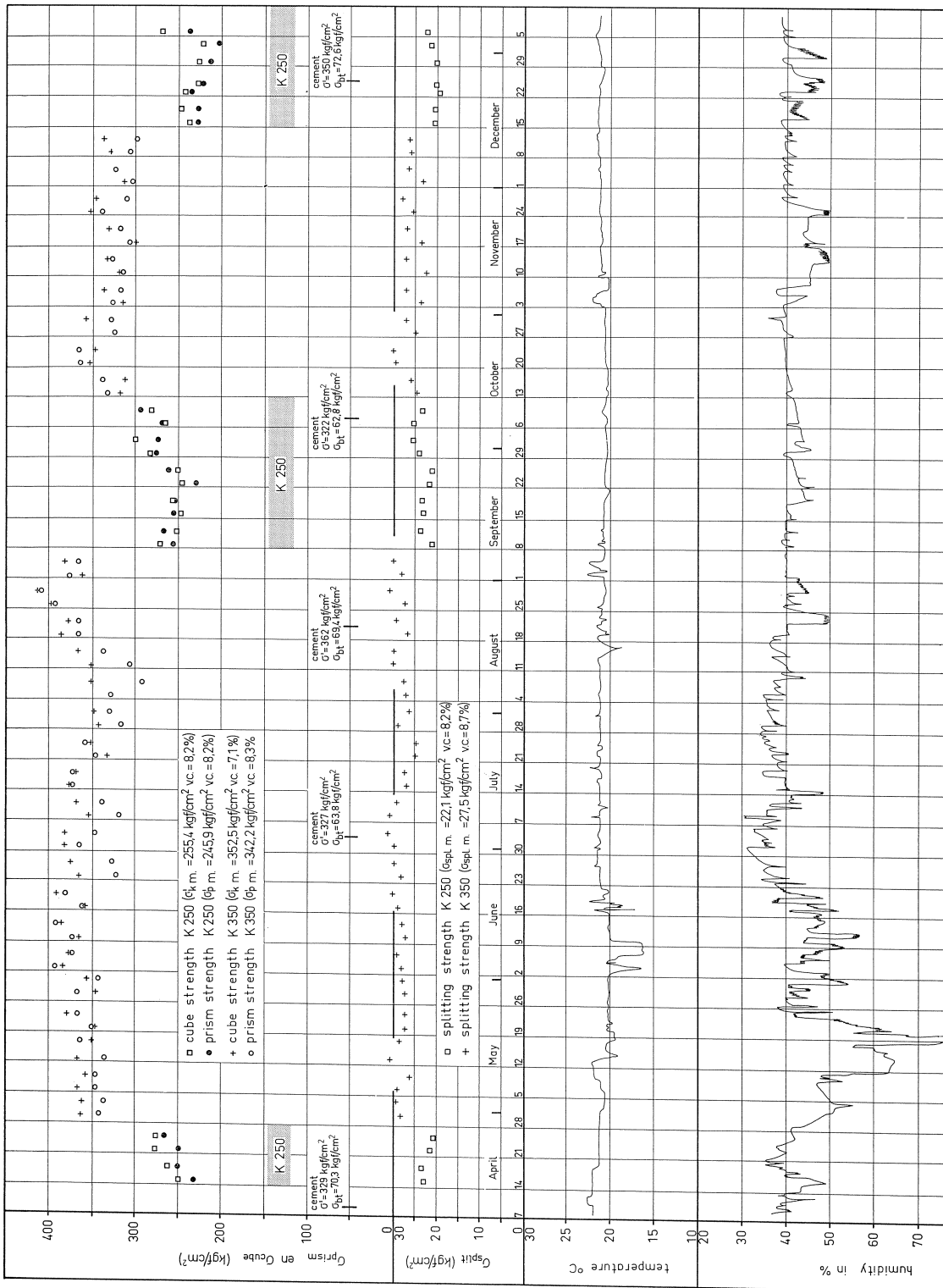


Fig. 30. Properties of the concrete and the hardening circumstances.

hardening and after 29 and 30 days of hardening. In a conventional testing frame compression tests were carried out on 2 cubes and 3 prisms and a splitting test on 2 cubes, respectively after 26 and 29 days of hardening. With the compression tests an effort was made to maintain a constant rate of loading of about 2,5 kgf/cm²/sec and with the splitting test a rate of loading of about 500 kgf/sec. The mean values of the compressive strength on cubes and prisms and of the splitting strength after 26 and 29 days of hardening are given in fig. 30. The deviation and the coefficient of variation of the several values of strength given in this figure are estimated by taking all test results into account. This figure also gives the humidity and the temperature of the room in which the specimens were stored for about 1 week for testing. The great deviation in temperature and humidity during the first period of testing (in which period the tests in the region of tension-tension were carried out) is a result of malfunctioning of the air-conditioning. This figure also gives the norm strength of the cement.

Figure 30 shows a relative high prism strength in comparison with the compression strength for both qualities of concrete (about 96%). In the previously described preliminary investigation (2.2.b and fig. 16) a mean value of about 0,86 was found for this factor, while the cube strength was about 8% lower. In both investigations the same mixture of concrete was used. The only difference was that in the definite investigation the specimens were stored during the last week of hardening in a room with a humidity of about 45% while the specimens in the preliminary investigation were stored during 26 days of hardening in a room with a humidity of 95%. The difference in strength has to be a result of the humidity of the specimens. The tests described in [58–60] proved that the humidity of a specimen has a great influence on the strength. It appeared that completely dried specimens had a strength of about 45% higher than completely saturated specimens. This can be the explanation for the difference in cube strength in the preliminary investigation and the biaxial investigation. Also the difference in sizes of the cubes and prisms can cause a difference in humidity of the specimen and as a result give a relatively higher strength of

Table IV: Comparison of the properties of the concrete after respectively 26 and 29 days of hardening

		26 days	29 days	σ_{29}/σ_{26}
K250	σ'_p mean	242	250	1,034
	coeff. of var.	8,1%	10,9%	
	σ'_c mean	255	256	1,005
	coeff. of var.	7,2%	9,3%	
	σ_{spl} mean	21,9	22,2	1,014
	coeff. of var.	8,3%	8,3%	
K350	σ'_p mean	341	343	1,007
	coeff. of var.	8,2%	8,4%	
	σ'_c mean	348	357	1,026
	coeff. of var.	7,5%	6,4%	
	σ_{spl}	27,0	27,9	1,033
	coeff. of var.	9,7%	7,3%	

the prism. The tests in the biaxial investigation were not carried out on specimens with the same age (between 26 and 30 days of hardening). This difference of age can be disregarded, as is shown in table IV.

5.2 Failure modes

Independent of the way of loading and also independent of the quality of the concrete the same crack pattern was observed at a certain stress ratio. Dissident failure modes were observed when the load was transmitted to the specimen by solid loading platens.

Region of tension-tension (III)

In this region at every stress ratio one crack occurred perpendicular to the largest tensile force and perpendicular to the free plane of the specimen (fig. 31). The situation of the crack appeared to be arbitrary. In the fracture only 10% of the coarse aggregate was broken, while at the other particles the fracture was situated in the boundary between mortar and aggregate. The cracks could be seen with the naked eye when the tensile strain was about $0,15\%$. It could also be ascertained that at the place of fracture the rods of the adjacent rod platens were separated from each other more than the other rods of these loading platens.

Region of compression-tension (II)

The above-mentioned failure mode did not change as long as the tensile stress was less than $1/30$ th of the compressive stress (fig. 31). For larger compressive stresses numerous cracks were observed perpendicular to the tensile force and perpendicular to the free plane of the specimen. When the stress ratio was about $-1 : 100$ or more numerous cracks occurred parallel to the free plane of the specimen. In that case several micro columns occurred parallel to the direction of the compressive force. The distance of the cracks in both directions was about 3 to 4 cm (maximum size of the aggregate was 32 mm!). Only a few of the coarse particles in the fracture were broken.

Region of compression-compression (I)

Up to a stress ratio of about $3 : 10$ the same failure mode was observed as described in region II with relatively high compressive stresses. Between the stress ratios of $3 : 10$ to $10 : 10$ only cracks parallel to the free plane of the specimen were observed (fig. 31). The distance between the cracks was 3 to 4 cm and only a few coarse particles were broken. When the load was transmitted to the specimen by rod platens, at any stress ratio the fracture was perpendicular to the direction of the greatest tensile strain. The shearing mode of failure, usually observed in uniaxial compression tests could not be affirmed.

From the difference in modes of failure in the three regions of a biaxial state of stress by using the rod platens or solid bearing platens (see fig. 31) can be concluded that by using solid platens the bearing of load by the adjacent platens already mentioned in 1.3 has influenced the test results.

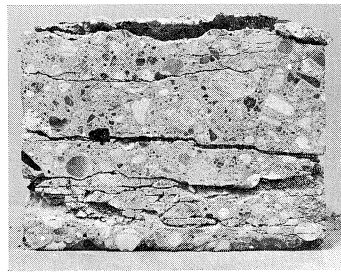
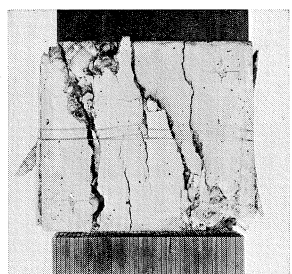
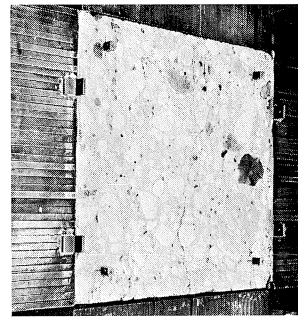
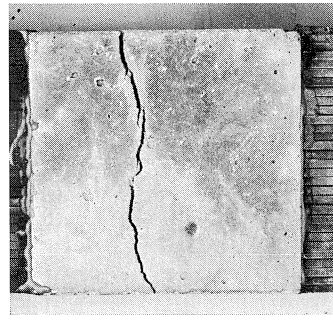
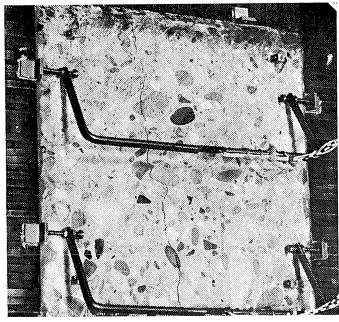
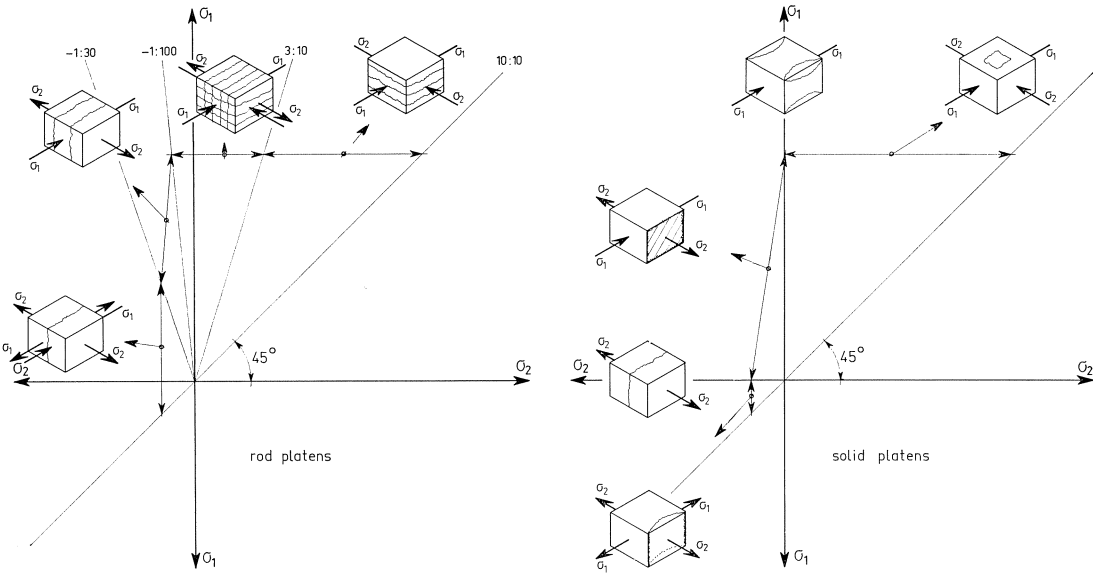


Fig. 31. Failure modes.

5.3 Ultimate load

All strength data are reported as fractions of the prism strength.

Region of tension-tension:

In fig. 32 a–e the ultimate load is given as a function of the stress ratio. In spite of a little influence of the compressive stress compared to a high tensile stress in the region of compression-tension (see hereafter), the uniaxial tensile strength appeared much smaller than the tensile strength estimated by the splitting test.

When it is assumed that the concrete behaves linear-elastically, then it can be calculated that in the critical zone of a specimen loaded by a concentrated force the compressive stress is about three times the tensile stress. The great difference in uniaxial tensile strength and splitting strength can be explained by:

- The line of action of the concentrated force in a splitting test stipulates the plane of fracture beforehand. The properties of the concrete in this plane determine the strength. On the other hand with the uniaxial tension tests the weakest plane of the specimen will cause the ultimate fracture.
- From the above-mentioned results of the biaxial tests it can be seen that a great part of the coarse aggregate in the plane of fracture was not broken. For this reason the plane of fracture in a splitting test does not occur in the plane of action of the load, but in several stages closer to the outside of the specimen.

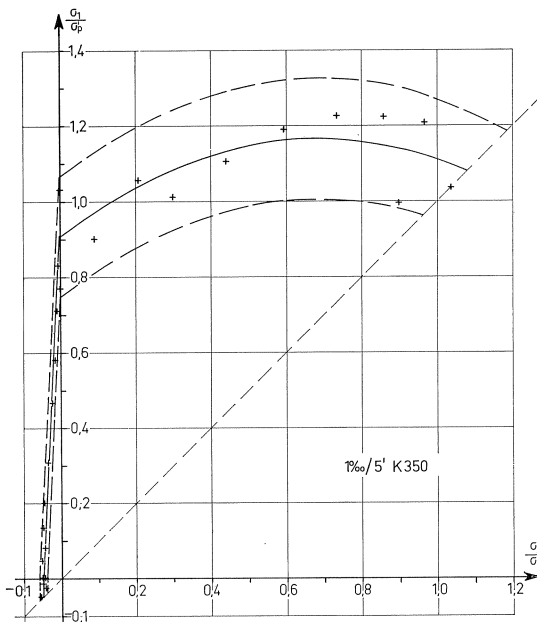


Fig. 32a

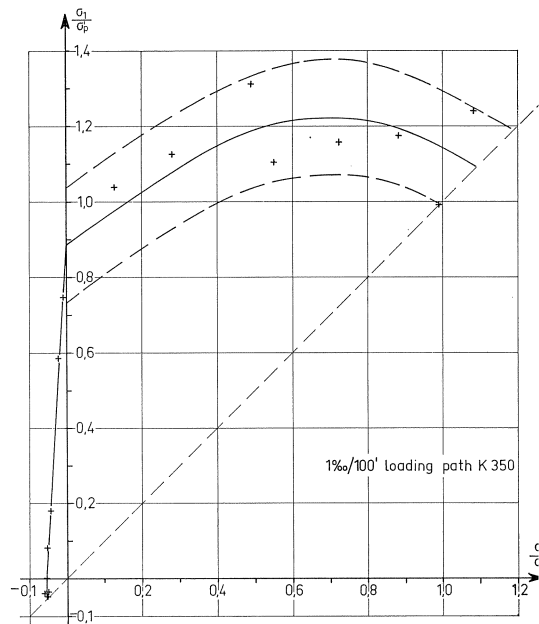


Fig. 32b

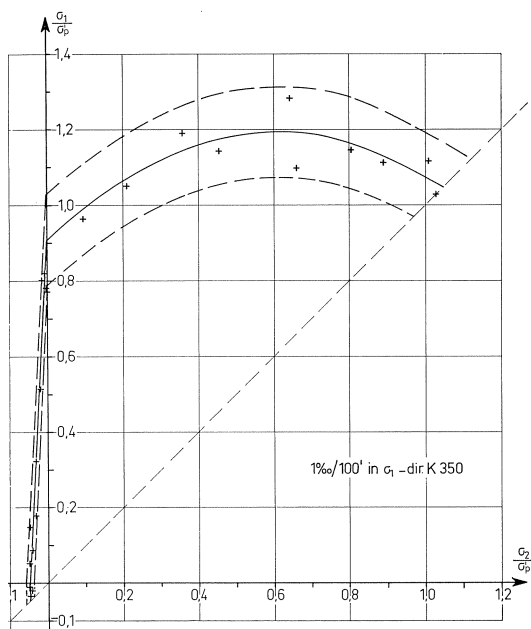


Fig. 32c

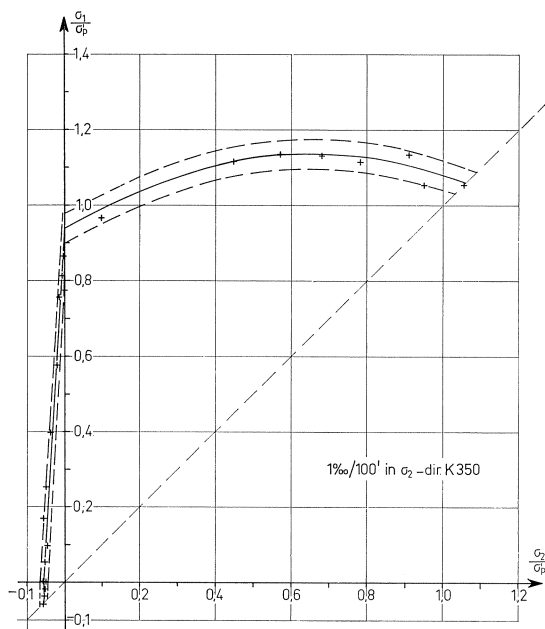


Fig. 32d

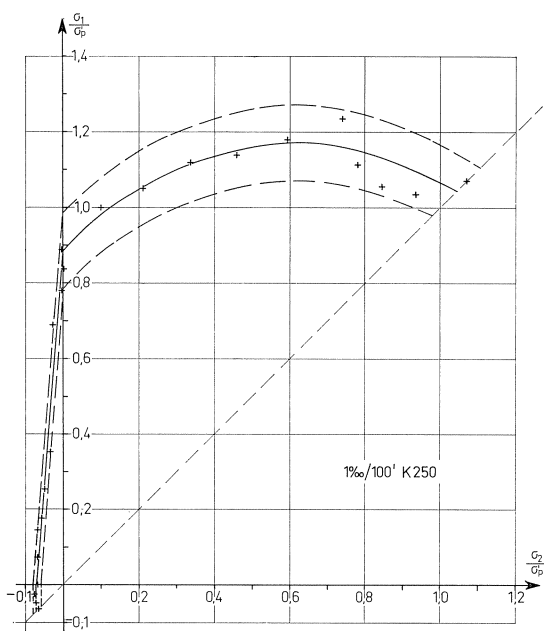


Fig. 32e

Fig. 32. The ultimate load as a function of the stress ratio.

- c. The greatest part of the difference in strength is a result of the hardening circumstances (see also Heilman [45]). It was necessary to store the specimen during the last week of hardening in a room with a humidity of 45% in order to get a layer of glue of sufficient strength. In this period the specimen dried and as a result the humidity of the specimen was no longer uniform. Tensile stresses or even cracking in the skin of the specimen are caused by this irregularity. With the splitting test the fracture starts at the inside of the specimen and there is only a little influence found on the ultimate load. The uniaxial tension test, however, causes a uniform tensile stress condition to the specimen. These stresses are added to the stresses introduced beforehand. As a result the ultimate load will be reached at a lower external force as compared to a specimen in which no shrinkage stresses occur.

A good comparison of the different test results is only possible when the hardening circumstances are constant. During the period of the tests in the region of tension-tension the air-conditioning did not function properly in the room in which the specimens were stored one week before testing. Consequently the humidity varied a lot. The sequence of the different tests was chosen in such a way that in every region of the biaxial stress condition the tests which belong together are carried out in as short a period as possible. By this sequence of testing it was possible to estimate the influence of the stress ratio on the ultimate load.

From the results it can be seen that the influence of the second principal stress on the ultimate load is very small. The modes of failure given in fig. 31 and the deformations in the direction of the greatest stress (see fig. 36) affirm this also. The results given in fig. 32 a–e are for this reason already multiplied by a factor in order to agree with the results in the region of compression-tension so that the influence of a different drying-up of the specimen can be eliminated.

Region of compression-tension:

From fig. 32 a–e it can be seen that the ultimate load in this region depends on the stress ratio. A small tensile stress in comparison to a compressive stress gives a great decrease in ultimate load. For every series of tests in which the way of loading was the same the best fitting parabolic curve or straight line for the ultimate load was estimated. It appeared that a straight line gave a better approximation of the test results (standard deviation about 30% smaller). The deviation of the test results around this best fitting straight line is estimated by the 95% confidence interval and given in fig. 32a–e.

Region of compression-compression:

The uniaxial ultimate load was about 90% of the cube strength. Such a high ultimate load compared to the cube strength can be explained by the difference in humidity of the specimens as a result of the hardening circumstances during the last week before testing as shown in 5.1. For each series of tests in this region, the best fitting

parabolic curve is estimated and given in fig. 32 a–e. These figures show that, in the region of biaxial compression, the second principal stress (that is the intermediate principal stress) influences the ultimate load.

A comparison of the several series of tests is given in fig. 33. The confidence intervals around the most fitting curves in the three regions of a biaxial state of stress overlap each other. For this reason it can be concluded that the different ways of loading have not had a significant influence on the ultimate load at the several stress ratios. Fig. 33 shows that in comparison to the uniaxial compressive strength a maximum increase of the ultimate load of 30% is achieved at a stress ratio of $\sigma_2 : \sigma_1 = 1 : 2$. When the stresses in both directions are equal to each other then this increases is only 20%. The uniaxial tensile strength was about 70% of the splitting strength.

From the test results it cannot be seen if the kink-way changes at the uniaxial compressive and tensile loading has appeared in reality. They can be seen as a simplification of a very sharp change of curvature in this region.

The test results with the solid loading platens (also given in fig. 33) show a great

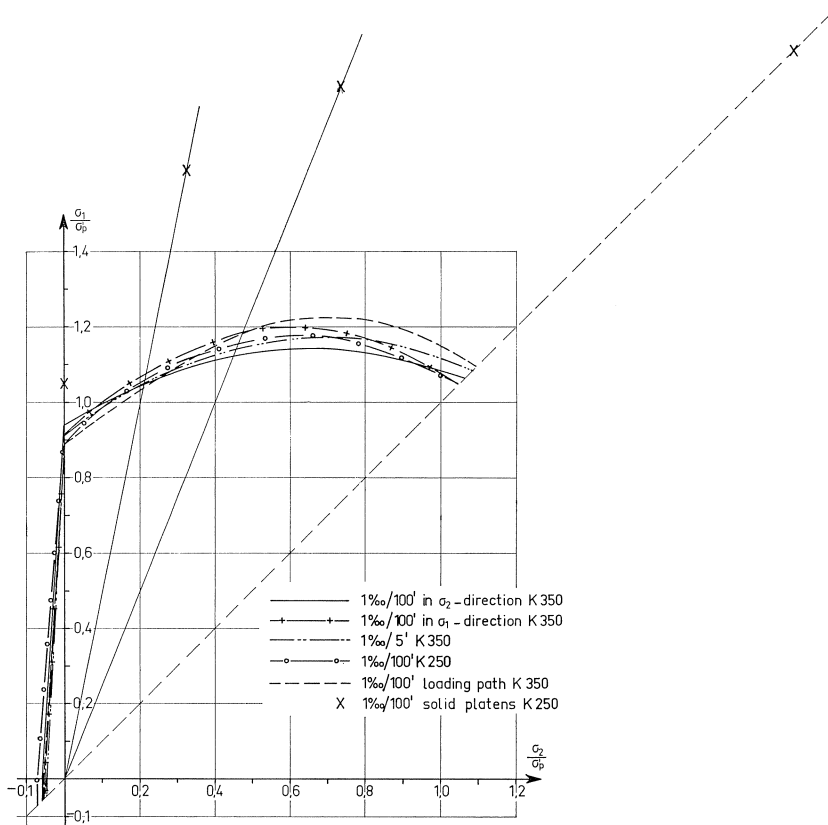


Fig. 33. The influence of the way of loading on the ultimate load under biaxial loading.

increase in strength in the region of biaxial compression. This apparent increase in strength is due to the restraint of the specimen. The great increase in strength found in the different previous tests (see appendix I) must, for this reason, also be a consequence of this external influence and cannot be a property of the material concrete itself.

5.4 *Stress-strain curves*

In fig. 34 the strains in the principal directions as a function of the largest stress for one way of loading in the three regions of the biaxial state of stress are given as an example. The descending part of the stress-strain curves is not given because this part of the curve depends on the situation of the measurement instruments. When all cracks which initiate the final fracture are situated within the measuring length then at the same stress a much larger deformation will be measured in comparison to the deformation when some cracks are situated outside this length.

Whether or not the test could come over the top of the stress-strain curve was dependent on the way of loading. A sudden rupture at the top of the stress-strain curve occurred in the regions of biaxial tension and compression-tension (till a stress ratio $\sigma_1 : \sigma_2 \sim 25 : -1$) when the load was raised by a constant strain rate in the direction of the smallest tensile stress or in the direction of the compressive stress. This is due to the fact that the deformation in the direction of the constant strain rate at these tests after reaching the top of the stress-strain curve did not increase any more, or even decreased. Because in all tests the loading apparatus was programmed with a constant increase in strain a sudden rupture occurred directly after reaching the top of the stress-strain curve.

This shows that the shape of the stress-strain curve depends on the direction in which the constant strain rate was maintained. The tests with a stress ratio of 2 : 10 and 3 : 10 in the region of biaxial compression in which the constant strain rate was maintained in the direction of the smallest stress could not be carried out because the regulation of the loading became unstable (see 2.2.a).

A great resistance against rupture was still found after reaching the top of the stress-strain curve (see, for instance, fig. 17) in all remaining tests. The very steep descending curve, often shown in literature, can be explained in most cases by external influences, such as not maintaining a constant strain rate. It may be expected that concrete with a porous aggregate and another bond between the aggregate particles and the cement paste will give a more steeply descending curve.

Different shapes of the stress-strain curves were observed at the tests in which the load was not increased by a constant stress ratio but following different stress paths.

The separated strain measurements, perpendicular to the direction in which the constant strain rate was maintained and parallel to the free plane of the specimen, were equal to each other at low stresses but deviated more with increasing load. This means that a material with uniform stiffness changes during loading in an irregular material probably as a result of microcracking.

Fig. 34. Stress-strain curves ($1^{0}/_{00}/100'$ in σ_1 -direction; K350).

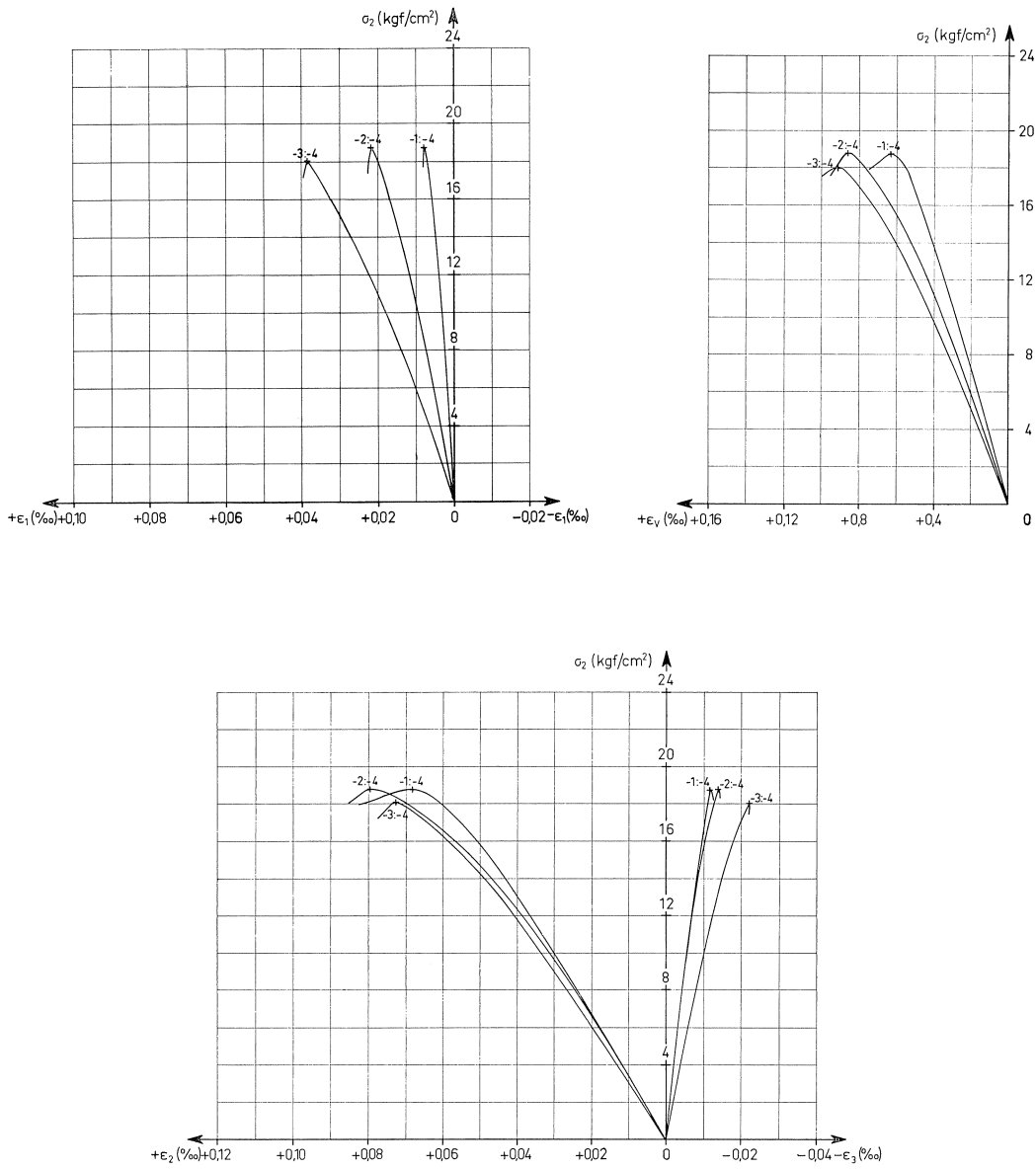


Fig. 34a. tension-tension.

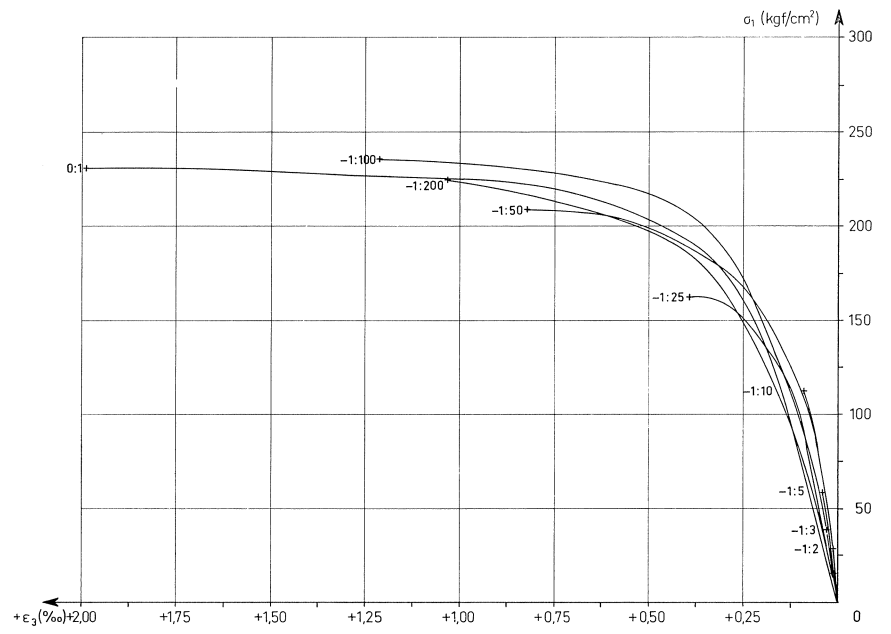
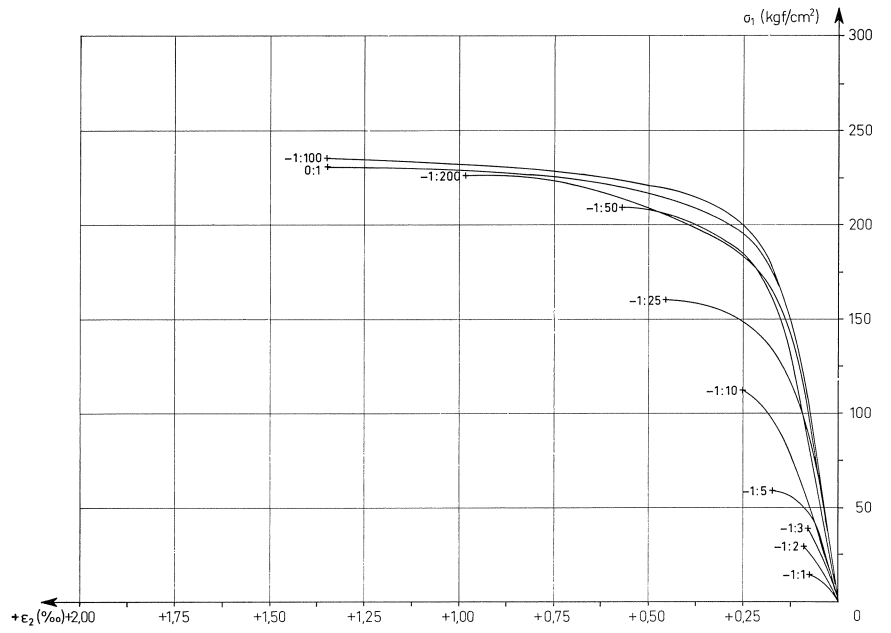
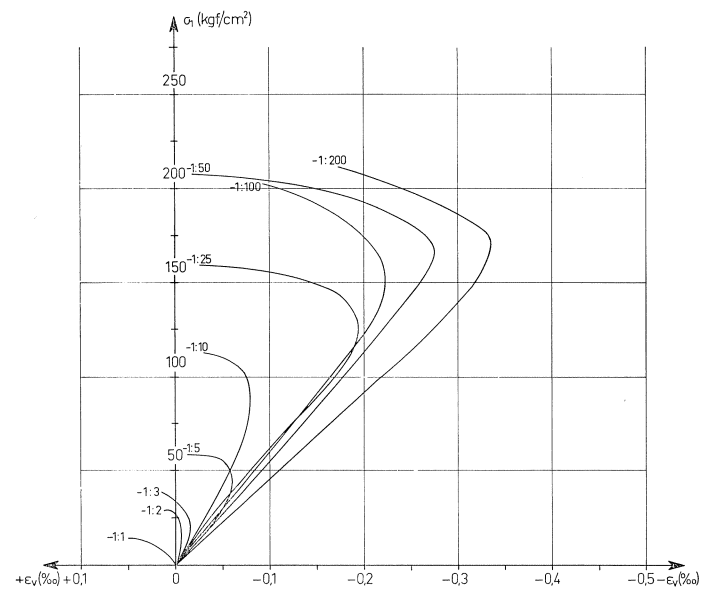
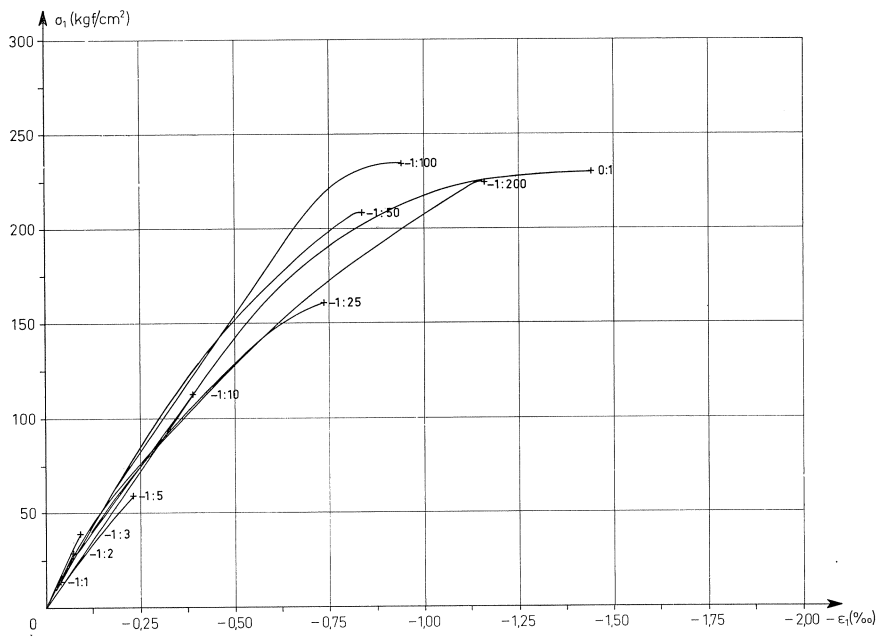


Fig. 34b. compression-tension



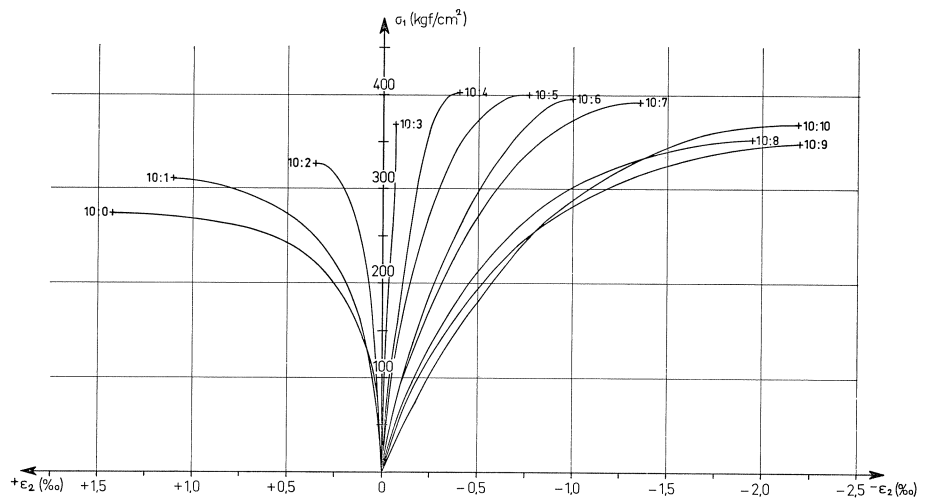
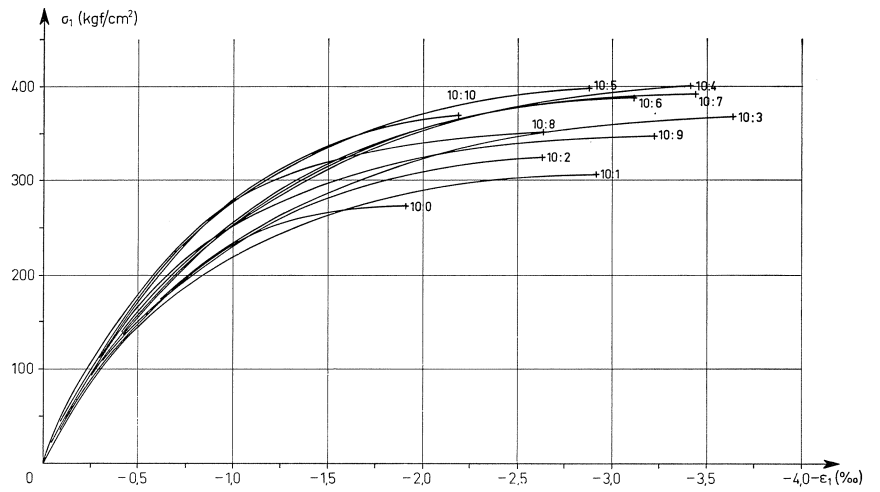
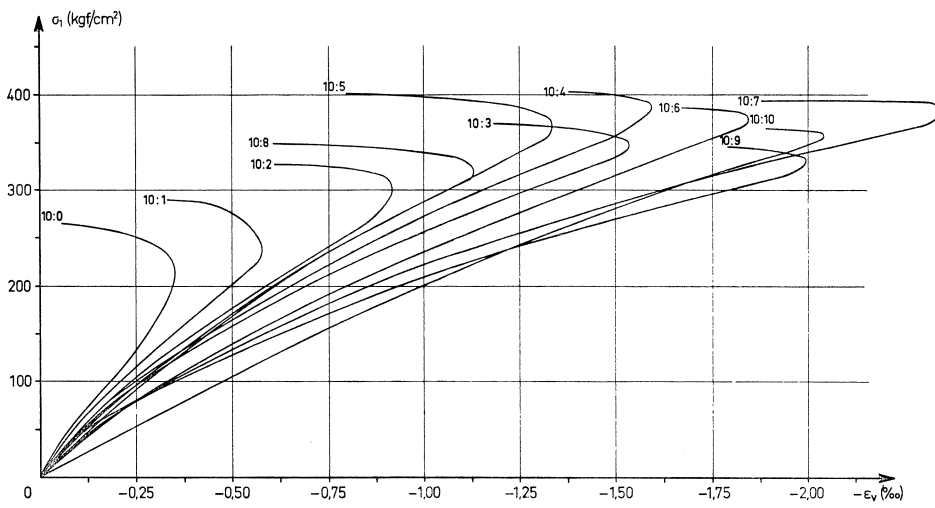
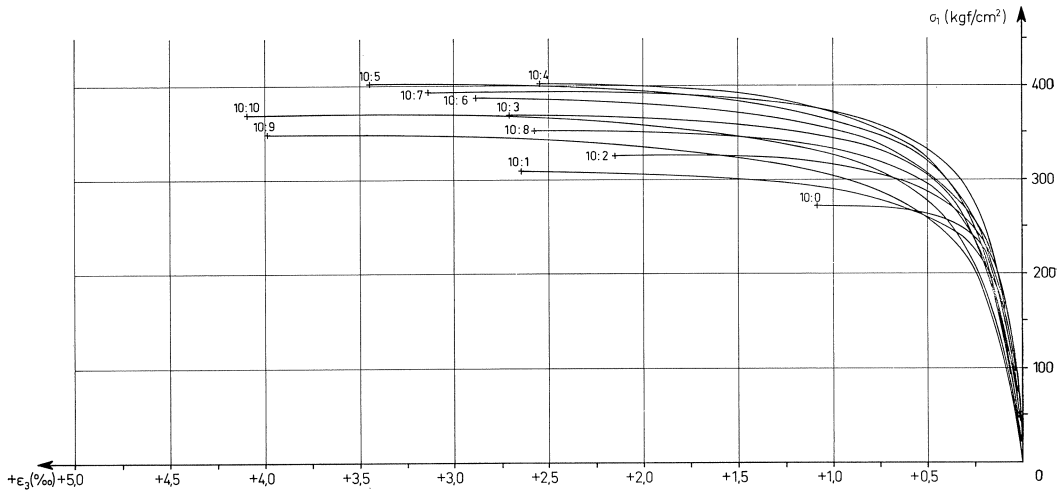


Fig. 34c. compression-compression.



Another presentation of stress-strain curves is given in fig. 35. From this figure it can be seen that there is no symmetry with respect to the 45° line. Maintaining a constant strain rate in one direction means in one half of the diagram a constant strain rate in the direction of the smallest compressive- and greatest tensile stress, but means in the other half of the diagram a constant strain rate in the direction of greatest compressive- and smallest tensile stress, respectively.

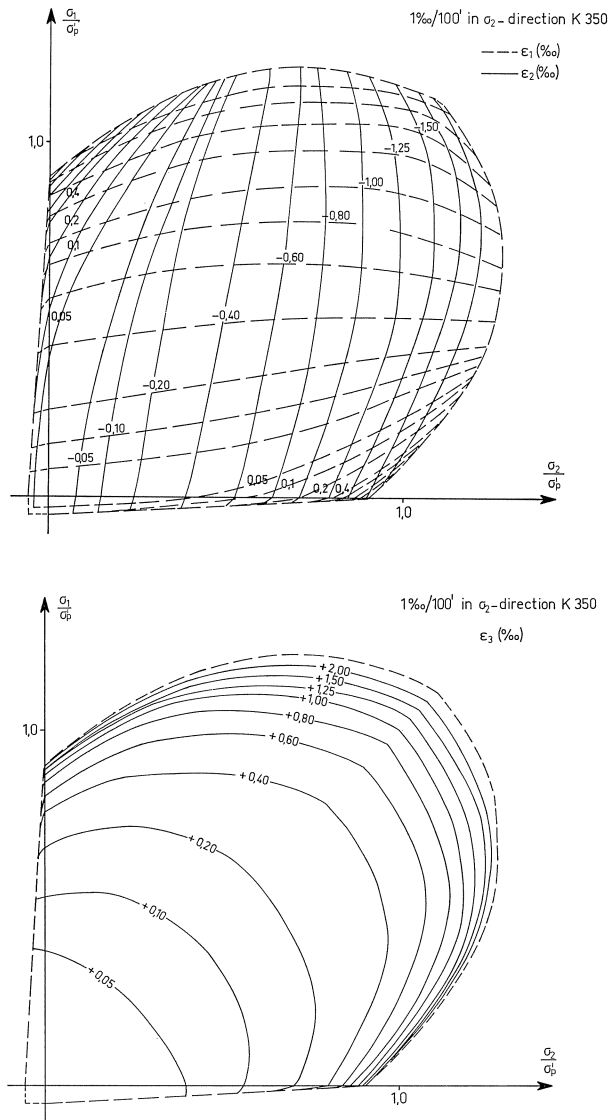


Fig. 35. The deformations as a function of the stress ratio.

5.4.a Maximum deformation

For the several series of tests the deformations at the top of the stress-strain curve (“maximum deformation”) are given in fig. 36 a–e as a function of

$$\alpha = \arctg\left(-\frac{\sigma_1}{\sigma_2}\right) \quad (\alpha = 0 \text{ corresponds with the uniaxial tension test}).$$

The maximum deformations in the directions of loading (ε_1 and ε_2) could not be given for the biaxial tests in the region of biaxial tension when the stress ratio was near to one, because the final fracture always occurred perpendicular to the direction of the stress. The deformations, perpendicular to this crack appeared to increase more under a relatively high stress than the deformation which was parallel to this crack.

The maximum deformations at the uniaxial compression tests depended on the direction of maintaining a constant strain rate. For this reason there is a discontinuity at that point in the maximum strains at the tests in which the constant strain rate was maintained in the region of compression-tension and biaxial tension in the direction σ_2 while in the region of biaxial compression this was done in the σ_1 direction.

A comparison of the different series of tests is given in fig. 37. From this figure it can be seen that the way of loading had an important influence on the deformations; especially the ε_1 -deformation in the region of compression-compression. A faster loading speed in this region gave a smaller maximum deformation in the direction of the greatest compressive stress. Following different stress paths also influenced the maximum deformation in this direction.

There can also be noticed that the relative sharp increase in ε_2 - and ε_3 -deformation in the region of compression-tension at a stress ratio $\sigma_2 : \sigma_1 \sim -1 : 25$ corresponds to the stress ratio at which the mode of failure changes from one crack perpendicular to the direction of the tensile stress to several cracks in the same direction (see fig. 31).

5.5 Energy

Fig. 38 a–c give as a function of

$$\alpha = \arctg\left(-\frac{\sigma_1}{\sigma_2}\right)$$

the total amount of energy and the energy in the two principal directions stored in the specimen before reaching the ultimate load for the several series of test. These figures show that the amount of energy stored in the specimen strongly depends on the stress ratio. The energy in the σ_2 -direction reaches a maximum in the region of compression-tension at a stress ratio of $\sigma_2 : \sigma_1 \sim -1 : 50$.

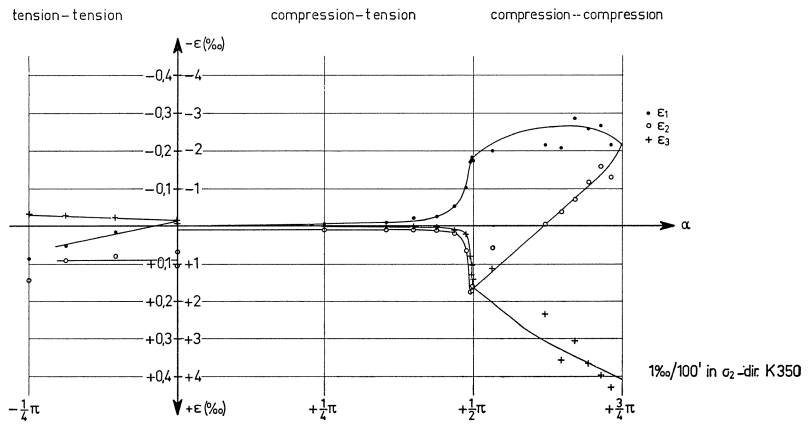


Fig. 36a

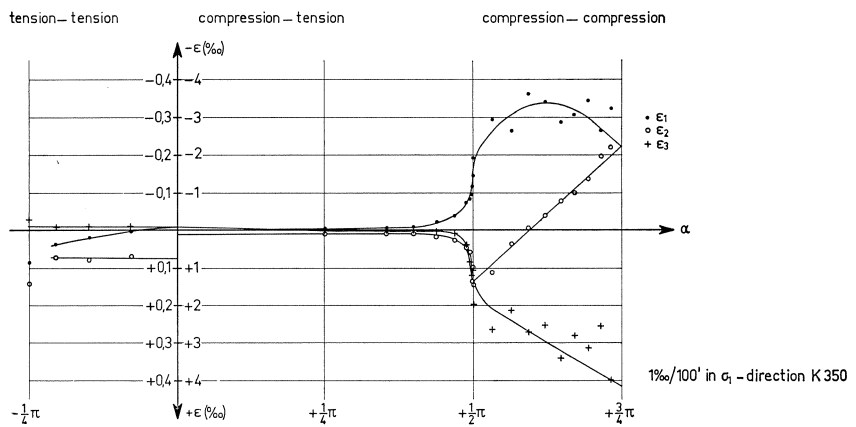


Fig. 36b

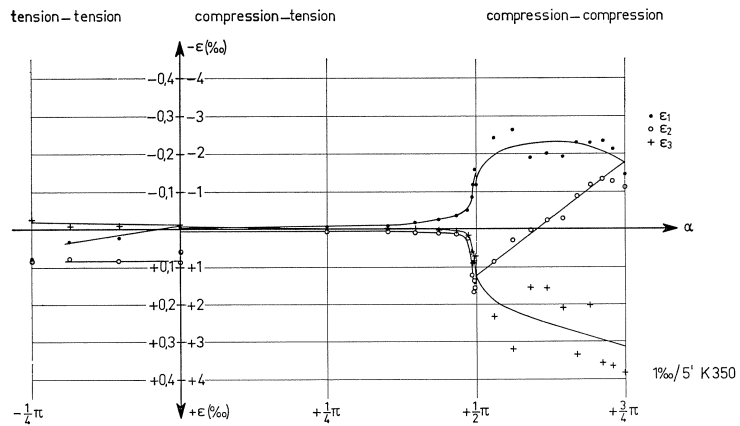


Fig. 36c

Fig. 36. The maximum deformations as a function of the stress ratio.

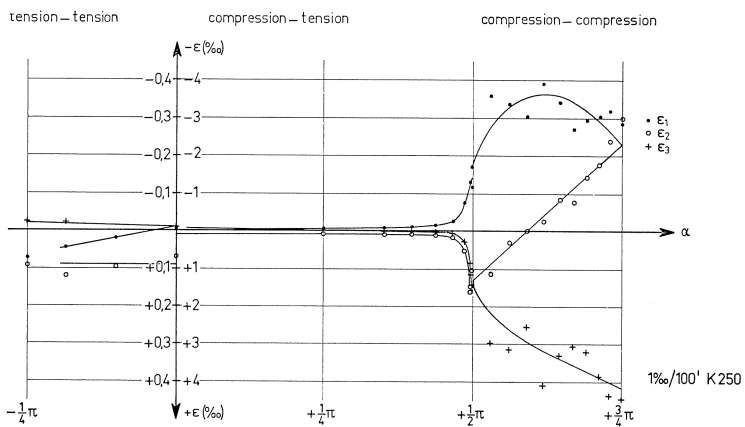


Fig. 36d

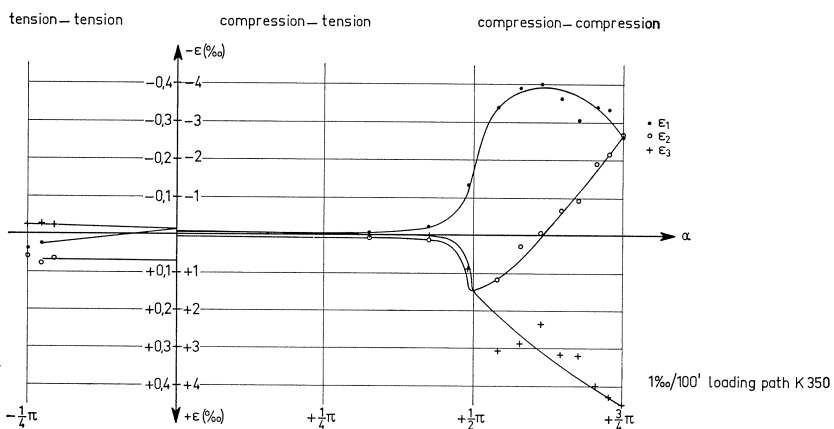


Fig. 36e

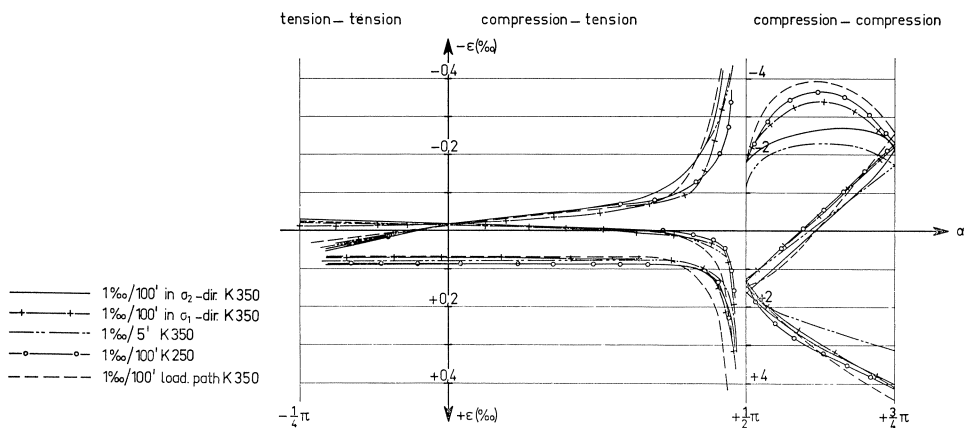
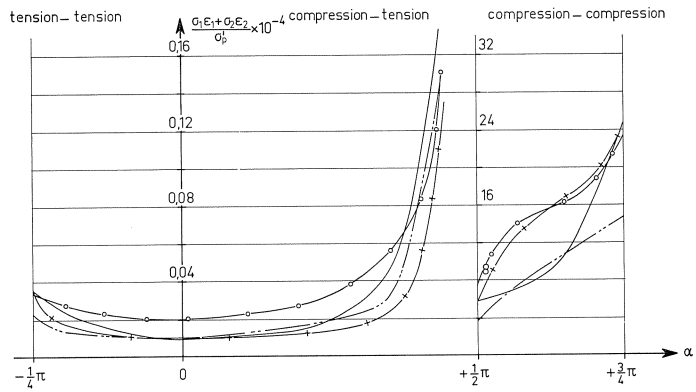
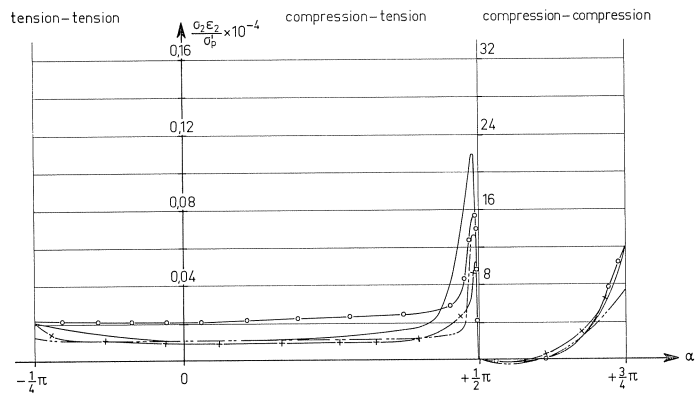


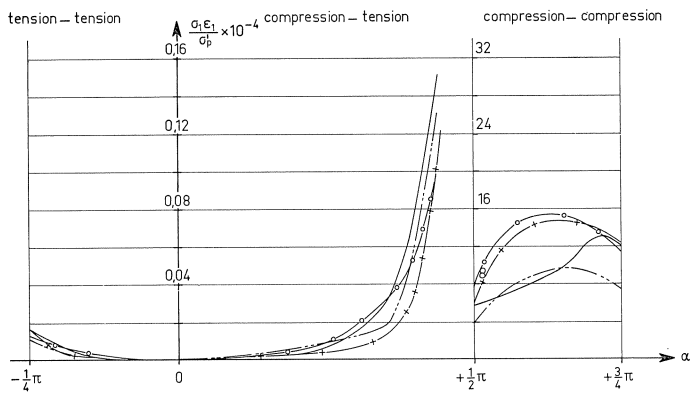
Fig. 37. The influence of the way of loading on the maximum deformations under biaxial loading.



a



b



c

- 1‰/100' in σ_2 -dir. K350
- - - 1‰/100' in σ_1 -dir. K350
- · · 1‰/5' K350
- ○ ○ 1‰/100' K250

Fig. 38. Energy stored in the specimen as a function of the stress ratio.

6 Failure criterion

The stress component σ_{ij} can be expressed in terms of the three principal stresses (σ_1 , σ_2 and σ_3) and the directions of principal axes cannot influence the failure. When a cartesian co-ordinate system is chosen in such a way that the directions of the axes correspond to the principal stresses, then the failure criterion $f(\sigma_1, \sigma_2, \sigma_3; C_1 \dots C_n = 0)$ may be thought of as the equation of a surface in a stress space. This surface is called the failure surface. The cross-section of this failure surface with one of the co-ordinate surfaces gives the failure curve of the biaxial state of stress. The failure criterion of a perfectly plastic material is not influenced by the presence, or absence of an overall hydrostatic pressure (or tension).

For this reason the failure surface must be a cylinder whose generators are all parallel to the hydrostatic axis ($\sigma_1 = \sigma_2 = \sigma_3$). As a result of this property the failure surface is defined by any plane which is perpendicular to the hydrostatic axis (equi-pressure cross-section: $\sigma_1 + \sigma_2 + \sigma_3 = C$). Furthermore, this cross-section must be a threefold symmetric one because an interchange of the arbitrarily numbered co-ordinate axes cannot influence the failure surface for an isotropic material.

It has been found experimentally that the failure surfaces for perfectly plastic materials fall between the von Mises' circle and the inner hexagon of this circle representing Tresca's theory of constant elastic strain energy of distortion. Huber and Hencky have also adopted the circle by assuming a constant octahedral shearing stress.

Isotropic materials with an appreciably different failure strength in compression and tension can have different failure surfaces. The condition of isotropy requires that any equipressure cross-section of the failure surface must show the threefold type of symmetry, but it is not necessary that the failure surface be convex when viewed from outside. Different failure criteria are also given for this kind of materials. According to the maximum normal stress theory the maximum principal stress determine the material failure, regardless of what the other principal stresses may be, provided that the latter are absolutely smaller.

A correction should be made on this theory for concrete because the uniaxial compressive- and tensile strength are not equal to each other. The failure curve representing this theory is a cube. The centre of this cube is situated on the space diagonal in the compression quadrant. A correction of this kind should also be made for the maximum elastic strain theory. The maximum shearing stress theory predicts failure when the maximum shearing stress just reaches a critical value. This value depends on the normal stress acting on the slip plane. Coulomb was the first one who formulated this theory by assuming a linear relationship between the maximum shearing stress and this normal stress. Mohr has generated this theory by assuming a certain non-linear relationship between the maximum shearing stress and the normal stress for a certain material. As a result the angle of slipping also depends on the state of stress. According to this theory a curve is found in the σ, τ co-ordinate plane as the locus of the points $P(\sigma, \tau)$ defining the limiting values of both components of

stress in the slip planes under the different states of stress to which the material may be subjected. Leon [61] further clarified additional conditions as far as the fracture of brittle materials is concerned and he assumed an ordinary parabola for the properties of the envelope.

It is also often assumed that the failure surface is a paraboloid of revolution. This amounts to the fact that the octahedral shearing stress is a square function of the mean value of the normal stresses. The properties of this curve depends on the relation between the uniaxial compressive and tensile strength. When these values are equal to each other then the paraboloid of revolution turns over in the failure surface of von Mises.

A good agreement with some of the previously mentioned theories was found in the different regions of the biaxial state of stress (see fig. 39 and compare with fig. 33). The maximum normal stress theory, the maximum elastic strain theory and the theory of Mohr proved to be in good agreement with the test results in the region of tension-tension. The theory of Mohr predicts the failure in the region of compression-tension quite well. However, no slip plane occurred in any test. In the region of biaxial compression the failure criterions could not predict the ultimate load. Furthermore, the energy stored in the specimen was not constant (see fig. 38). It seems less significant to estimate the failure surface from the biaxial tests. Because the biaxial state of stress only gives an arbitrary cross-section of the failure surface with one of the co-ordinate surfaces and also because not all of the influences on the fracture are completely investigated, only an indication about possible influences is obtained. Furthermore none of the classical theories gives a good prediction and explanation of the failure in all of the three regions of the biaxial state of stress.

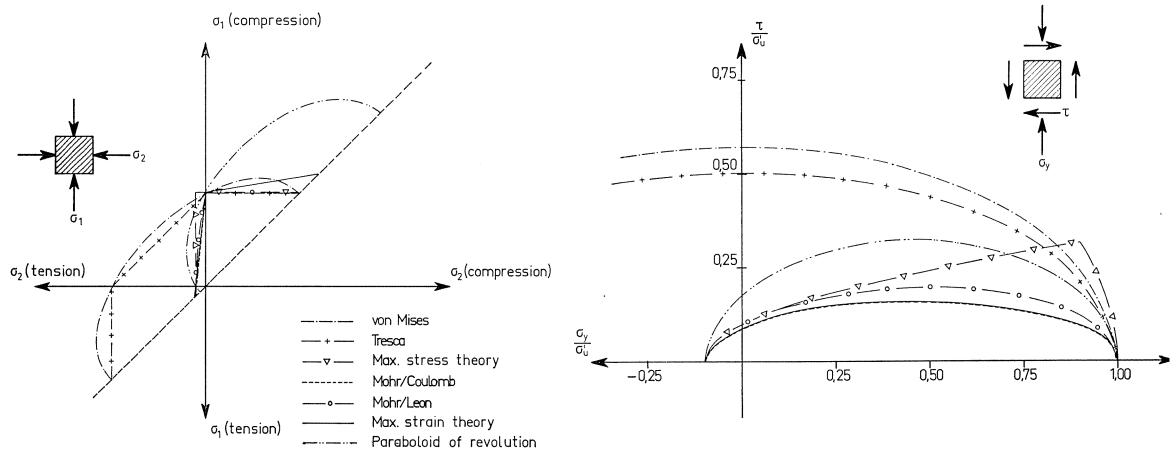


Fig. 39. Different classical failure criterions.

With the presentday knowledge a very simple mathematical formulation, based on certain critical values of the material is more realistic. These critical values can be based on the uniaxial compressive and tensile strength. Such a theory is essential for solving structural problems and for this reason this theory has to be as simple as possible. A mathematical formulation can provide the answer to what is happening at a certain loading. One must bear in mind that this formulation is based on experimental results on the macroscopic level, and, therefore, cannot provide a physical explanation as to what is happening or why certain phenomena occur.

6.1 Long-term strength under biaxial loading

The first investigators who established that the failure of concrete is introduced by microcracks were probably Richart, Brandtzaeg and Brown [4]. In order to get a more physical explanation about the failure of concrete many investigators have tried to measure indirectly or directly the stress at which progressive microcracking occurs [63–67]. The effects of micro-cracking under uniaxial compression on certain properties of concrete is given in fig. 40.

- a. The volume of the specimen decreases under uniaxial compressive loading, roughly in proportion to the load applied, up to about two-thirds of the ultimate load. Above this load, the material is further condensed by a load increase. However, the rate of change in volume decreases up to the point in which a small increase in load causes no corresponding change in volume (at about 80% of the ultimate load, depending on the age of the concrete, the aggregate content, etc.). At higher loads the volume increases with an increase in load, so that at ultimate load the apparent volume of the tested specimen becomes actually larger than it was before the load was applied as a result of the application of compressive load.

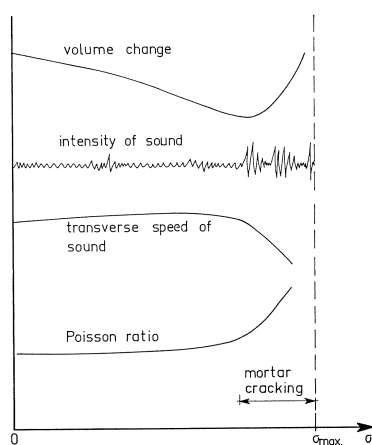


Fig. 40. Effects of microcracking under uniaxial compression on certain properties of concrete.

- b. The Poissons ratio, which can be estimated only with uniaxial tests on concrete, depends on the applied load. This ratio can be estimated by:
- the total deformation from the start of loading
 - the differences in deformation at a certain load increase.
- The Poissons ratio, calculated with the latter method is constant up to approximately 35% of the ultimate load. Above this load the ratio will increase slowly under uniaxial compression and attains the value of 0,5 at a load of approximately 85% of the ultimate load.
- c. The ultrasonic pulse velocity in the direction of loading remains constant when the load is increased to failure. In the transverse direction, however, there is a decrease in the pulse velocity at only a fraction of the ultimate load, and further decreases occur as the load is increased to failure. It is deduced from these tests that the microcracking starts at a fraction of the ultimate load and the cracks are oriented parallel to the direction of loading.
- d. X-ray photography and microscopy provide an even more detailed picture. Accordingly, microcracks at the interface between coarse aggregate and mortar exist in concrete before it is subjected to any load. Above approximately 30% of the ultimate compressive load these bond cracks begin to increase in length, width and number while cracks in the mortar remain negligible. At about 80% of the ultimate load, cracks through the mortar begin to increase noticeably and begin to form continuous crack patterns by bridging the bond cracks.

An indication of the long-term strength of concrete under biaxial loading in the described investigation can be obtained from the measured deformations. The volume strain as a function of the stress in the three regions of biaxial loading at several stress ratios is given in fig. 34. In the region of biaxial compression these curves can be characterized as follows. Directly from the beginning of loading the rate of change in volume decreases was more than proportional to the applied stress. At a certain stress level a bending point occurred. Above this stress a minimum in volume was obtained and the volume increased. At ultimate load the volume could even be larger than it was when the load was applied.

Depending on the stress ratio a different relationship between the volume strain and the applied stress occurred in the region of compression-tension. At stress ratios larger than $\sigma_2 : \sigma_1 \sim 1 : 25$ (a large compressive stress in comparison to the tensile stress) the change in volume decreases was less than proportional to the applied load when the load increased. At a certain stress level a small increase in load caused no change in volume, and above this load the volume increases with increase in load. A bending point in the curve did not occur at these tests, but a load at which the volume was minimal did occur at these tests till the stress ratio $\sigma_2 : \sigma_1 = -1 : 1$. When the tensile stress was larger in comparison to the compressive stress and also in the region of biaxial tension the volume increased immediately when the load was applied.

A bending point or a minimum volume did not occur in these curves.

From the above-mentioned it can be concluded that it is very difficult to estimate the long-term strength with the help of the strain measurements only. A more fundamental investigation into the development of microcracks under loading is necessary in order to estimate the properties of concrete in the macroscopic level [68–71].

The tendency in the relationship between the volume strain and the stress is approximately the same for all tests in the region of biaxial compression and of compression-tension till the stress ratio $\sigma_2 : \sigma_1 = -1 : 25$. For these stress ratios the long-term strength can be estimated by the stress at which there is a bending point in the curve and the stress at which the volume is minimal (as has been established by several investigators with uniaxial compression tests).

In the region of biaxial compression, departing from a stress ratio $\sigma_2 : \sigma_1 = 1 : 10$, the load at which a minimal volume occurred was approximately 91% of the ultimate load (coefficient of variation 5%). This load was about 77% of the ultimate load from the stress ratio $\sigma_2 : \sigma_1 = 1 : 10$ till $\sigma_2 : \sigma_1 = -1 : 25$ (coefficient of variation 10%). The load at which a bending point occurred in the region of biaxial compression was about 76% of the ultimate load (coefficient of variation 9%). This load did not occur at the region of compression-tension and at the uniaxial compression test. These percentages proved to be independent of the way of loading and the applied stress ratio.

7 Conclusions

The different modes of failure in the three regions of the biaxial state of stress show that a bearing of load by the adjacent loading platens occur when these are solid platens (see 1.3). In the region of biaxial compression an apparent increase in strength was also established with these tests (more than 75% in comparison to the uniaxial compression test). In the region of compression-tension and biaxial tension the ultimate load at the several stress ratios proved to be almost equal to the ultimate load, estimated by loading with rod platens. An apparent increase in strength in the region of compression-tension was prevented by an early fracture of the connection glue-concrete. The tests in the region of biaxial tension carried out with solid loading platens showed an apparent increase in stiffness of about 40% in comparison to the uniaxial tension test. This increase was also established in a calculation with the help of the finite element method, in which the stiffness of the uniaxial tension test was used for the description of the properties of the different concrete elements. Furthermore, it followed from this calculation that directly next to the layer of glue the stress in the edges was about 7 times that in the middle of the specimen. An apparent increase in strength in the region of biaxial tension (as was established in the region of biaxial compression) was nullified by this irregular distribution of the stresses.

In the following only the tests in which the load was transmitted to the specimen by rod platens will be considered. From the previous chapters it can be seen that by using rod platens the applied load is not disturbed by this way of loading and as a

result that the state of stress in the specimen is almost independent of the deformations of the concrete.

7.1 The ultimate load

In 5.3 it is shown that a parabolic function gives the best fitting curve for the results in the region of biaxial compression. A simple approximation of this parabolic curve is obtained by two straight lines. The largest increase of the ultimate load in the region of biaxial compression was attained at a stress ratio $\sigma_2 : \sigma_1 = 1 : 2$. In previous investigations (see appendix I) this maximum increase was also attained at this stress ratio.

A straight line is chosen in such a way that it passes the ultimate load at the stress ratios $\sigma_2 : \sigma_1 = 0 : 1$ and $\sigma_2 : \sigma_1 = 1 : 2$. The other straight line passes the ultimate load at the stress ratios $\sigma_2 : \sigma_1 = 1 : 1$ and $\sigma_2 : \sigma_1 = 1 : 2$. When a formulation for the ultimate load is made in this way then the calculated ultimate load can be considered as a safe value. The ultimate load in the region of biaxial tension and compression-tension can be calculated by two straight lines (see 5.3) cutting each other at the stress ratio $\sigma_2 : \sigma_1 = -1 : 0$ (uniaxial tension test).

Starting from the prism strength and the splitting strength, the ultimate load can be formulated in each biaxial region by:

Compression-compression

$$\sigma_1 = \frac{2(p-1)}{p} \cdot \sigma_2 + k\sigma'_p \quad 0 \leq \sigma_2 \leq 0,5\sigma_1 \quad (1)$$

$$\sigma_1 = \frac{2(q-p)}{2q-p} \cdot \sigma_2 + \frac{p \cdot q \cdot k}{2q-p} \cdot \sigma'_p \quad 0,5\sigma_1 \leq \sigma_2 \leq \sigma_1 \quad (2)$$

Compression-tension

$$\sigma_1 = k \left(\frac{s}{l} \cdot \sigma_2 + \sigma'_p \right) \quad (3)$$

Tension-tension

$$\sigma_2 = -\frac{l}{s} \cdot \sigma'_p \quad (4)$$

$$p = \frac{\sigma'_{1\max} \text{ (at } \sigma_2 : \sigma_1 = 1 : 2)}{\sigma'_{\max} \text{ (uniaxial compression)}}$$

$$q = \frac{\sigma'_{1\max} \text{ (at } \sigma_2 : \sigma_1 = 1 : 1)}{\sigma'_{\max} \text{ (uniaxial compression)}}$$

$$k = \frac{\sigma'_{\max} \text{ (uniaxial compression)}}{\sigma'_p}$$

$$s = \left| \frac{\sigma'_p}{\sigma_{spl}} \right|$$

$$l = \frac{\sigma_{\max} \text{ (uniaxial tension)}}{\sigma_{spl}}$$

The different coefficients in these equations can also be made dependent on the hardening circumstances, the kind of aggregate, the age of testing and the duration of the loading. A simple and universal calculation of the ultimate load under biaxial loading is the result. The equations for the tests described in this report are (see fig. 33 and eq. 1-4):

Compression-compression

$$\sigma_1 = 0,46\sigma_2 + 0,9\sigma'_p \quad 0 \leq \sigma_2 \leq 0,5\sigma_1 \quad (1a)$$

$$\sigma_1 = -0,18\sigma_2 + 1,28\sigma'_p \quad 0,5\sigma_1 \leq \sigma_2 \leq \sigma_1 \quad (2a)$$

Compression-tension

$$\sigma_1 = 16\sigma_2 + 0,9\sigma'_p \quad (3a)$$

Tension-tension

$$\sigma_2 = -0,055\sigma'_p \quad (4a)$$

From 6.1 it can be seen that the load at which severe micro-cracking occurs is a constant percentage of the ultimate load at every stress ratio in the regions of biaxial compression and compression-tension (till $\sigma_2 : \sigma_1 = -1 : 25$). In the case of the remaining stress ratios such a load could not be determined with the tests. The micro-cracking could not be determined directly, and furthermore it was not possible to get an indication concerning a certain load from the volume strain as a function of the applied stress. Tests by Heilmann [45] and Hansen [72] showed that the long-term strength of concrete under uniaxial tension is almost an equal percentage of the short-term strength as is the case for the uniaxial compression test. As long as no tests of long duration are carried out it seems, however, that we are justified in estimating the long-term strength under biaxial loading as a constant percentage of the short-term strength. In the three regions of biaxial loading the deviation around the most fitting curve proved to be as large as is usually found with uniaxial compression and splitting tests. For the determination of the design values of the ultimate load in the three regions of biaxial loading the same coefficients can, for these reasons

be used as are normally used for the determination of the design values of the uniaxial strength. With regard to the uniaxial tension strength, one must bear in mind that the circumstances of hardening have a great influence on the stress distribution in the specimen (see 5.3). It is doubtful if the sharp reduction of the ultimate load under uniform drying of the section also occurs in the construction. For this reason it is perhaps better to determine the uniaxial tension strength with the help of the splitting test ($l = 1$ in the equations 3 and 4) because with the latter test the irregular drying of the specimen has no significant influence on the ultimate load.

The different modes of failure and the previous investigations of the microcracking as a function of the loading [63–69] have shown that for gravel aggregate the bond strength between the coarse aggregate and the mortar determines the ultimate load and the shape of the stress-strain curve. The ultimate load is much smaller in comparison to normal concrete, when the gravel aggregate for instance is coated with a silicone rubber material to substantially eliminate the bond between the paste and the aggregates [66]. Furthermore, the load at which a minimum volume is obtained was about 15% of the ultimate load with coated aggregates, while it was about 75% with untreated aggregates. The bond strength between the mortar and the aggregate is in general much better when lightweight aggregates are used. The stiffness and the strength of these aggregates are, however, much smaller. Lightweight concrete behaves, in general, in a more homogeneous manner and as a result the bond between the mortar and the aggregates does not determine the ultimate load. These properties also give a different shape to the stress-strain curve. A preliminary investigation in the Stevin-laboratory has shown that with uniaxial tests on different kinds of lightweight concrete the stress-strain relationship is more linear, and after reaching the top of the diagram it has a much steeper descending curve (the deformation in the direction of loading even decreased after reaching the top of the diagram). The capacity of rotation of a section by using this kind of concrete is for this reason, probably less than by using normal concrete. Furthermore, indications of the failure of a construction and a clear visual bending or formation of cracks will also be less. For these kinds of concrete it is perhaps better to use an extra reduction on the design value of the ultimate load, which reduction should resemble that used with normal concrete when bending and a normal force act together on a section.

7.2 *Stress-strain relationship*

The deformations as a function of the loading in the regions of biaxial compression and compression-tension (up to a stress ratio $\sigma_2 : \sigma_1 = -1 : 25$) can be described by the following equations:

$$\varepsilon_1 = a\sigma_1 + b\sigma_2 \quad (5)$$

$$\varepsilon_2 = b\sigma_1 + a\sigma_2 \quad (6)$$

$$\varepsilon_3 = b\sigma_1 + b\sigma_2 \quad (7)$$

When a and b are also made dependent on the strain rate, the quality of the concrete and the kind of concrete, etc. then it is possible with these equations in combination with the equations 1–4 to get a good approximation of the deformations as a function of the stress under biaxial loading. From the tests it appeared that for the above-mentioned stress ratios a and b can be described by:

$$a = a_0 + a_1 \cdot \frac{t}{t_u} + a_2 \cdot \left(\frac{t}{t_u}\right)^2 \quad (8)$$

$$b = b_0 + b_1 \cdot \frac{t}{t_u} + b_2 \cdot \left(\frac{t}{t_u}\right)^2 \quad (9)$$

In this equation t_u is the time in minutes required to reach the top of the stress-strain curve (after this to be called maximum duration of the test) and t is the time in minutes expired after applying the load.

The strains ε_1 and ε_3 as a function of the loading in the regions of biaxial tension and compression-tension (up to $\sigma_2 : \sigma_1 = -1 : 25$) can be calculated by equating a and b respectively with 1, $1a_0$ and $1b_0$ (for a_0 and b_0 the values belonging to the uniaxial compression test have to be used). When the constant strain rate is maintained in the σ_1 -direction, then ε_2 can also be calculated in this way. However, when the constant strain rate is maintained in the σ_2 -direction then a bilinear stress-strain curve fits better. Until the top of the diagram is reached ε_2 can be calculated by using 1, $1a_0$ and 1, $1b_0$ (see above). The second (horizontal) part of the diagram can be estimated by multiplying the maximum deformation calculated above by a factor 1,5.

For a certain strain rate and a certain quality and kind of concrete the deformation in the top of the stress-strain curve at every stress ratio can be calculated with the help of the equations 1–9 by equating $t/t_u = 1$. When, for instance, the constant strain rate is maintained in the σ_1 -direction, then with the help of equation 5 the stress at a certain ε_1 -deformation can be calculated. After this, with the help of the equations 6 and 7 the ε_2 and ε_3 deformations at that stress can be estimated.

When the load is first raised to a certain stress and then maintained constant (creep test), the deformations and stresses under short-time loading can be calculated as described above. The maximum deformations which occur after maintaining this load constant can be estimated with the help of a and b , as used in the equations for the test with infinite duration.

The deformations from the tests at which the load in the two directions was not raised in a constant ratio can also be estimated by the equations 1–9. When, for instance, first the stress in one direction is raised to a certain value (as is done in the described tests on the influence on the loading path), then the deformations under this loading can easily be calculated. When after this, the load in the second direction is raised, in a short time until a certain stress ratio is attained, the deformations which occur during this loading can be calculated with the help of the equations 5–9 and $t/t_u = 0$. After reaching the desired stress ratio, then we get the deformations which results from raising the load in this ratio.

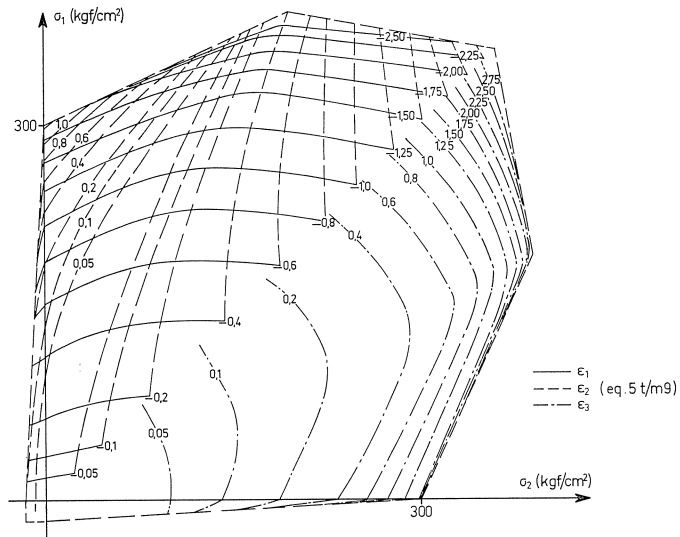


Fig. 41a. The calculated deformations as a function of the stress ratio.

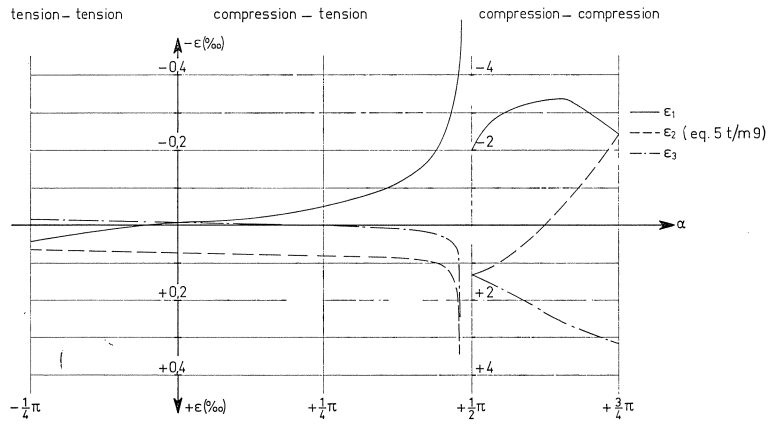


Fig. 41b. The calculated maximum deformations as a function of the stress ratio.

For the tests on the quality of concrete K350 in which the load is raised by a constant strain rate of $1^0/_{00}/100'$ the equations for the calculation of a and b (see equations 8 and 9) are given as an example.

$$a_0 = -(2784,1 - 565,5K) \times 10^{-9}$$

$$a_1 = -\{3347,7 + 1696,4K - 3123 \operatorname{arctg}(10,19K) + 3480 \operatorname{arctg}(6,77K)\} \times 10^{-9}$$

$$a_2 = -\{368,2 - 1130,9K + 3480 \operatorname{arctg}(6,77K) + 6246 \operatorname{arctg}(10,19K)\} \times 10^{-9}$$

$$b_0 = (432,3 - 203,8K) \times 10^{-9}$$

$$b_1 = 611,4K \times 10^{-9}$$

$$b_2 = (3964,6 - 407,6K) \times 10^{-9}$$

$$K = \frac{\sigma_2}{\sigma_1}$$

For $K = 0$ (uniaxial compression test) and $t/t_u = 0$ (applying the load) can be calculated the "module of elasticity" E_0 and the "ratio of Poisson" ν_0 belonging to the uniaxial compression test. From the equations 5-7 follows:

$$E_0 = -\frac{1}{a_0} \quad \text{en} \quad \nu_0 = -\frac{b_0}{a_0}$$

For the above-mentioned way of loading can be calculated:

$$E_0 = \frac{1}{2784,1} \times 10^9 = 3,59 \times 10^5 \text{ kgf/cm}^2$$

$$\nu_0 = \frac{432,3}{2784,1} = 0,155$$

The deformations as a function of the load and the maximum deformation calculated with the help of the equations 1a-4a and 5-9 are shown in fig. 41a-b (compare fig. 34, 35 and 37).

7.3 Some remarks about the practical use of the test results

We shall look at the bearing capacity of some constructions in every region of the biaxial state of stress. Beforehand, we shall show what, in general, has been learned from the tests with respect to the ultimate strength of concrete (fig. 42).

Hitherto almost all calculations have been based on the uniaxial compressive and tensile strength: the first one estimated by the cube or prism test; the latter one almost

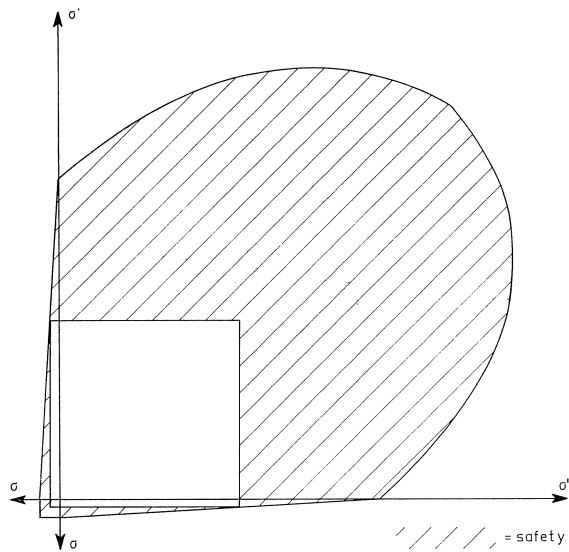


Fig. 42. The safety of constructions under biaxial loading.

always estimated by the splitting test. From the biaxial results it can be seen that in the region of biaxial compression this results in a safe construction; the safety is however more than is presumed. In the region of compression-tension the safety is less than presumed; the difference between the real bearing strength and the calculated one depends on the stress ratio. In the region of biaxial tension the calculation gives a good estimation of the bearing strength. When the splitting strength is the basis of the calculations in this region, then some underestimation of the ultimate load is possible. From this it can be concluded that, in particular, constructions on which a compression-tension state of stress acts needs a lot of attention in the calculations.

Constructions under tension-tension

From the results it can be seen that in these constructions the moment of cracking can be calculated with the aid of the uniaxial tension or splitting test. From slab and beam tests we learned that in the stage of an uncracked section the behaviour of a beam can be calculated by assuming a linear-elastic behaviour of the material. These two test results give the possibility of calculating the behaviour of, for instance, two-way spanning slabs with the aid of the linear-elastic theory up to the moment of cracking. Only a very small deviation of the real behaviour occurs because of the fact that the Poissons ratio is not constant and the $\sigma-\epsilon$ curve is not completely linear under tension. Furthermore, the test results have shown that the tensile strength depends very strongly on the humidity of the concrete. For this reason a higher safety factor is necessary than that for concrete under compression.

Constructions under compression-tension

Fig. 42 has shown that, in particular, in this region a modification of the usual

calculation method is necessary. Some examples of the kind of constructions belonging to this region are given in fig. 43. The stress ratio depends on the sizes of these structures and the loading. The load at which cracking occurs can be calculated with the aid of the biaxial test results. When there is only a little amount of reinforcement then the collapse load can also be estimated.

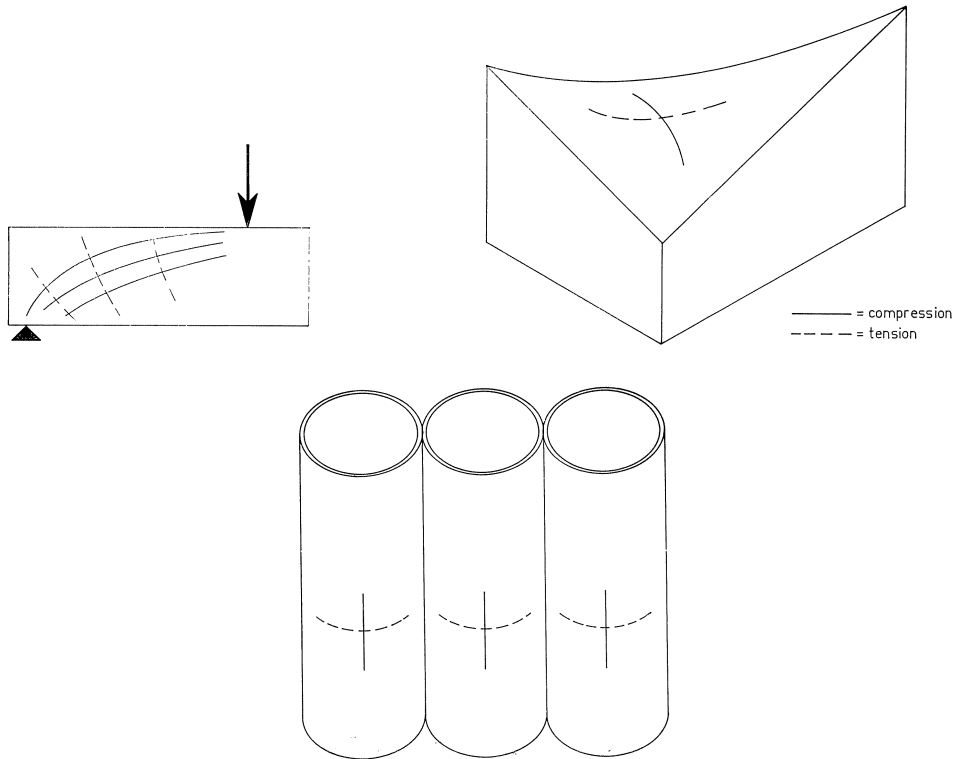


Fig. 43. Constructions under compression-tension.

The behaviour of a beam loaded by shearing forces will be treated as an example. First we have to remark that the usual method of calculation is based on the ultimate shearing stresses that can be resisted. From the biaxial tests it can be seen that in the region of compression-tension (which can be compared with the region of shearing stresses) the only shearing failure we see is a fracture perpendicular to the direction of the tensile stresses. It is impossible to use these test results directly in the region of shearing forces for all kinds of beams, because the stress condition in a beam in this region depends on the sizes of the beam, the amount of reinforcement, etc. In a prestressed beam, for instance, when the first crack occurs not as a result of tensile bending stresses, then the ultimate load can be calculated with the aid of the test results. This mode of fracture is a dangerous one, because it occurs without warning; it is a brittle fracture.

An example of the safety of such a structure against failure is given in the following.

Assume a uniform divided prestressing of $\sigma_x = -40 \text{ kgf/cm}^2$ over the cross-section. Consider also a shearing stress $\tau = 15 \text{ kgf/cm}^2$ as a result of the surface load. The principal stresses belonging to this state of stress can be calculated by the usual equations of equilibrium: $\sigma_1 = -45 \text{ kgf/cm}^2$ and $\sigma_2 = +5 \text{ kgf/cm}^2$.

In order to control the safety of this structure according to the codes, the load has to be multiplied by the safety factor (for instance 2) and the calculated principal stresses belonging to this state of stress may just reach the uniaxial compressive and/or tensile strength. In this example ($\tau = 30 \text{ kgf/cm}^2$ and $\sigma_x = -40 \text{ kgf/cm}^2$) the principal stresses are $\sigma_1 = -56 \text{ kgf/cm}^2$ and $\sigma_2 = +16 \text{ kgf/cm}^2$. When the calculating value of the tensile strength is just $+16 \text{ kgf/cm}^2$ then according to the codes we may speak of a safe structure. From the biaxial test results in the region of compression-tension it can be seen, however, that this structure is an unsafe one: the safety factor is only 1.73 (principal stresses: $\sigma_1 = -52 \text{ kgf/cm}^2$ and $\sigma_2 = +13 \text{ kgf/cm}^2$).

Constructions under compression-compression

Some examples of constructions in this region are given in fig. 44. Hitherto, the bearing strength of, for instance, two-way spanning slabs and one-way spanning beams with transversal prestressing in the compression zone was based on the ultimate strength and the stress strain relationship of concrete under uniaxial compression.

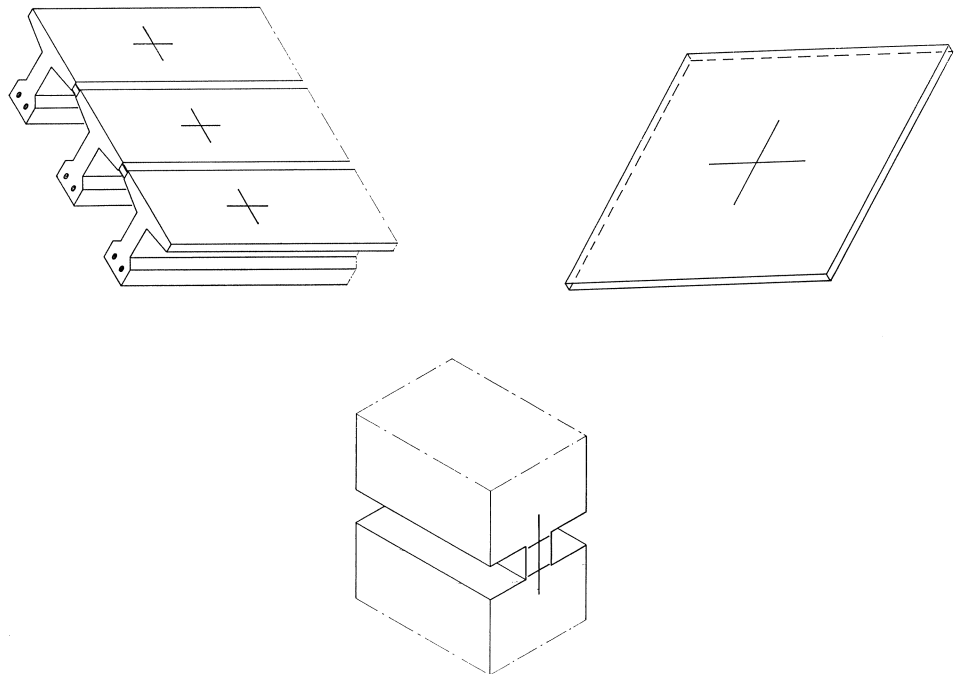


Fig. 44. Constructions under compression-compression.

The biaxial test results have shown that, when the concrete under compression estimates the failure, then the safety of such a structure will be greater than the calculated one. When the yielding of the steel estimates failure, then a higher percentage of steel is possible. The situation of the neutral axis will be somewhat different too, because of a different relationship between stress and strains under biaxial compression.

From many tests it is already known that the bearing strength of a concrete line-hinge is higher than the uniaxial compressive strength multiplied by the area of the hinge. From the biaxial tests we can learn that this occurs only when there is a biaxial compression state of stress. For this reason a good reinforcement on both sides of the hinge is necessary to prevent cracking (according to 2.2.b a fine spaced reinforcement is favourable). Tests on concrete hinges have also shown a smaller stiffness against rotation than can be calculated in the usual way. This difference may be declared by the more pronounced deformations under biaxial loading compared to the deformations under uniaxial loading.

Literature

1. KRAHL, N. W. e.a., The behaviour of plain mortar and concrete under triaxial stresses. Proc. of A.S.T.M. V. 65-1965, p. 697-709.
2. KÁRMÁN, TH. VON, Festigkeitsversuche unter allseitigen Druck. Zeitschrift des Vereins Deutscher Ingenieure no. 42, 1911.
3. BÖKER, R., Die Mechanik der bleibenden Formänderung in kristallinisch aufgebauten Körpern. Mitteilungen über Forschungsarbeiten, Heft 175-176, Berlin 1915, 51 p.
4. RICHART, F. E., A. BRANDTZAEG and R. L. BROWN, The behaviour of plain and spirally reinforced concrete in compression. University of Illinois Engineering Experiment Station. Bulletin no. 190, April 1929, 72 p.
5. AKROYD, T. N. W., Concrete under triaxial stresses. Magazine of Concrete Research. V. 13 no. 39, Nov. 1961, p. 111-119.
6. FUMAGALLI, E., The strength characteristics of concrete under conditions of multi-axial compression. Models and Structures Experimental Institute, Bergamo, report no. 30, Oct. 1965, p. 1-16.
7. CHINN, J. and R. M. ZIMMERMAN., Behaviour of plain concrete under various high triaxial compression loading conditions. University of Colorado, Aug. 1965.
8. CONSIDÈRE, A., Résistance à la compression du béton armé et du béton fretté. Le genie civil 1902.
9. BEN-ZVI, E., G. MULLER and I. ROSENTHAL., Effect of the active triaxial stress on the strength of concrete elements. Proc. of A.C.I. V. 63, Oct. 1966, p. 112-128.
10. RENGERS, N. J., Tests on columns of concrete and reinforced concrete. De Ingenieur No. 27, 31, 40 and 48, 1933 and De Ingenieur No. 1, 9 and 27, 1934.
11. RÜSCH, H. and S. STÖCKL, Versuche an Wendelbewehrten Stahlbetonsäulen unter kurz- und langfristig wirkende zentrischen Lasten. Deutscher Ausschuss für Stahlbeton. Heft 205, Berlin 1969.
12. MCHENRY, D. and J. KARNI, Strength of concrete under combined tensile and compressive stresses. Journal of A.C.I., Apr. 1958, p. 829-839.
13. BELLAMY, C. J., Strength of concrete under combined stresses. Journal of A.C.I., Oct. 1961, p. 367-380.
14. MALČOV, K. A. and A. PAK, Betonfestigkeit bei mehrachsiger Beanspruchung. Festigkeitsprobleme des Betons. Internationales Kolloquium Dresden 1968. Sonderdruck der Wissenschaftl. Zeitschrift der T.U. Dresden, p. 1519-1520.
15. BRESLER, B. and K. S. PISTER, Failure of plain concrete under combined stresses. A.S.C.E., Apr. 1955, no. 2897, p. 1049-1059.

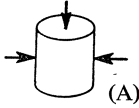
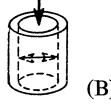
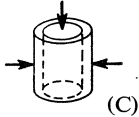
16. BRESLER, B. and K. S. PISTER, Strength of concrete under combined stresses. *Journal of A.C.I.* V. 30 no. 3, Sept. 1958, p. 321–345.
17. TSUBOI, Y. and Y. SUENAGA, Experimental study on failure of plain concrete under combined stresses. Part 3. *Transactions of the architectural Institute of Japan.* No. 64, Febr. 1960, p. 25–36.
18. GOODE, C. D. and M. A. HELMY, The strength of concrete under combined shear and direct stress. *Magazine of Concrete Research.* V. 19, No. 59, June, 1967, p. 105–112.
19. JOHNSON, R. P. and P. G. LOWE, Behaviour of concrete under biaxial and triaxial stress. *International Conference on Structure, Solid Mechanics and Engineering Design.* Civil Engineering Materials. Southampton University, 21–25 Apr. 1969, p. 89/1–89/13.
20. KOK, A. W. M., Finite element method. The theory of the finite element method with displacements as fundamental unknowns. *Stevin-report 8–67–4*, 27 p.
21. FÖPPL, A., Abhängigkeit der Bruchgefahr von der Art des Spannungszustandes. *Mitteilungen dem Mechanisch-Technischen Laboratorium der K. Technischen Hochschule.* Heft 27, München 1900.
22. WÄSTLUND, G., Nya rön angående Betongens Grundläggande Halfasthetsegenskaper. *Betong 1937.* Haft 3, p. 189–205.
23. GLOMB, J., Die Ausnutzbarkeit zweiachsiger Druckfestigkeit des Betons in Flächentragwerken. Paper of the F.I.P., third congress 1958, p. 3–14.
24. WEIGLER, H. and G. BECKER, Untersuchungen über das Bruch- und Verformungsverhalten von Beton bei zweiachsiger Beanspruchung. *Deutscher Ausschuss für Stahlbeton.* Heft 157, Berlin 1963, 65 p.
25. SUNDARA RAJA IYENGAR, K. T., K. CHANDRASHEKHARA and K. T. KRISHNASWAMY, Strength of concrete under biaxial compression. *Journal of A.C.I.* V. 62 no. 2, Febr. 1965, p. 239–249.
26. VILE, G. W. D., Behaviour of concrete under simple and combined stresses. *Imperial College of Science and Technology, London,* Sept. 1965, 559 p.
27. SMITH, G. M., Failure of concrete under combined tensile and compressive stresses. *Journal of A.C.I.* V. 50 no. 2, Oct. 1953, p. 137–140.
28. OPITZ, H., Festigkeit und Verformungseigenschaften des Betons bei zweiachsiger Beanspruchung. *Festigkeitsprobleme des Betons. Internationales Kolloquium Dresden 1968.* Sonderdruck der *Wissenschaftl. Zeitschrift der T.U. Dresden*, p. 1520–1523.
29. HRUBAN, I. and B. VITEK, Die Festigkeit des Betons bei ein- und zweiachsiger Beanspruchung. *Festigkeitsprobleme des Betons. Internationales Kolloquium Dresden 1968.* Sonderdruck der *Wissenschaftl. Zeitschrift der T.U. Dresden*, p. 1523–1525.
30. HILSDORF, H. K., Bestimmung der zweiachsigen Festigkeit des Betons. *Deutscher Ausschuss für Stahlbeton.* Heft 173, Berlin 1965, 68 p.
31. KUPFER, H., H. K. HILSDORF and H. RÜSCH, Behaviour of concrete under biaxial stresses. *Journal of A.C.I.*, Aug. 1969, p. 656–666.
32. NIWA, Y., S. KOBAYASHI and W. KOYANAGI, Failure criterion of lightweight aggregate concrete subjected to triaxial compression. *Memoires of the faculty of engineering, Kyoto University*, 29 (1967) 2, p. 119–131.
33. ROSS, A. D., Experiments on the creep of concrete under two-dimensional stressing. *Magazine of Concrete Research*, no. 16, June 1954, p. 3–11.
34. MEYER, H. G., Beitrag zur Frage des Querkriechens von Beton unter ein- und zweiachsiger Druckbeanspruchung. *Mitteilungen aus dem Institut für Materialprüfung und Forschung des Bauwesens der T.H. Hannover*, Heft 5, 1967, 247 p.
35. GOPALAKRISHNAN, K. S., A. M. NEVILLE and A. GHALI, Creep poisson's ratio of concrete under multi-axial compression. *University of Calgary Journal of A.C.I.*, Dec. 1969, p. 1008–1016.
36. NEWMAN, K., Concrete control tests as a measure of the properties of concrete. *Symposium on Concrete Quality.* 10–12 Nov. 1964, London.
37. KOTTE, J. J., Z. G. BÉRCZES, J. GRAMBERG and TH. R. SELDENRATH, Stress-strain relations and breakage of cylindrical rock specimens under uniaxial and triaxial loads. *Int. J. Rock Mech. Min. Sci.* V. 6, p. 581–595. Pergamon Press 1969.
38. KJELLMANN, W., Om Undersdening av Jordartes Deformations Egenskaper. *Teknisk Tidskrift, Stockholm*, No. 8, Aug. 1936.
39. MÄNGEL, S., Beitrag zur Prüfung von Betonwürfeln. *Betonsteinzeitung*, Heft 4, 1968, p. 197–201.
40. WESTLEY, J. W., Some experiments on concrete cubes with non-plane surfaces. *Magazine of Concrete Research*, V. 18, No. 54, March 1966, p. 35–37.

41. TURNER, P. W. and P. R. BARNARD, Stiff constant strain rate testing machine. *The Engineer*, 27th July 1962, V. 214, No. 5557, p. 146–149.
42. GLUCKLICH, J., The influence of sustained loads on the strength of concrete. *Bulletin Rilem*, No. 5, Dec. 1959, p. 14–18.
43. HUGHES, B. P. and G. P. CHAPMAN. The complete stress-strain curve for concrete in direct tension. *Bulletin Rilem*, No. 30, March 1966, p. 95–98.
44. RASCH, C., Spannungs-Dehnungslinien des Betons und Spannungsverteilung in der Biegedruckzone bei konstanter Dehngeschwindigkeit. *Deutscher Ausschuss für Stahlbeton*, Heft 154, Berlin 1962, 72 p.
45. HEILMAN, H. G., H. HILSDORF and K. FINSTERWALDER, Festigkeit und Verformung von Beton unter Zugspannungen. *Deutscher Ausschuss für Stahlbeton*, Heft 203, Berlin 1969, 94 p.
46. NADAI, A., *Theory of flow and fracture of structures solids*. McGraw Hill book Co. Ny. 1950.
47. RÜSCH, H., Research toward a general flexural theory for structural concrete. *Journal of A.C.I.*, July 1960, p. 1–28.
48. SELL, R., Investigations into the strength of concrete under sustained load. *Bulletin Rilem* No. 5, Dec. 1959, p. 5–17.
49. GROOT, A. K. DE and A. C. VAN RIEL, The stability of columns and walls of unreinforced concrete. *Heron*, V. 15, No. 3/4, 1967, p. 65–112.
50. LEEUWEN, J. VAN, Investigation into the influence of fine-spaced reinforcement on cracking, stiffness and strength of plates under bending. *Stevin-report 5-68-1-SV6*, Febr. 1968, 11 p.
51. MÜLLER, R. K., Der Einfluss der Messlänge auf die Ergebnisse bei Dehnungsmessungen an Beton. *Beton* 14 (1964), p. 205–209.
52. DRAGOSAVIĆ, M., Stability of walls in prefabrication. *Heron* V. 12, No. 2, 1964, p. 51–71.
53. MUSKHELISHVILI, N. I., Some basic problems of the mathematical theory of elasticity. 1963, p. 381–398.
54. NEWMAN, K. and O. T. SIGVALDSON, Testing machine and specimen characteristics and their effect on the mode of deformation, failure and strength of materials. *Machines for material and environmental testing*. Manchester 6–10 Sept. 1965.
55. TONGEREN, H. P. VAN, Surface treatment of concrete, before glueing. T.N.O.-report BI-67-24/22h33.
56. BUEREN, R. VAN, The influences of the sizes of the specimen and the effect of the wall on the compression strength of concrete. *Stevin-report 5-67-3-DR-1*, 10 p.
57. DEKKER, A. J. CHR., The vibration of concrete. *Cement XIX* (1967), No. 4, p. 130–133.
58. TAYLOR, W. H., *Concrete technology and practice*. American Elsevier publishing Co. Inc., 1965, p. 163–173.
59. WALKER, S. and D. L. BLOEM, Effects of curing and moisture distribution on measured strength of concrete. *Proc. Highw. Res. Bd.* 36, 1957, p. 334–346.
60. DAHMS, J. Einfluss der Eigenfeuchtigkeit auf die Druckfestigkeit des Betons. *Betontechnische Berichte*, 1968, p. 113–127.
61. LEON, A., Über die Scherfestigkeit des Betons. *Beton und Eisen*, 1935, p. 130–135.
62. RÜSCH, H., R. SELL, C. H. RASCH and S. STÖCKL, Investigations into the strength of concrete under sustained load. *Rilem Colloquium*, 1958, München.
63. BERG, O. JA., Die Hauptentwicklungsrichtungen der Theorie des Festigkeit und Verformungen des Betons. *Kolloquium Festigkeitsprobleme des Betons Dresden 1968*. Sonderdruck der Wissenschaftl. Zeitschrift der T.U. Dresden, p. 1489–1496.
64. STURMAN, G. M., S. P. SHAH and G. WINTER, Microcracking and inelastic behaviour of concrete. *Proc. of A.C.S.E.–A.C.I. International symposium on Flexural Mechanics of reinforced concrete*, Nov. 1964, p. 473–499.
65. RÜSCH, H., Physikalischen Fragen der Betonprüfung. *Zement-Kalk-Gips*, Heft 1, 1959, p. 1–10.
66. SHAH, S. P. and S. CHANDRA, Critical stress, volume change and microcracking of concrete. *A.C.I. journal*, Sept. 1968, p. 770–781.
67. DESAYI, P. and C. S. VISWANATHA. The ultimate strength of plain concrete. *Bulletin Rilem*, No. 36, Sept. 1967, p. 163–174.
68. INGLIS, C. E., Stresses in a plate due to the presence of cracks and sharp corners. *Transactions Institute of Naval Architects*, V. 60, London 1913.
69. GRIFFITH, A. A., The phenomena of rupture and flow in solids. *Philosophical Transactions, Royal Society of London, Series A*, V. 221, 1920, p. 163–198.

70. OROWAN, E., Fracture and strength of solids. Reports on Progress in Physics, V. 12. Physical Society of London, 1948-49, p. 185-232.
71. SACK, R. A., Extension of Griffith's theory of rupture to three dimensions. Proc. Physical Society of London, 1946, p. 729-736.
72. HANSEN, T. C., Creep and Stress Relaxation of Concrete. Proc. no. 31, Swedish Cement and Concrete Research Institute at the Royal Institute of Technology, Stockholm 1960.
73. LEVI, F. and C. E. CALLARI, Introduction à une tentative d'établissement d'une méthode générale pour le calcul des dalles en flexion. C.E.B. Bulletin d'information no. 38, March 1963, p. 35-59.

APPENDIX

APPENDIX I Survey of previous investigations

	Name	Region	Loading set up	Sizes of the specimen (cm)	Material	Speed of loading
Solid cylinders (1.1)	v. Kármán Böker [2-3]	C-C	 (A)	$\varnothing 4 \times 10$	Carrara-marble	
	Richart et al. [4]	C-C	A	$\varnothing 10 \times 25$	concrete mortar	
	Akroyd [5]	C-C	A	$\varnothing 2,5 \times 7,5$	concrete	
	Fumagalli [6]	C-C	A	$\varnothing 10 \times 20$	concrete $\begin{cases} \text{K75} \\ \text{K170} \\ \text{K280} \end{cases}$ $\varnothing_{\max} = 20 \text{ mm}$	
	Chinn-Zimmerman [7]	C-C	A	$\varnothing 15 \times 30$	concrete $\begin{cases} \text{K350} \\ \text{K500} \\ \text{K700} \end{cases}$	max. duration of the test 2 till 3 hours
Hollow cylinders (1.2.a)	McHenry-Karni [12]	C-T	 (B)	$\varnothing_i = 25$ $\varnothing_e = 35$ $l = 60$	concrete $\sigma'_c = \begin{cases} 200 \\ 350 \\ 450 \end{cases}$ $\varnothing_{\max} = 20 \text{ mm}$	
	Bellamy [13]	C-C	 (C)	$\varnothing_i = 7,5$ $\varnothing_e = 15$ $l = 30$	concrete $\varnothing_{\max} = 4,5 \text{ mm}$	160 kgf/cm ² min.
	Malčov-Pak [14]	T-T		$\varnothing_i = 50$ $\varnothing_e = 56$ $l = 120$	concrete	
		C-T	B	$\varnothing_i = 27,6$ $\varnothing_e = 30$		
C-C		C	$l = 71$			

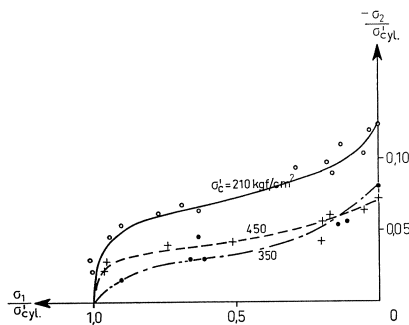


Fig. I.1

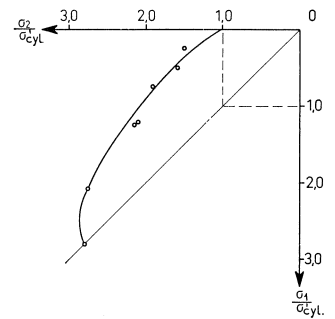


Fig. I.2

Remarks	Results
<ul style="list-style-type: none"> - no coating used against penetration of the fluid - restraint of axial deformation is estimated 	<ul style="list-style-type: none"> - σ'_u biaxial $\sim 1,3\sigma'_u$ uniaxial - brittle material behaves more plastic under increasing fluid pressure
<ul style="list-style-type: none"> - penetration of fluid prevented - restraint of axial deformation is not estimated 	<ul style="list-style-type: none"> - σ'_u biaxial $\sim 1,3\sigma'_u$ uniaxial - there is an influence of the quality of the concrete on this increase in strength
<ul style="list-style-type: none"> - the specimen is coated to prevent the penetration of the fluid 	<ul style="list-style-type: none"> - the humidity influences the ultimate load (a dried specimen gives a higher strength)
<ul style="list-style-type: none"> - restraint of axial deformation as much as possible reduced but not estimated - penetration of fluid not prevented 	<ul style="list-style-type: none"> - σ'_u biaxial $\sim 1,35\sigma'_u$ uniaxial - fracture occurred normal to the plane of loading
<ul style="list-style-type: none"> - neoprene coating of the specimen against penetration of the fluid - restraint of axial deformation estimated 	<ul style="list-style-type: none"> - σ'_u biaxial $\sim 1,25\sigma'_u$ uniaxial - the quality of the concrete had a little influence - following different loading paths had a little influence
<ul style="list-style-type: none"> - rubber coating against penetration of the fluid - assumed a uniform stress distribution over the wall 	<ul style="list-style-type: none"> - following different loading paths had a little influence - fig. 1.1
<ul style="list-style-type: none"> - neoprene coating against penetration of the fluid - assumed a uniform stress distribution over the wall 	<ul style="list-style-type: none"> - fig. 1.2
<ul style="list-style-type: none"> - rubber coating against penetration of the fluid - tensile force by bars - compressive force by movable stamps - the assumed stress distribution is not given in the report 	<ul style="list-style-type: none"> - fig. 1.3

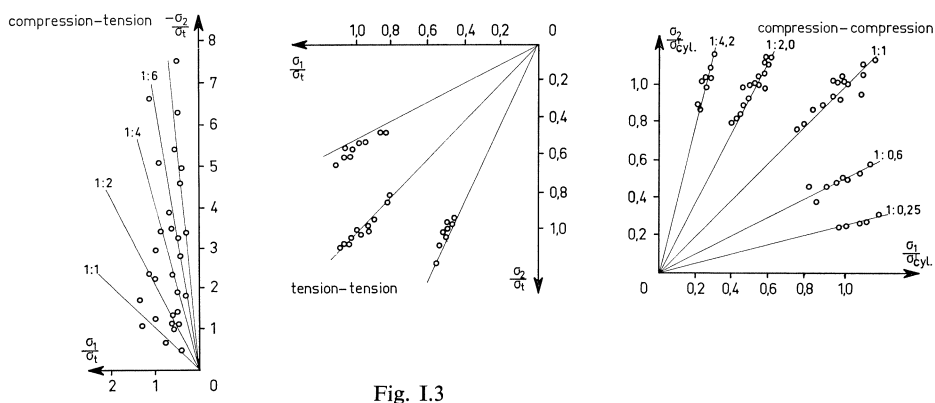
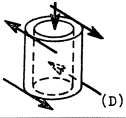


Fig. 1.3

	Name	Region	Loading set up	Sizes of the specimen (cm)	Material	Speed of loading
Hollow cylinders (1.2.b)	Bresler-Pister [15, 16]	C-T		$\varnothing_i = 15$ $\varnothing_e = 21$ $l = 76$	concrete $\sigma'_e = 200$	Max. duration of the test 5400 min.
	Tsuboi-Suenaga [17]	C-T	B D			
	Goode-Helmy [18]	C-T	D	$\varnothing_i = 15$ $\varnothing_e = 20$ $l = 60$	concrete K200 to K500 $\varnothing_{max} = 10$ mm	max. duration of the test 2½ hours
	Isenberg [19]	C-T	D	$\varnothing_i = 9,7$ $\varnothing_e = 11,4$ $l = 29$	concrete $\varnothing_{max} = 4,8$ mm	

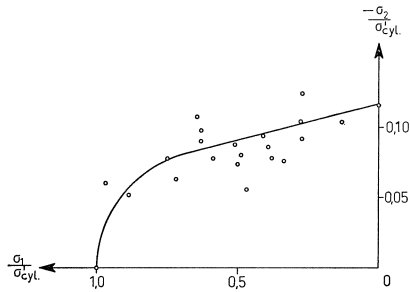


Fig. I.4

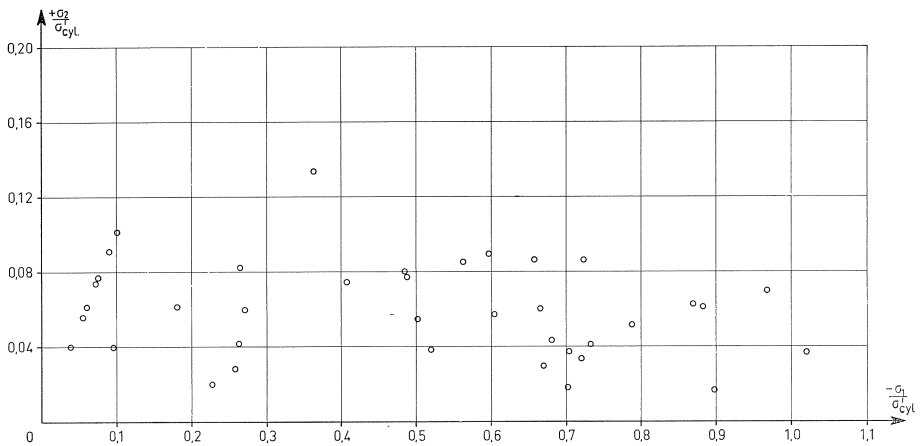


Fig. I.6

Remarks

Results

- restraint of axial deformation and friction of the loading mechanism estimated
 - assumed a uniform stress distribution over the wall
 - assumed a uniform stress distribution over the wall
 - the great deviation in test results is probably the result of a relative thin wall compared to the maximum size of the aggregate (only factor 2)
 - the stress distribution over the wall calculated for a linear-elastic material
 - only a little attention is made for the turning and axial deformation of the specimen
 - assumed a uniform stress distribution over the wall
 - discontinuity point is the load at which ψ deviates more than 6×10^{-6} rad. from the straight $M-\psi$
- no difference in strength by following different loading paths
 - no influence of the quality of the concrete
 - fig. 1.4
 - fig. 1.5
 - σ'_u torsion $\sim 0,65\sigma$ splitting
 - fig. 1.6
 - fig. 1.7

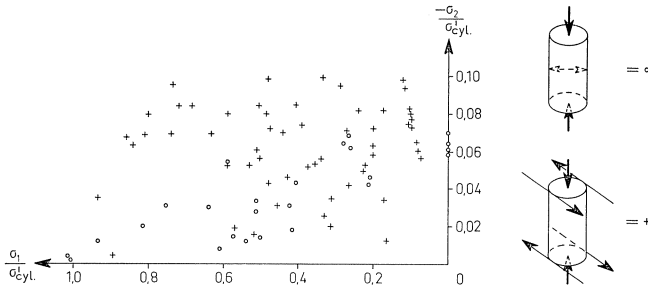


Fig. I.5

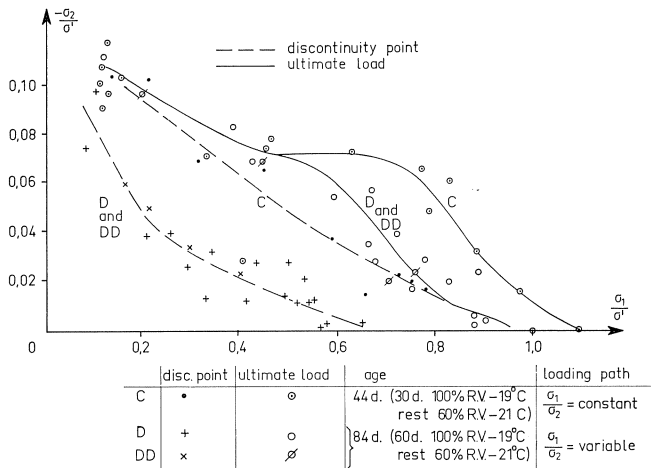


Fig. I.7

	Name	Region	Loading set up	Sizes of the specimen (cm)	Material	Speed of loading
Cubes plates (1.3)	Föppl [21]	C-C	cube	7×7×7	mortar	
	Wästlund [22]	C-C	cube	15×15×15	concrete	
	Glomb [23]	C-C	cube	20×20×20 10×10×10	concrete K160 K225	1 till 1,5 kgf/cm ² /sec.
	Weigler-Becker [24]	C-C	plate	10×10×2,5	cementstone K225 concrete K300 K600 $\varnothing_{\max} = 7$ mm	max. duration of the test 30 min.
	Sundara Raja Iyengar et al. [25]	C-C	cube	15×15×15 10×10×10	concrete K500 mortar K150	
	Vile [26]	C-C C-T	plate	25×25×10	concrete mortar lightweight concrete $\varnothing_{\max} = 20$ mm K200 to K575	5 kgf/cm ² /min. 0,8 kgf/cm ² /min.
	Opitz [28]	C-C	plate	20×20×5	concrete K225 K300 K450	
	Kupfer et al. [31]	C-C C-T T-T	plate	20×20×5	concrete $\sigma'_p = 190$ 315 590 $\varnothing_{\max} = 15$ mm	max. duration of the test 20 min. tried $d\varepsilon/dt = k$

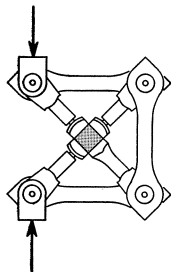


Fig. I.8

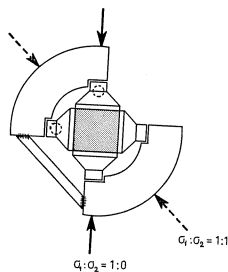


Fig. I.9

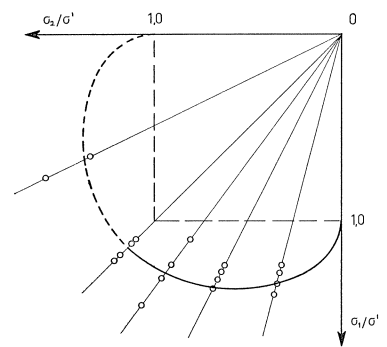


Fig. I.1

Remarks	Results
<ul style="list-style-type: none"> - looked after the influence of the medium between loading platen and specimen - testing frame, see fig. 1.8 	<ul style="list-style-type: none"> - the medium between loading platen and specimen has a great influence on the ultimate load
<ul style="list-style-type: none"> - a lubricant of 1 cm rubber - how the uniaxial compressive strength is estimated is not given in the report - testing frame see fig. 1.9 	<ul style="list-style-type: none"> - fracture occurred in the direction of the tensile strain.
<ul style="list-style-type: none"> - a lubricant of paraffine - stiff testing frame with 4 vessels - assumed: $\sigma'_{u \text{ uniaxial}} = 0,855\sigma'_{\text{cube}}$ 	<ul style="list-style-type: none"> - ultimate load is proportional to the stress ratio (maximum increase 40% at 1:1) - the quality of the concrete does not have an influence on this increase - fracture occurred in the direction of the tensile strain (reinforcement in this direction resulted in an extra increase of 50%)
<ul style="list-style-type: none"> - no lubricant - testing frame: see fig. 1.11 	<ul style="list-style-type: none"> - fig. 1.12
<ul style="list-style-type: none"> - no lubricant - the two loading frames in both directions can move separately from each other 	<ul style="list-style-type: none"> - fig. 1.13
<ul style="list-style-type: none"> - no lubricant - very stiff testing frame (fig. 1.14) 	<ul style="list-style-type: none"> - fig. 1.15
<ul style="list-style-type: none"> - a lubricant consisting of sheets of polytetrafluoroethylene (3,5 × 3,5 × 0,4 cm) + brass of a thickness of 0,2 mm 	<ul style="list-style-type: none"> - following different loading paths increased the strength with 5% in comparison to a constant stress ratio - the load at which a minimum volume occurred was a constant percentage of the ultimate load. - fig. 1.16
<ul style="list-style-type: none"> - used brushes (loading platens built up of separate rods) - the brushes were glued to the specimen in order to transmit tensile forces 	<ul style="list-style-type: none"> - fig. 1.17

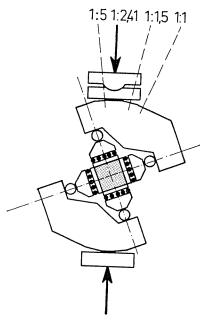


Fig. I.11

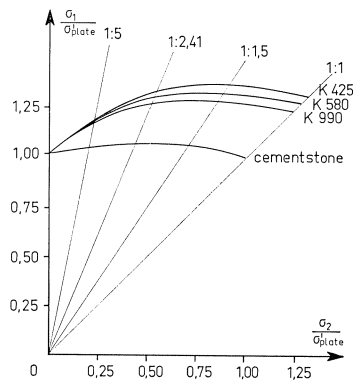


Fig. I.12

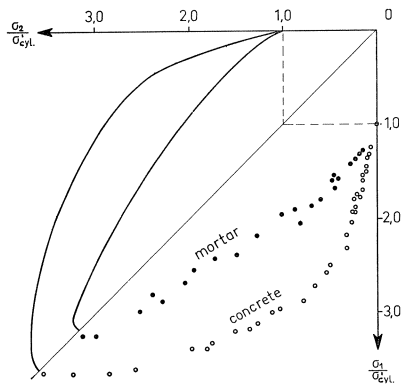


Fig. I.13

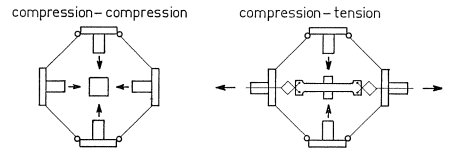


Fig. I.14

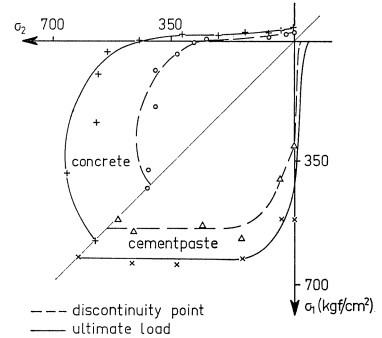


Fig. I.15

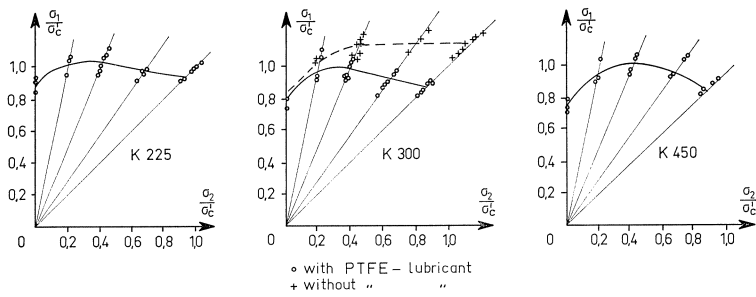


Fig. I.16

	Name	Region	Loading set up	Sizes of the specimen (cm)	Material	Speed of loading
Creep tests	Ross [33]	C-C	plate	15 × 15 × 3	concrete	$\sigma_{\max} = 35$
		C-T	B	$\varnothing_i = 12$ $\varnothing_e = 15$ $l = 60$	$\varnothing_{\max} = 10$ mm	kgf/cm^2 1:0 1:1 1:2 1:3
	Meyer [34]	C-C	plate	40 × 40 × 6	concrete $\varnothing_{\max} = 7$ mm	$\sigma_{\max} = 0,3\sigma'_{\text{cut}}$ 1:1 1:2
Gopala-Krishnan et al. [35]	C-C	cube	25 × 25 × 25	concrete K300 $\varnothing_{\max} = 20$ mm	$\sigma_{\max} = 0,5\sigma'_{\text{cut}}$	

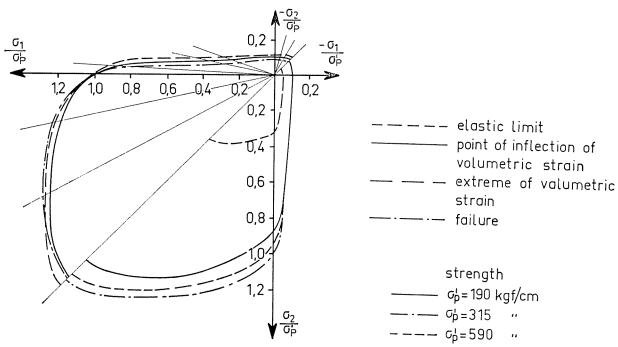


Fig. I.17

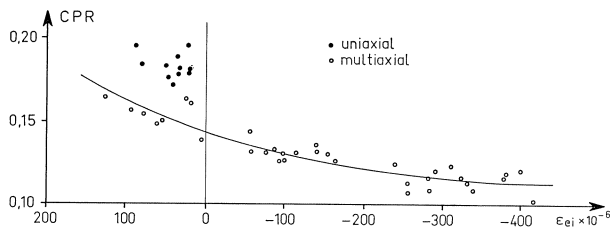


Fig. I.18

Remarks	Results
<ul style="list-style-type: none"> - no lubricant - assumed a uniform stress distribution over the wall - rubber coating against penetration of the fluid 	<ul style="list-style-type: none"> - no lateral contraction under long time loading
<ul style="list-style-type: none"> - a lubricant of hestaflon of 2 mm thickness 	<ul style="list-style-type: none"> - creep deformation can be calculated by the principle of counting
<ul style="list-style-type: none"> - a lubricant consisting of 3 sheets of aluminium (0,001 mm) with between these sheets polar grease 	<ul style="list-style-type: none"> - fig. I.18

APPENDIX II Calculation of the rod-platens

Calculation of the instability (see fig. II-1)

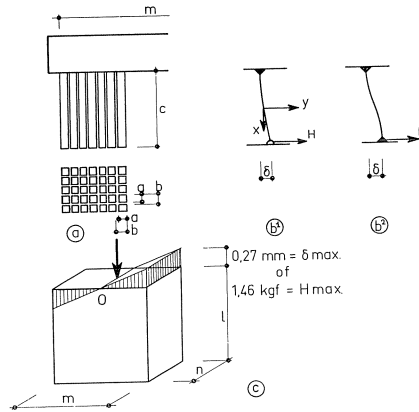


Fig. II.1. Calculation of the rod-platen.

The most unfavourable length occurs when the rod is pinned on the concrete. Assuming a straight rod, the maximum force that can be borne by a single rod can be calculated by

$$P_s = \frac{\pi^2 EI}{(2c)^2} \quad (\text{II.1})$$

Every loading platen consists of q rods:

$$q = \frac{m \cdot n}{b^2} \quad (\text{II.2})$$

Every loading platen can transmit:

$$(1) + (2) \rightarrow P_t = q \cdot \frac{\pi^2 EI}{(2c)^2} = \frac{\pi^2 E a^4 m n}{48 b^2 c^2} \quad (\text{II.3})$$

The first condition that has to be fulfilled is that $P_{t_{\min}} = 100.000 \text{ kgf}$. From this condition and (II.3) follows:

$$\frac{a^4}{b^2 c^2} > 10^{-3} \quad (\text{II.4})$$

Insurance against turning over [52].

For this calculation it is assumed that the rods are fixed to the concrete. This can be controlled after calculating.

It is necessary to have a horizontal force (H) to turn over the single rod. When a rod of infinite stiffness is assumed, then from calculation of the equilibrium follows (see fig. II-2):

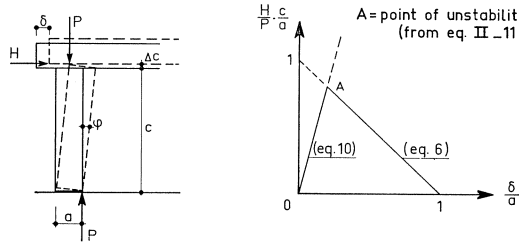


Fig. II.2. Unstability calculation for a single rod.

$$\frac{H}{P} = \frac{a - \delta}{c + \Delta c} \quad (\text{II.5})$$

If $\Delta c \ll \ll c$ then:

$$\frac{H}{P} \cdot \frac{c}{a} = 1 - \frac{\delta}{a} \quad (\text{II.6})$$

The bending line of a rod with normal stiffness can be calculated from:

$$\frac{d^2 y}{dx^2} = -\frac{Mx}{EI} = -\frac{1}{EI}(Py + Hx) \quad (\text{II.7})$$

The following universal solution satisfies equation (II.7):

$$y = C_1 \cos kx + C_2 \sin kx - \frac{H}{P}x \quad \text{with} \quad k^2 = P/EI \quad (\text{II.8})$$

The value of the constants C_1 and C_2 can be calculated from:

$$\begin{aligned} x = 0 \quad \text{and} \quad \frac{d^2 y}{dx^2} = 0 &\rightarrow C_1 = 0 \\ x = \frac{1}{2}c \quad \text{and} \quad \frac{dy}{dx} = 0 &\rightarrow C_2 = \frac{H}{P} \cdot \frac{1}{k \cos \frac{1}{2}kc} \end{aligned} \quad (\text{II.9})$$

From the condition $x = \frac{1}{2}c \rightarrow y = \frac{1}{2}\delta$ follows the force H needed to give the single rod a displacement of δ .

$$\frac{\delta}{2} = \frac{H}{P} \cdot \frac{\text{tg} \frac{1}{2}kc}{K} - \frac{H}{P} \cdot \frac{c}{2} \rightarrow \frac{H}{P} \cdot \frac{c}{a} = \frac{\delta}{a} - \frac{1}{\frac{\text{tg} \frac{1}{2}kc}{\frac{1}{2}kc} - 1} \quad (\text{II.10})$$

The rod will become unstable when the equations (II.10) and (II.6) are equal to each other (see fig. II.2):

$$\frac{H}{P} \cdot \frac{c}{a} = \frac{\frac{1}{2}kc}{\operatorname{tg} \frac{1}{2}kc} \quad (\text{II.11})$$

The equations (II.7) to (II.11) are correct when the entire contact area between concrete and rod transmits the axial force. This last assumption is fulfilled when the excentricity of the force in this section is less than $1/6a$:

$$H \cdot \frac{1}{2}c + P \cdot \frac{1}{2}\delta \leq P \cdot \frac{a}{6} \rightarrow \frac{H}{P} \cdot \frac{c}{a} \leq \frac{1}{3} - \frac{\delta}{a} \quad (\text{II.12})$$

The sizes of the single rods ($4 \times 4 \times 100$ mm) are chosen in such a way that the entire contact area does not transmit the normal force ($e_0 > 1/6a$). In comparison to the theoretical calculated joint for instability (II.11) there still exists a security factor of about 2, which follows from the next calculation:

The horizontal force H (see fig. II.1b) needed to give the single rod a displacement of δ can be calculated from:

$$H = \frac{p\delta EI}{c^3} \quad (\text{II.13})$$

In this equation $p = 12$ when the rod is completely fixed to the concrete (most unfavourable). The maximum strain of concrete is assumed to be $3^0/00$ and the deformation of the concrete is linear with the distance to the middle of the specimen, as is fulfilled by the loading frame (see fig. II.1). The expected maximum deformation of a single rod is $\delta = 3 \cdot 10^{-3} \times \frac{1}{2} \cdot m \sim 0,27$ mm.

For this displacement a horizontal force $H = 1,46$ kgf is needed. With the assumption of a rod fixed completely to the concrete, the rod would turn over when the horizontal displacement was 0,59 mm, caused by a horizontal force $H = 2,71$ kgf and an axial force of $P = 97,3$ kgf.

In reality the factor of security will be less than 2 because the rod is not effectively fixed to the specimen.